Image Cover Sheet

CLASSIFICATION	SYSTEM NUMBER
UNCLASSIFIED	103645

TITLE

DEVELOPMENT OF RANDOM RESPONSE ANALYSIS CAPABILITY FOR THE VAST FINITE ELEMENT PROGRAM - PHASE I

System Number:

Patron Number:

Requester:

Notes:

DSIS Use only:

Deliver to: JR

UNLIMITED DISTRIBUTION

National Defence
Research and Development Branch

Défense nationale
Bureau de recherche et développement

DREA CR/91/424

DEVELOPMENT OF RANDOM RESPONSE ANALYSIS CAPABILITY FOR THE VAST FINITE ELEMENT PROGRAM - PHASE I -

by
I.R. Orisamolu - M.E. Norwood - M.W. Chernuka

MARTEC LIMITED
1888 Brunswick Street, Suite 400
Halifax, Nova Scotia, Canada
B3J 3J8

CONTRACTOR REPORT

Prepared for

Defence Research Establishment Atlantic

Centre de Recherches pour la Défense Atlantique

Canada

PLEASE DIRECT ENQUIRIES TO:

THE CHIEF,
DEFENCE RESEARCH ESTABLISHMENT ATLANTIC,
PO BOX 1012,
DARTMOUTH, NOVA SCOTIA,
CANADA.

UNLIMITED DISTRIBUTION

National Defence
Research and Development Branch

Défense nationale
Bureau de recherche et développement

DREA CR/91/424

DEVELOPMENT OF RANDOM RESPONSE ANALYSIS CAPABILITY FOR THE VAST FINITE ELEMENT PROGRAM - PHASE I -

by
I.R. Orisamolu - M.E. Norwood - M.W. Chernuka

MARTEC LIMITED
1888 Brunswick Street, Suite 400
Halifax, Nova Scotia, Canada
B3J 3J8

Scientific Authority D.C. Stredulinsky

W7707-0-0956/01-OSC
Contract Number

March 1991

CONTRACTOR REPORT

Prepared for

Defence Research Establishment Atlantic

Centre de Recherches pour la Défense Atlantique

Canada

ABSTRACT

This report contains a description of the work done in the first phase of a contract awarded by the Defence Research Establishment Atlantic (DREA) for the provision of an in-house random response analysis capability. A concise description of the theoretical basis of the finite element random vibration analysis methodology is given. A description of available procedures for computing the assembled cross-spectral density matrix for a finite element model of structures excited by distributed random loads is also presented. Special emphasis is given to marine structures subjected to random pressure loads induced by random ocean waves. Computer programs for performing random vibration analysis developed during the course of this work have been incorporated into the VAST finite element program as a new module called RANVIB. A suite of computer programs for the generation of random loads for ship structures were also developed. Descriptions of all programs together with operational procedures and input data preparation are provided. Example problems illustrating the operation of RANVIB are given. The report also gives some remarks about the capabilities developed and recommendations for future work.

RÉSUMÉ

Le présent rapport décrit les travaux effectués au cours de la première phase d'un contrat attribué par le Centre de recherche pour la défense Atlantique (CRDA) pour la création d'un service interne d'analyse des réponses aléatoires. Une description concise de la base théorique de la méthode d'analyse des vibrations aléatoires par éléments finis est donnée. Une description des méthodes disponibles pour calculer la matrice des densités trans spectrales élaborée pour un modèle aux éléments finis de structures excitées par des charges aléatoires est aussi présentée. L'accent est mis sur les ouvrages marins soumis à des pressions aléatoires exercées par des vagues océaniques aléatoires. Les logiciels d'analyse des vibrations aléatoires, élaborés au cours de ces travaux, ont été incorporés dans le programme aux éléments finis VAST sous fourme d'un nouveau module appelé RANVIB. Une suite de logiciels générant des charges aléatoires pour des constructions navales ont aussi été élaborés. Des descriptions de tous les programmes ainsi que des modes opératoires et du traitement des données d'entrée sont fournies. Des exemples illustrant le fonctionnement de RANVIB sont donnés. Le rapport renferme aussi quelques remarques sur les compétences acquises et des recommandations de travaux futurs.

TABLE OF CONTENTS

	Page
Abstract	
Table of Contents	
List of Figures	
List of Tables	
1.0 INTRODUCTION	1.1
2.0 RANDOM VIBRATION THEORY	2.1
2.1 Classification of Random Processes	2.1
2.2 Introduction to Random Vibration Terminology	2.3
2.3 Stationary Random Vibration Analysis of Linear Systems	2.7
2.3.1 Response of a Single Degree-of-Freedom System	2.9
2.3.2 Response of Multi Degree-of-Freedom Systems	2.11
3.0 RANDOM LOAD DESCRIPTION	3.1
3.1 Wave Loads on Marine Structures	3.1
3.2 Ocean Wave Spectra	3.4
3.3 Determination of Random Pressure Loads	3.11
3.4 Determination of the Cross Spectral Density Matrix of the Applied Loads	3.14
3.4.1 Procedure Implemented in this Work for Random Load Description	3.18
4.0 COMPUTER PROGRAMS FOR RANDOM RESPONSE ANALYSIS	4.1
4.1 Program RANVIB	4.1
4.2 Computer Programs for Random Load Generation	4.12
5.0 GRAPHICS SUPPORT FOR RANDOM VIBRATION ANALYSIS	5.1
6.0 EXAMPLE PROBLEMS	6.1
7.0 CONCLUSIONS AND RECOMMENDATIONS FOR FUTURE WORK	7.1
REFERENCES	
APPENDIX A - Description of Input Data File Preparation for Running Program RANVIB	
APPENDIX B - Input Data for Program PREHPC	

LIST OF FIGURES

FIGURE 4.1 A Flow Diagram Showing Various VAST Modules Required for a Virgin Random Vibration Analysis

FIGURE 4.2 Simplified Flow Diagram of Program RANVIB

FIGURE 4.3 Flow Diagram of Subroutine PRERDM used for Preparing Information for Random Vibration Analysis

FIGURE 4.4 Flow Diagram of Subroutine MODRES for Computing the Cross Spectral Densities and Covariance Matrix of Modal Displacements

FIGURE 4.5 Flow Diagram of Subroutine RANRES which Directs the Computation of the Response Statistics for all Processes

FIGURE 4.6a Flow Diagram for the Computation of the Spectral Densities of Primary Responses in Subroutine POWERS

FIGURE 4.6b Flow Diagram for the Computation of the Spectral Densities of Secondary Responses in Subroutine POWERS

FIGURE 4.7a Flow Diagram for the Computation of the Covariance Matrix of Displacements in Subroutine COVARC

FIGURE 4.7b Flow Diagram for the Computation of the Covariance Matrix of Velocities in Subroutine COVARC

FIGURE 4.7c Flow Diagram for the Computation of the Covariance Matrix of Accelerations in Subroutine COVARC

FIGURE 4.7d Flow Diagram for the Computation of the Covariance Matrix of Stresses in Subroutine COVARC

FIGURE 4.7e Flow Diagram for the Computation of the Covariance Matrix of Strains in Subroutine COVARC

FIGURE 4.8 Flow Diagram of Subroutine CORELA for the Computation of Correlation Functions

FIGURE 4.9 Flow Diagram of Subroutine APFREQ for the Computation of Apparent Frequencies

FIGURE 4.10a Flow Diagram of Subroutine PRNTRR for Printing the Response Results in the VAST Output File (PREFX.LPT)

FIGURE 4.10b Flow Diagram Illustrating the Order in which the Various Response Statistics are Printed out for Each Process

LIST OF FIGURES (Continued)

FIGURE 4.11 Procedure for Generating the Consistent Cross Spectral Density Matrix of the FEM of a Ship whose Hydrodynamic Pressure Transfer Functions are Computed by the HPCFEM Suite of Programs

FIGURE 4.12 Procedure for Generating the PREFX.PSD File for Random Wave Loads

FIGURE 6.1 A Five Bay Beam Excited by Jet Noise

LIST OF TABLES

TABLE 6.1 Natural Frequencies of Five Bay Beam

TABLE 6.2 Power Spectral Densities of Displacements

TABLE 6.3 Power Spectral Density of Modal Forces for the First Mode (SFM(1,1)) at Various Forcing Frequencies

TABLE 6.4A Root Mean Square Displacement Response

TABLE 6.4B Root Mean Square Slope Response

1.0 INTRODUCTION

The fact that uncertainty is inherent in virtually all natural and man-made phenomena is widely accepted. The use of deterministic concepts such as the factor of safety to account for uncertainties associated with some problems is inadequate for the cases in which the level of uncertainty is high or where a high degree of precision is needed to describe system behaviour. The probabilistic approach to system uncertainties provides a very good framework for dealing with this class of problems because it is based on a rational and realistic methodology for dealing with such uncertainties.

In the field of structural dynamics, in particular, considerable efforts have been directed toward the computation of the response of engineering structures subjected to random excitations over the years. This is because many modern structures and their components must be designed to withstand a variety of excitations that are best described as nondeterministic. Such structures include aircrafts flying in gusty atmospheres; high-rise buildings, suspension bridges, and suspended roofs subjected to wind and earthquake loads; aerospace structures and missiles subjected to jet noise excitations; vehicles travelling on rough tracks; ships, submarines and offshore structures subjected to the hostile environment of the confused sea; aircrafts landing on imperfect runways; and heat exchanger tubes subject to turbulent flows.

Primarily, it has been the applications in aerospace engineering which have sped the development of the probabilistic techniques in the area of structural dynamics. However, these techniques are being increasingly accepted and applied for the design and analysis of the integrity of other engineering structures, including ship and offshore structures.

Ocean waves, which constitute major loadings for ships and offshore platforms, are inherently random in terms of both temporal and spatial characteristics. As such, stochastic modelling plays an important role in the design, operation and service of these marine structures. The probabilistic characterizations and determinations of their responses have attracted the attention of scientists and engineers. A number of interesting studies addressing this subject area have been published, see for example [1,2,3].

In realization of the need to adopt a probabilistic approach for the design and structural integrity assessment of Canadian naval ships, the Defence Research Establishment Atlantic (DREA) has decided to provide an in-house capability to perform the required computations. Three important components are required for this capability. First, an adequate description of the random wave loads imparted on the ship structures by the random sea surface elevation is needed. Secondly, the capability to determine the random vibration response to the random excitations in a finite element setting must also be available. Finally, provision must be made for the utilization of the response statistics available in the second capability for the estimation of the reliability of the ship structure. This third and final component is the ultimate goal of any probabilistic approach to design or the assessment of the integrity of an engineering structure.

A two-phase contract was recently awarded to Martec Limited to meet some of the objectives described in the preceding paragraph. In the first phase, a methodology for describing the random pressure loads imparted on ship structures travelling in rough seas with known wave spectra is to be provided. The random loading is to be described in a form suitable for input into the finite element program that will be used for the computation of the random response quantities. Secondly, a random vibration analysis capability is to be provided in the finite element program VAST. In the second phase of the work, a state-of-the-

art literature survey is to be carried out for the purpose of identifying suitable probabilistic methodologies to be adopted for the accurate (fatigue) reliability assessment of naval ships.

The present document represents the final report of the first phase of the contract work. In Chapter 2, a brief introduction to the theory of Random Vibration is given especially the part that is of relevance to the one implemented in the current work. In Chapter 3, a description of the random load generation is presented. A detailed description of the implementation of the random vibration analysis module in VAST called RANVIB is presented in Chapter 4. A description of the set of computer programs developed for the computation of the random wave loads imposed on ship hulls is also given. The provision of a graphics support for the RANVIB module is given in Chapter 5. Example problems used for the verification of program RANVIB and illustrating its use are presented in Chapter 6. Chapter 7 closes the report by giving a few remarks about the work done during the course of this work and some recommendations for additional work that would enhance the versatility of the capabilities that have been provided.

2.0 RANDOM VIBRATION THEORY

The subject of random vibrations is concerned with the application of probabilistic methods for the determination of the response of certain or uncertain systems subjected to dynamic loads that are best described as nondeterministic. As a technical discipline, therefore, random vibration is a combination of structural dynamics and probability theory.

A dynamic excitation representable as a function of time is said to be nondeterministic or random if the function cannot be given any explicit certain description. In other words the variation of the value of the function with time is so irregular and uncertain that it can only be described in a statistical or averaged sense and so the excitation is said to constitute a random process.

If, in addition to randomness in time, there is also spatial randomness, the excitation is referred to as a random field. Thus, the key concepts from probability theory are those of random processes and random fields which are used as stochastic models for excitation and response histories.

2.1 Classification of Random Processes

Based on a statistical regularity classification scheme [4], time-parametered random processes are generally grouped into two main categories: stationary and nonstationary. Analogously, space-parametered random processes are classified as homogeneous or nonhomogeneous.

A stationary process is one in which the statistical behaviour does not vary with time. Its complete probability structure, which for a stochastic process is defined by a system of probability distribution functions, is independent of a shift in the time origin across the ensemble. Thus, the properties of this process can hypothetically be

described at any instant of time by computing average values over the collection of sample functions which describe the random process and they will be found to be time-invariant. For an excitation that can be so classified, its duration is usually relatively long compared with the period of the lowest frequency spectral components of the excited system [5]. Similarly, a random field is said to be homogeneous with respect to a particular spatial coordinate if its probability distributions are invariant with respect to translations of the origin along the axis of that coordinate.

On the other hand, a nonstationary (nonhomogeneous) process is one whose probability distribution functions depend upon the values of time (space) parameters explicitly. In other words, its statistical behaviour depends upon the absolute origin of time (space). Furthermore, a non-stationary (nonhomogeneous) excitation is such that its duration is not much longer than the fundamental time (spatial) period of the system. Nonstationary random processes are in general much more difficult to handle than their stationary counterparts: measurement or description, response prediction, and drawing conclusions about reliability. The majority of disturbances encountered in real-life applications are actually nonstationary by definition. This is because all engineering random process must have a beginning and ending. In many cases, however, it is acceptable to assume a kind of uniformity or regularity for the random field or random process describing such disturbances for the lifetime or piecewise portions thereof. Fortunately, the case of interest in this work falls into the category of problems that can reasonably be assumed to be stationary in time and homogeneous in space. As such, all further discussions of the theory of random vibration will focus on stationary excitations and response computations.

A stationary random process may be further classified as ergodic or non-ergodic. An ergodic process is one in which, in addition to all the ensemble averages being stationary with respect to a change of the time

scale, the averages taken along any single sample are the same as the ensemble averages. In practical terms, each sample function of an ergodic process is completely representative of the ensemble that constitutes the random process. For a non-ergodic stationary process, the averages over a single realization of the random phenomenon cannot be used to describe the ensemble average.

2.2 Introduction to Random Vibration Terminology

For completeness of this report, the definitions of a few Random Vibration terminologies are given in what follows.

Let X(t) represent a random process that is time stationary. The probability distribution function of X(t), denoted $F_X(x)$, is the probability that X assumes a value less than x, i.e.

$$F_X(x) = P(X \leq x) \tag{2.1}$$

In practice it is more convenient to deal with the derivatives of the probability distribution functions, called the probability density functions, $p_X(x)$, defined as:

$$p_X(x) = \frac{dF_X(x)}{dx} \tag{2.2a}$$

Thus, for a process X(t), p(x)dx is the fraction of the total elapsed time for which X(t) lies in the band x to x+dx. Alternatively, equation (2.2a) may be expressed as

$$P(X \leq x) = \int_{-\infty}^{x} p(\epsilon)d\epsilon \tag{2.2b}$$

The expected value of a random variable x is defined as

$$E[X] = \int_{-\infty}^{\infty} x p_X(x) dx \tag{2.3}$$

An expected value is synonymously called an ensemble average (or mean), or statistical average (or mean), or mathematical expectation.

The mean square of X is given by

$$E[X^2] = \int_{-\infty}^{\infty} x^2 p_X(x) dx \tag{2.4}$$

and the variance, σ^2, is given by

$$\sigma^2 = E[(X-E[X])^2] \tag{2.5a}$$

or $$\sigma^2 = E[X^2] - (E[X])^2 \tag{2.5b}$$

The mean and the mean square of a random variable or a random process depend on the first-order probability distribution as can be seen in equations (2.3) and (2.4). These are the most basic and common statistical averages used in the description of random processes. For a zero-mean process, the variance is the same as the mean square value which gives a rudimentary description of the intensity of the random process.

While the probability density function p(x) gives an amplitude domain description of the process, the autocorrelation and power spectral density functions furnish similar information in the time and frequency domains, respectively. If $f(\underset{\sim}{x}_1, t_1)$ is a random field, the space-time correlation function is the ensemble average of the product $f(\underset{\sim}{x}_1, t_1) f(\underset{\sim}{x}_2, t_2)$. In general, this is a function of the two locations and the two times. If

the field is stationary then the correlation is merely dependent on the difference $\tau = t_2 - t_1$ of the two times. Similarly, for a homogeneous process, the correlation depends only on the spatial distance $\underline{x}_2 - \underline{x}_1$.

For a time-stationary process, the autocorrelation function, $R_{xx}(\tau)$ is defined as

$$R_{xx}(\tau) = E[x(t)x(t+\tau)] \tag{2.6a}$$

while the cross-correlation function of two processes x(t) and y(t) is defined as

$$R_{xy}(\tau) = E[x(t)y(t+\tau)] \tag{2.6b}$$

The Fourier transform of the correlation function of a stationary process is called the cross-spectral density function and is mathematically expressed as

$$S_{xy}(\omega) = \frac{1}{2\pi} \int_{-\infty}^{\infty} R_{xy}(\tau)\exp(-i\omega\tau)d\tau \tag{2.7}$$

Thus, when the cross spectral density function is known, the cross correlation function may be readily obtained using the expression:

$$R_{xy}(\tau) = \int_{-\infty}^{\infty} S_{xy}(\omega)\exp(i\omega\tau)d\omega \tag{2.8}$$

Of particular practical significance is that the value of the autocorrelation function evaluated at $\tau=0$ gives the mean square value, i.e.:

$$E[X^2] = R_{xx}(\tau=0) = \int_{-\infty}^{\infty} S_{xx}(\omega)d\omega \tag{2.9}$$

Equation (2.9) represents the area under the graph of power spectrum versus frequency.

The two Fourier transform pairs in (2.7) and (2.8) are the well-known Wiener-Khintchine relations [6,7]. The importance of the correlation and spectral density functions as statistical descriptors of random processes stem from the fact that they provide average amplitude and frequency information about the sample histories. Furthermore, they can be measured with available data-processing techniques; they are mathematically closed with respect to linear time-invariant operations in the sense that if these statistics are known for the excitation, then it is possible to obtain the corresponding statistics for the response of a linear time-invariant dynamic system; and, finally, they often provide adequate information about the response for making vital engineering decisions concerning the severity of the vibration, extent of deformation, and the reliability or safety of the system [8]. Note that definitions of (2.7) and (2.8) vary in that the factor $1/2\pi$ or other factors may be used as a multiplier in Equation (2.8).

The correlation function is a measure of the dependence between two random processes. It also gives information about the frequencies present in a random process indirectly as can be seen by examination of the Wiener-Khintchine relations given above. The time history $x(t)$ of a sample function of a naturally occurring random process is not periodic and so it cannot be represented by a discrete Fourier series. Furthermore, for a stationary process, $x(t)$ goes on forever and the integrability condition

$$\int_{-\infty}^{\infty} |x(t)|dt < \infty \tag{2.10}$$

is not satisfied. This is why the frequency content of a signal is studied either from its autocorrelation function which is amenable to

classical Fourier methods or a truncated version $x_T(t)$ of the random process. Until recently, the first approach just mentioned was the one usually adopted for estimating the spectrum of a discrete time series. However, the second approach is now heavily favoured in modern signal processing and analysis since the development of the Fast Fourier Transform (FFT) which has revolutionized the methodology for performing discrete Fourier transforms. In this latter approach, rather than estimate the spectrum by first determining the autocorrelation function and then calculating the Fourier transform, the spectra are more efficiently and more accurately computed directly from the original time signal. We shall see later that a knowledge of the spectrum of a random excitation is very vital in the application of frequency domain methods for the calculation of random responses to such excitations.

2.3 Stationary Random Vibration Analysis of Linear Systems

Random vibration analysis involves the use of probabilistic methods to perform structural dynamic analysis. The probabilistic description of the random excitation is used to determine the statistical properties of the random response. In general, the response of a linear time-invariant system to a stationary excitation is also stationary. The only exception to this rule is if the system has no damping or is unstable [8]. In the application which is of interest in this work, it is very safe to consider our random response to be stationary because all real-life structures possess some degree of damping and we, of course, assume our structure to be stable.

In conventional vibration or structural dynamics analysis, there are two main techniques for the solution of dynamic problems. In the first technique, the equations of motion are directly integrated using either implicit or explicit time-stepping numerical integration schemes to determine the dynamic response. This technique is popularly referred to as the time domain method. In the second approach, the power of the

Fourier series for period functions or Fourier transforms for nonperiodic functions is applied. The beauty of this approach for linear systems lies in the applicability of the principle of superposition whereby the response of the dynamic system is obtained as the summation of the responses of each of the terms of the Fourier series expansion or the discrete Fourier transform of the excitation function. This latter technique known as the frequency domain approach is particularly attractive for linear systems because the numerical integration involved in the direct method is replaced by finite sums by using the powerful FFT. The frequency domain approach may be further subdivided into the direct frequency response method and the modal frequency response method. Linear dynamic analysis using modal superposition (or the normal-mode method) is computationally inexpensive apart from providing useful insight into the dynamic behaviour of the system. Details of the above methods can be found in any classical textbook on vibrations or structural dynamics.

Similar to conventional vibration analysis, the computation of the stationary random response of a system subjected to stationary random excitation can proceed via a time-domain approach or a frequency-domain approach. The important difference is that the equations of motion (or their Fourier transforms in the case of the frequency-domain approach) are dealt with in a probabilistic sense through the statistical properties of the excitation. In the time-domain case, the auto- and cross-correlation functions represent the description of the applied forces in time while the auto- and cross-spectral densities are the frequency-domain descriptors of the statistical properties of the forces. As was mentioned earlier on, the modern use of the powerful FFT technique has made it possible to directly obtain the spectral densities of random processes. As such, the application of a frequency-domain approach to the random response analysis of linear structures subjected to stationary loads is very attractive.

2.3.1 Response of a Single Degree-of-Freedom System

Consider a single degree-of-freedom (SDF) system comprising of mass m, viscous damping coefficient c, stiffness k, and whose motion is governed by the equation:

$$m\ddot{x} + c\dot{x} + kx = F(t) \tag{2.11}$$

where $F(t)$ is the stationary random force applied to the mass, $x=x(t)$ is the corresponding stationary random displacement response, $\dot{x}(t)$ is the velocity and $\ddot{x}(t)$ is the acceleration. Let $\bar{F}(i\omega)$ denote the Fourier transform of $F(t)$ and $\bar{X}(i\omega)$ denote the Fourier transform of $x(t)$. Taking the Fourier transform of both sides of Equation (2.11) gives:

$$(-\omega^2 m + i\omega c + k)\bar{X}(i\omega) = \bar{F}(i\omega) \tag{2.12a}$$

or $$\bar{X}(i\omega) = (k - \omega^2 m + i\omega c)^{-1}\, \bar{F}(i\omega) \tag{2.12b}$$

or $$\bar{X}(i\omega) = H(i\omega)\bar{F}(i\omega) \tag{2.12c}$$

where

$$H(i\omega) = (k - \omega^2 m + i\omega c)^{-1} \tag{2.12d}$$

is the well-known complex frequency response function or receptance of the system.

If the random function $F(t)$ is truncated so that it becomes zero outside the interval $(-T,+T)$ to give a new function $F_T(t)$, then the power spectral density of $F(t)$ can be expressed in the form [9]

$$S_{FF}(\omega) = \lim_{T\to\infty} \frac{\pi}{T} \left|[\bar{F}_T(i\omega)]\right|^2 \tag{2.13a}$$

$$S_{FF}(\omega) = \lim_{T\to\infty} \frac{\pi}{T} [\bar{F}_T(i\omega)] \cdot [\bar{F}_T^*(i\omega)] \tag{2.13b}$$

where $\bar{F}_T^*(i\omega)$ is the complex conjugate of $\bar{F}_T(i\omega)$. Henceforth, $\bar{F}_T(i\omega)$ and

$\bar{X}_T(i\omega)$ will be used interchangeably with $\bar{F}(i\omega)$ and $\bar{X}(i\omega)$ respectively. In other words, Equation (2.13b) may also be written as:

$$S_{FF}(\omega) = \lim_{T\to\infty} \frac{\pi}{T} [\bar{F}(i\omega)][\bar{F}^*(i\omega)] \tag{2.14}$$

In a similar manner, the power spectrum of x(t) may be expressed as

$$S_{XX}(\omega) = \lim_{T\to\infty} \frac{\pi}{T} [\bar{X}(i\omega)][\bar{X}^*(i\omega)] \tag{2.15}$$

Substituting the expression for $\bar{X}(i\omega)$ (equation (2.12c)) into Equation (2.17) gives

$$S_{XX}(\omega) = \lim_{T\to\infty} \frac{\pi}{T} [H(i\omega)\bar{F}(i\omega)][H(i\omega)\bar{F}(i\omega)]^* \tag{2.16a}$$

or $$S_{XX}(\omega) = H(i\omega) \cdot \lim_{T\to\infty} \{\frac{\pi}{T} [\bar{F}(i\omega)][\bar{F}^*(i\omega)]\} \cdot H^*(i\omega) \tag{2.16b}$$

Invoking the definition of $S_{FF}(\omega)$ as given by equation (2.14) in equation (2.16b) gives

$$S_{XX}(\omega) = H(i\omega) \cdot S_{FF}(\omega) \cdot H^*(i\omega) \tag{2.17a}$$

or $$S_{XX}(\omega) = |H(i\omega)|^2 \cdot S_{FF}(\omega) \tag{2.17b}$$

Equation (2.17a) or (2.17b) gives the all-important fundamental relationship between the power spectral density of the forcing function and that of the corresponding response for a single input-single output system. The implication of this relationship is that the statistical properties of the response can be determined from those of the input provided the system frequency response function is known. The mean value can also be shown to be given by [8]:

$$E[X(t)] = H(0)E[\bar{F}(t)] \tag{2.18}$$

It is pertinent to point out that the relations (2.17) and (2.18) are independent of the probability distributions involved.

2.3.2 Response of Multi Degree-of-Freedom Systems

The results derived for the single degree-of-freedom system in the preceding subsection extend formally to multiple input-multiple output time-invariant linear systems and so can be readily applied to discrete multi degree-of-freedom systems or continuous structures discretized by a numerical technique such as the finite element method.

The governing equation of motion of a continuous structure discretized by the finite element method is of the form:

$$\underline{M}\underset{\sim}{\ddot{X}} + \underline{C}\underset{\sim}{\dot{X}} + \underline{K}\underset{\sim}{X} = \underset{\sim}{F}(t) \qquad (2.21)$$

In Equation (2.21), $\underline{M}$ is the assembled mass matrix, $\underline{C}$ is the damping matrix, $\underline{K}$ is the assembled stiffness matrix, $\underset{\sim}{X}(t)$ is the vector displacement response to the vector excitation $\underset{\sim}{F}(t)$, $\underset{\sim}{\dot{X}}(t)$ is the random velocity vector, and $\underset{\sim}{\ddot{X}}(t)$ is the random acceleration vector. For our present interest, it is assumed that the system parameters $\underline{M}$, $\underline{C}$, and $\underline{K}$ are known deterministic quantities thereby leaving $\underline{F}(t)$ the only random input for which the random output $\underset{\sim}{X}(t)$ is sought. For a structure discretized in this mannner with a total of NS global degrees of freedom, $\underline{M}$, $\underline{C}$, and $\underline{K}$ are (NSxNS) square matrices while both $\underset{\sim}{X}$ and $\underset{\sim}{F}$ are vectors with NS components.

It can be shown, in a manner similar to the single degree-of-freedom case, that the cross-spectral density of the vector random displacement reponse is related to that of the vector random force excitation via the expression

$$[S_{XX}(\omega)] = [H(i\omega)][S_{FF}(\omega)][H(i\omega)]^{T*} \tag{2.22}$$

where, now, $[S_{FF}(\omega)]$ and $[S_{XX}(\omega)]$ are matrices of excitation and response spectra including auto- and cross-spectral density functions, and $[H(i\omega)]$ is the complex frequency response function matrix corresponding to Equation (2.21). On taking the Fourier transform of both sides of Equation (2.21), it is easy to see that $[H(i\omega)]$ is given by

$$[H(i\omega)] = [\underline{K} - \omega^2\underline{M} + i\omega\underline{C}]^{-1} \tag{2.23}$$

The procedure for computing $[S_{XX}(\omega)]$ by using Equations (2.22) and (2.23) involves an inversion of the matrix shown on the right hand side of Equation (2.23) at each discrete frequency and is known as the direct frequency response method of analysis. The inversion of this usually large and complex matrix is computationally intensive even with the use of conventional elimination procedures [9].

An attractive alternative to using a direct analysis is to use the normal mode approach mentioned earlier on. In the application of this method, it is first required to perform an eigenvalue analysis of the structural system to determine its natural frequencies and mode shapes. The orthonormalized mode shapes or eigenvectors are used to form a modal transformation matrix $\underline{R}$ which is used to uncouple the system of equations of motion into normal modes or generalized coordinates. The main advantage gained by dealing with the uncoupled equations is that the complex frequency response function matrix is now a diagonal matrix and hence the determination of its inverse for use in the relation (2.22) becomes a trivial computational operation. The only price paid is that the modal response obtained must be transformed back to the original global degrees of freedom of the finite element model of the structure. A restriction of the normal mode procedure is that the damping matrix must be such that the same transformation matrix $\underline{R}$ that diagonalizes the mass and

stiffness matrices will do the same for the damping matrix. For this to be so, the damping matrix must be some form of a linear combination of the mass and stiffness matrices. This is known as Rayleigh or proportional damping and is considered to be an adequate representation of the damping in many structural applications. It is also common practice to assume a modal damping ratio for each of the vibration modes used for the response computations. Another disadvantage of the modal method is that only some of the modes are used in the computation of the responses and in some cases the omitted modes could contribute significantly to the response even though their frequencies lie outside the range of the exciting forces [9]. This problem can be overcome by using the residual flexibility method which is not implemented in this work. In spite of these shortcomings, the normal mode approach provides an elegant, powerful, and cost effective method for dealing with the random response of discretized structures. As such, it has been popularly applied in research studies and commercial finite element programs [10,11,12].

Consider, once again, the discretized matrix equation of motion given in (2.21). The natural frequencies (ω_r) and mode shapes (ϕ_r) of the system are first computed to determine [R] using $\underline{M}$ and $\underline{K}$ which are determined by the finite element program. Next, the assembled cross-spectral density matrix $[S_{FF}(\omega)]$ must be determined as a function of the forcing frequencies of interest from the user specified auto- and cross-spectral densities of the applied point loads and/or distributed loads.

Let a transformation between the global degrees of freedom $\underset{\sim}{X}$ of the finite element model and the NM modal (generalzed) coordinates $\underset{\sim}{q}$ be defined such that

$$\underset{\sim}{X} = \underline{R}\ \underset{\sim}{q} \tag{2.22}$$

where $\underline{R}$ is the mass-orthonormalized modal matrix described earlier. Substituting the transformation relation (2.22) in (2.21) and pre-multiplying both sides of the latter by the transpose ($\underline{R}^T$) of $\underline{R}$ gives:

$$\underline{R}^T \underline{M} \underline{R} \underset{\sim}{\ddot{q}} + \underline{R}^T \underline{C} \underline{R} \underset{\sim}{\dot{q}} + \underline{R}^T \underline{K} \underline{R} \underset{\sim}{q} = \underline{R}^T \underset{\sim}{F}(t) \tag{2.23}$$

in which the nature of $\underline{R}$ is such that

$$\underline{R}^T \underline{M} \underline{R} = \underline{I} \tag{2.24a}$$

$$\underline{R}^T \underline{C} \underline{R} = [2\xi_r \omega_r] \tag{2.24b}$$

$$\underline{R}^T \underline{K} \underline{R} = [\omega_r^2] \tag{2.24c}$$

$$\underset{\sim}{f}_r(t) = \underline{R}^T \underset{\sim}{F}(t) \tag{2.24d}$$

$$\underline{R} = [R] = [\{\phi_1\} \{\phi_2\} \cdots \{\phi_{NM}\}] \tag{2.24e}$$

In the above, $\underline{I}$ is the (NMxNM) identity matrix, $[2\xi_r \omega_r]$ and $[\omega_r^2]$ are (NMxNM) diagonal matrices in which ξ_r is the equivalent modal damping for the rth mode, ω_r is the natural frequency corresponding to mode r out of a possible total number of NM modes, $\underset{\sim}{f}_r(t)$ is the random modal force, and $\{\phi_r\}$, r=1,2,...,NM, are the eigenvectors of the NM modes. Thus, Equation (2.23) may be alternatively written as

$$\underline{I} \underset{\sim}{\ddot{q}}_r + [2\xi_r \omega_r] \underset{\sim}{\dot{q}}_r + [\omega_r{}^2] \underset{\sim}{q}_r = \underset{\sim}{f}_r(t), \quad r=1,2,...NM. \tag{2.25}$$

In the normal mode procedure adopted in this work, we shall solve Equation (2.25) in a probabilistic sense to obtain the random modal displacement response and convert back to the response referred to the original degrees of freedom using the transformation relation defined in (2.22). This is because the uncoupled set of Equations (2.25) is easier to handle than the original Equation (2.21) because of reasons we have previously described.

The first step is to determine the cross spectral density matrix of the modal force $[S_{ff}(\omega)]$ from the cross spectral density matrix of the applied force referred to the original global degrees of freedom using the relation:

$$\underset{(NMxNM)}{[S_{ff}(\omega)]} = \underset{(NMxNS)}{[R]^T} \underset{(NSxNS)}{[S_{FF}(\omega)]} \underset{(NSxNM)}{[R]} \tag{2.26}$$

This relation follows directly from the linear transformation relation between f(t) and F(t) defined in Equation (2.24d). An important property of cross spectral density matrices of real processes is that they are Hermitian, that is,

$$[S_{FF}(\omega)] = [S_{FF}(\omega)]^{T*} \tag{2.27a}$$

or

$$S_{FF}^{ij}(\omega) = S_{FF}^{ji*}(\omega) \tag{2.27b}$$

The Hermitian property of complex matrices is a generalization of the symmetry property of real matrices. Thus the cross-spectral density of the input excitation to the modal system described in Equation (2.25) is now known.

The second step is to compute the cross-spectral density of the modal displacement response in Equation (2.25) using the complex frequency response functions of this modal system and the input-output relations expressed in (2.22). Thus, the cross-spectral density of the random modal displacement response is given by

$$[S_{qq}(\omega)] = [H(i\omega)]\,[S_{ff}(\omega)]\,[H(i\omega)]^{T*} \tag{2.28}$$

Equation (2.28) represents the frequency-domain probabilistic description of the solution to the modal system of Equations (2.25). We emphasize, once again, that the computational advantage of solving Equation (2.25) instead of (2.21) lies in the fact that the complex frequency response function in (2.28) is a diagonal matrix thus making it easier to deal with. The frequency response function $[H(i\omega)]$ matrix is computed according to the type of damping used.

For the present work, the damping is classified into three categories. The first type of damping requires the specification of the damping ratio ξ_r, for each mode r of the NM modes involved. This is a ratio of viscous damping to the critical damping. Denoting, the element (r,r) of the diagonal matrix $[H(i\omega)]$ by $H_{rr}(i\omega)$, then for this type of modal damping for any forcing frequency ω

$$H_{rr}(i\omega) = \{(\omega_r^2 - \omega^2) + (2\xi_r\omega_r\omega)i\}^{-1} \tag{2.29a}$$

The second type of damping is the proportional damping or Rayleigh damping described earlier. For this case, the damping matrix is assumed to be of the form

$$\underline{C} = \alpha_M\underline{M} + \alpha_K\underline{K} \tag{2.29b}$$

where α_M and α_K are real constants.

For this case, $H_{rr}(i\omega)$ is given by

$$H_{rr}(i\omega) = \{(\omega_r^2-\omega^2) + (\alpha_M+\alpha_K\omega_r^2)\ \omega i\}^{-1} \tag{2.29c}$$

The third type of damping option is structural damping for which the damping force is represented as a complex stiffness term in the form:

$$\underset{\sim}{C}\dot{\underset{\sim}{X}} = ig\underset{\sim}{K}\underset{\sim}{X} \tag{2.29d}$$

where g is the structural damping factor.

Unlike modal damping and Rayleigh damping, structural damping is a non-viscous form of damping that is usually employed for modelling internal energy dissipation per cycle (due to internal friction) for structures. Thus, for this third case, $H_{rr}(i\omega)$ is given by:

$$H_{rr}(i\omega) = \left\{(\omega_r^2-\omega^2) + (g\omega_r^2)i\right\}^{-1} \tag{2.29e}$$

All these three damping options have been implemented with the user defining his/her choice by means of the parameter IDAMP which may assume values of 1, 2, or 3.

The final step is the transformation of the cross-spectral density of the modal response to the displacement response referred to the original global degrees of freedom, using the relation:

$$\underset{(NSxNS)}{[S_{xx}(\omega)]} = \underset{(NSxNM)}{[R]}\ \underset{(NMxNM)}{[S_{qq}(\omega)]}\ \underset{(NMxNS)}{[R]^T} \tag{2.30}$$

Again, Equation (2.30) is a direct consequence of the linear transformation relation between $\underset{\sim}{X}$ and $\underset{\sim}{q}$ defined by the expression (2.22). All the spectral density matrices in (2.28) and (2.30) satisfy the same Hermitian property described in (2.27). Thus, Equation (2.30) is the frequency-domain probabilistic description of the random displacement response. Formally, a knowledge of the cross-spectral density matrix of the displacements completes the solution process. However, in practice, a knowledge of other statistical properties of displacements or those of other related processes are usually of interest. These related processes

include derivative processes such as velocities and accelerations and secondary processes such as stresses and strains that are directly (linearly) related to displacements.

The cross-spectral densities of velocities and accelerations can be obtained from those of displacements by using the property of derived processes. Denoting the cross spectral density matrices of velocites and accelerations as $[S_{VV}(\omega)]$ and $[S_{AA}(\omega)]$ respectively, then the following relations are used for their computation:

$$[S_{VV}(\omega)] = \omega^2[S_{XX}(\omega)] \tag{2.31}$$

$$[S_{AA}(\omega)] = \omega^4[S_{XX}(\omega)] \tag{2.32}$$

For stresses and strains (referred to as secondary responses in this work) the procedure is not as straightforward as those given in equation (2.31) and (2.32) above. This is because neither the stress nor the strain is a time derivative of the displacement. Although, for linear finite element analysis, the stresses and strains are related to displacements through a linear transformation, some additional effort is required for the determination of the transformation matrices. Once these transformation matrices are determined, the rule used for the computation of the cross-spectral densities of modal force from those of the global nodal forces can then be applied.

Let [T] be the transformation matrix relating the stress $\{\sigma\}$ at a given set of points to the modal displacements $\{q\}$ and let [W] be the corresponding matrix for the strains $\{\epsilon\}$. Then

$$\{\sigma\} = [T]\{q\} \tag{2.33}$$

and

$$\{\epsilon\} = [W]\{q\} \tag{2.34}$$

A typical component T_{ij} of the matrix [T] represents the stress at point i due to a normalized oscillation in the oscillation mode j. In other words, therefore, [T] is the modal stress transformation matrix corresponding to the points and stress components of interest in the structure. The same goes for the definition of the components of [W]. Comparing Equations (2.33) and (2.34) with the transformation relation (2.22), it is easy to see that the [T] and [W] play the same role for stresses and strains as the modal matrix [R] does for displacements. Once [T] and [W] have been determined, the cross spectral density matrices of stresses and strains are obtained from the relations:

$$[S_{\sigma\sigma}(\omega)] = [T]\,[S_{qq}(\omega)]\,[T]^T \tag{2.35}$$

and

$$[S_{\epsilon\epsilon}(\omega)] = [W]\,[S_{qq}(\omega)]\,[W]^T \tag{2.36}$$

With Equations (2.30), (2.31), (2.32), (2.35), and (2.36), the cross spectral densities of any of the random response quantities that may potentially be of interest in a random vibration analysis may be computed. However, in practical applications, other statistical properties of the random responses may be additionally required or indeed preferred to the cross spectral densities. In what follows, a brief description of these other properties are presented.

Let $X_1=X_1(t)$ and $X_2=X_2(t)$ be two random processes or components of a random vector process. The covariance of X_1 and X_2 denoted $Cov(X_1X_2)$ or $C_{X_1X_2}$ is defined as

$$Cov(X_1X_2) = C_{X_1X_2} = E[[X_1(t) - \mu_1(t)]\bullet[X_2(t) - \mu_2(t)]] \tag{2.37}$$

where μ_1 and μ_2 are the mean values of X_1 and X_2 respectively and the

operator E denotes the mathematical expectation defined earlier on. For zero values of μ_1 and μ_2,

$$C_{X_1X_2} = E[X_1X_2] \tag{2.38a}$$

and for the special case where X_1 and X_2 are the same random process (i.e. $X_1(t) = X_2(t)$), then

$$C_{X_1X_2} = C_{X_1X_1} = E[X_1X_1] = E[X_1^2] \tag{2.38b}$$

Thus, the covariance of X_1 and itself usually called the autocovariance (or simply variance) of X_1 is nothing but the mean square value of X_1 provided X_1 is a zero-mean process which we assume throughout this work. Let {y} be a random vector process of order n. Then the covariance of {y} is an nxn matrix defined as

$$[C_{yy}] = E[\{y\}\bullet\{y\}^T] \tag{2.39a}$$

or

$$[C_{yy}] = \begin{bmatrix} E[y_1^2] & E[y_1y_2] & \cdots & E[y_1y_n] \\ & E[y_2^2] & & \\ \text{Sym.} & & & \\ & & & E[y_n^2] \end{bmatrix} \tag{2.39b}$$

It can be seen from Equation (2.39b) that for zero-mean processes, the diagonal terms of the covariance matrix give the mean square responses.

The cross and auto correlation functions are related to the cross and auto spectral density functions through the well-known Wiener-

Khintchine relations which were presented earlier (Equations (2.7) and (2.8)). The cross-correlation function between x and y is given by

$$R_{xy}(\tau) = \int_0^\infty S_{xy}(\omega)e^{i\omega\tau}\, d\omega \tag{2.40}$$

Thus, with a knowledge of $S_{xy}(\omega)$, $R_{xy}(\tau)$ may be computed by taking the inverse discrete Fourier transform (DFT) of $S_{xy}(\omega)$ using the FFT algorithm. For auto-correlation functions, in particular

$$R_{xx}(\tau) = \int_{-\infty}^{\infty} S_{xx}(\omega)\, e^{i\omega\tau} d\omega = 2\int_0^\infty S_{xx}(\omega)\, \cos\,\omega\tau\, d\omega \tag{2.41a}$$

or

$$R_{xx}(\tau) = \int_{-\infty}^{\infty} G_{xx}(\omega)\, \cos\,\omega\tau\, dw \tag{2.41b}$$

where

$$G_{xx}(\omega) = 2S_{xx}(\omega) \tag{2.41c}$$

is called the one-sided power spectral density which has zero values for negative values of the circular frequency, ω.

Recalling that

$$E[x^2] = R_{xx}(\tau)\big|_{\tau=0} = R_{xx}(0) \tag{2.42a}$$

it is easy to see from (2.41) that

$$E[x^2] = \int_{-\infty}^{\infty} S_{xx}(\omega)d\omega = 2\int_0^\infty S_{xx}(\omega)\, d\omega \tag{2.42b}$$

Similarly, since $E[x(t)y(t+\tau)] = R_{xy}(\tau)$, and

$$R_{xy}(\tau)\big|_{\tau=0} = E[x(t)y(t)] = Cov(xy) = C_{xy} \tag{2.43a}$$

it follows that

$$E[xy] = \int_{-\infty}^{\infty} S_{xy}(\omega)\, d\omega = 2\int_{0}^{\infty} S_{xy}(\omega)\, d\omega = \int_{0}^{\infty} G_{xy}(\omega)\, d\omega \tag{2.43b}$$

Thus, the off-diagonal terms of the covariance matrix defined in (2.39b) may be computed from the cross-spectral densities using (2.43) while the diagonal terms may be computed from the auto spectral densities using (2.42). The diagonal terms popularly referred to as the variances or mean square responses are often of interest while off-diagonal terms may also be of interest in reliability studies.

The above procedures for calculating the covariances of the responses is straightforward. However, it is time-consuming from a computational implementation point of view.

Let us consider a random vector process {y} that is related to another random vector process {z} through a linear transformation matrix [T] such that

$$\{z\} = [T]\{y\} \tag{2.44}$$

The cross spectral density matrices of {z} and {y} are related through

$$[S_z(\omega)] = [T][S_y(\omega)][T]^T \tag{2.45}$$

Similarly, the covariance matrix of {z} and {y} are related via the expressions

$$[C_z] = [T][C_y][T]^T \tag{2.46}$$

Suppose the cross spectral density $[S_y(\omega)]$ of $\{y\}$ is known and the covariance of $\{z\}$ is to be computed. Then two alternative approaches are available. In the first, $[S_z(\omega)]$ is computed for all the applied frequencies using the relation (2.45). Then $[C_z]$ is determined by using the matrix form of the relation (2.43), namely

$$[C_z] = 2\int_0^\infty [S_z(\omega)]\, d\omega \tag{2.47}$$

In the second approach, the covariance matrix $[C_y]$ of $\{y\}$ is computed using the relation

$$[C_y] = 2\int_0^\infty [S_y(\omega)]\, d\omega \tag{2.48}$$

and then the covariance matrix of $\{z\}$ is computed using equation (2.46).

It can be seen that the first approach involves the calculation of the triple matrix product on the right hand side of (2.45) for each of the applied forcing frequencies. For a total number of NAF applied frequencies, therefore, the triple matrix product has to be evaluated NAF times and so the procedure is computationally intensive. In the second approach, however, the integration in Equation (2.48) is first performed and then the triple matrix product in (2.46) is evaluated only once. Thus, the first approach involves one numerical integration and NAF evaluations of a triple matrix product while the second involves one numerical integration and the evaluation of only one triple matrix product. The second approach is much more preferred, especially when the structural model size is large or when there are more than a few forcing

frequencies because of the significant savings in computation time. The only situation in which the first procedure would be preferable, of course, is when the cross spectral density $[S_Z(\omega)]$ has been previously computed or is otherwise known.

In terms of the response quantities of interest in this work, the above discussion of the computation of covariances of responses translates to the following. For displacements, for example, if the spectral densities are not of interest but say the mean squares are, then they are best computed by first computing the covariance matrix of modal displacements from the corresponding cross spectral density matrix, that is

$$[C_{qq}] = 2\int_0^\infty [S_{qq}(\omega)]\, d\omega \tag{2.49}$$

It will be recalled that $[S_{qq}(\omega)]$ has been previously computed as the second step in the random response analysis, Equation (2.28). Then the covariance matrix of displacements $[C_{xx}]$ is computed from

$$[C_{xx}] = [R][C_{qq}][R]^T \tag{2.50}$$

The diagonal terms of $[C_{xx}]$ represent the mean square displacements. Similar procedures apply to other response quantities. For example, for stresses, the covariance matrix is computed from the relation

$$[C_{\sigma\sigma}] = [T][C_{qq}][T]^T \tag{2.51}$$

and the diagonal terms of $[C_{\sigma\sigma}]$ give the mean square stresses. Higher order spectral moments of any of the random response quantities may also be computed by using the cost effective second approach. This was used, for example, by Karadeniz et al [13] for the spectral analysis of the

probabilistic reliability analysis of the fatigue limit state of gravity and jacket-type structures.

The mean square response is a very important statistical property because it can be used for calculating the probability of failure (and hence the reliability) of a structural system once the probability density function of the random response process is known. It is an interesting fact of life that many naturally occurring random vibrations have the well-known "bell-shaped" probability distribution function known as the normal or Gaussian probability distribution. Accordingly, a random process that possesses this type of distribution is known as a Gaussian process. An important property of linear time-invariant systems excited by Gaussian random process is that the resulting response is also Gaussian and hence possesses the same probability density function as the excitation. The probability density function of the random process x has the form

$$p(x) = \frac{1}{\sqrt{2\pi}\,\sigma} \exp\left[-(x-m)^2/2\sigma^2\right] \tag{2.52}$$

where m is the mean $E[x]$ and σ^2 is the variance $E[(x-E[x])^2]$. The normal distribution function is completely characterized by the two parameters m and σ^2. For a zero-mean process (i.e. for m=0), σ^2 is the same as the mean square. Thus the mean square value of x can be used to compute the probability that x=x(t) will lie in a certain interval (say $x_1(t)$ and $x_2(t)$) using the relation

$$\text{Prob}[x_1 \leq x(t) \leq x_2] = P(x_2) - P(x_1) = \int_{x_1}^{x_2} p(x)dx \tag{2.53}$$

Note that in equation (2.53), $P(x_i)$ denotes the probability that x=x(t) will not exceed the value x_i, that is,

$$\text{Prob}[x(t) \leq x_i] = \int_{-\infty}^{x_i} p(x)dx \tag{2.54}$$

Thus, if, for example, failure is assumed to occur if x=x(t) goes outside the range $x_1 \leq x(t) \leq x_2$, then from (2.53), the probability of failure is 1 - Prob $[x_1 \leq x(t) \leq x_2]$. Consequently, the reliability is 1 - (probability of failure) = Prob$[x_1 \leq x(t) \leq x_2]$. If failure is assumed to occur if x=x(t) exceeds a critical value x_i, say, then the probability of failure is Prob$[x(t) > x_i]$ = 1 - Prob$[x(t) \leq x_i]$ which is readily obtained from (2.54). In this case, the reliability is Prob$[x(t) \leq x_i]$ because the reliability, r, is always related to the probability of failure, p_f, through

$$r = 1 - p_f \tag{2.55}$$

For the cases where there are two or more random variables or for vector-valued random processes such as we have in the analysis of multi-degree-of-freedom systems, the first-order probability density function is no longer sufficient to describe the probability structure of the Gaussian process. A full definition of the multi-dimensional Gaussian distribution must include, not only the first-order probability density function given by (2.52), but also corresponding second and higher order joint densities. For the case of two jointly Gaussian random variables x and y, for example, the second-order probability density function is [5]:

$$p(x,y) = \frac{1}{2\pi\sigma_x\sigma_y\sqrt{(1-\rho^2_{xy})}}\, e^{-\frac{1}{2(1-\rho^2_{xy})}\left\{\frac{(x-m_x)^2}{\sigma^2_x} + \frac{(y-m_y)^2}{\sigma^2_y} - \frac{2\rho_{xy}(x-m_x)(y-m_y)}{\sigma_x\sigma_y}\right\}} \tag{2.56}$$

where m_x and m_y are the mean values of x, and y, σ^2_x and σ^2_y are the variances of x and y and ρ_{xy} is a correlation coefficient defined as

$$\rho_{xy} = \frac{E[(x-m_x)(y-m_y)]}{\sigma_x \sigma_y} \tag{2.57}$$

and called the normalized covariance. Notice that if $\rho_{xy} = 0$, x and y are statistically independent because then (2.56) may be factorized to give

$$p(x,y) = \left[\frac{1}{\sqrt{2\pi}\sigma_x} e^{-(x-m_x^2/2\sigma_x^2)}\right] \cdot \left[\frac{1}{\sqrt{2\pi}\sigma_y} e^{-(y-m_y^2/2\sigma_y^2)}\right]$$

$$= p(x) \cdot p(y) \tag{2.58}$$

The numerator of the right hand side of Equation (2.57), it will be recalled, is a typical term of the covariance matrix of x and y. It represents an off-diagonal term for $x \neq y$ and a diagonal term for $x=y$. Thus it can be seen that the off-diagonal elements of the covariance matrix are also important in the application of higher order joint densities for the computation of failure probabilities or in reliability analysis. Zero-valued off-diagonal terms of the covariance matrix correspond to zero correlation and the higher-order joint density functions become simply the products of the first-order density functions as in (2.58). However, for MDF system excited by random excitations it is not uncommon for the off-diagonal terms to take on non-zero values because the response process is actually a vector random process in which the components are like correlated random variables. This is the motivation for including the capability for the computation of cross spectral densities and cross terms of the covariances of responses in this work. It is hoped that future work involving the application of advanced reliability analysis techniques will benefit immensely from the broad framework that has been established during the course of this first phase of the contract.

Another statistical property of response that is usually of interest in probability structural dynamics is the apparent frequency or the

expected (or effective) equivalent frequency. This is defined as the expected value of the number of zero crossings with positive slope per unit time denoted N_o or $E[N+(o)]$. For a random process $x=x(t)$ whose corresponding time-derivative process is $x=x(t)$, it is mathematically defined as:

$$N_o = E[N+(o)] = \frac{1}{2\pi}\frac{\sigma_x}{\sigma_x} \tag{2.59}$$

where σ_x is the variance of x and σ_x is the variance of the corresponding rate process [14]. For a zero mean process then

$$N_o = \frac{1}{2\pi}\left[\frac{\int_{-\infty}^{\infty} \omega^2 S_{xx}(\omega)\, d\omega}{\int_{-\infty}^{\infty} S_{xx}(\omega)\, d\omega}\right]^{1/2} \tag{2.60}$$

In the relation (2.60), $S_{xx}(\omega)$ is the auto spectral density of x and so it is easy to see that the denominator is the mean square of x while the numerator is the mean square of $\dot{x}$. In view of the discussions previously given concerning the efficient computation of mean square responses, a knowledge of the spectral density of x is not essential in the computation of its apparent frequency. Both the denominator and the numerator in (2.60) can be computed directly from the covariances of the modal displacements and modal velocities respectively. The apparent frequency is very useful in fatigue analysis and so the capability for computing this statistical property for any of the possible physical processes has been provided in this work.

3.0 RANDOM LOAD DESCRIPTION

The analysis procedure presented in the preceding chapter is based on the assumption that the cross spectral density matrix of the applied forces referred to the original global degrees of freedom of the finite element model is available. However, this is not the case in practice. Although the user defines the spectra and/or cross spectra of the point loads and/or distributed (i.e. pressure) loads acting on the structure, a procedure is required for calculating the consistent assembled cross spectral density matrix of the system due to all the applied random loads in a finite element setting. This operation is analogous to the computation of the assembled consistent load vector in a conventional deterministic analysis using the finite element method.

The primary goal of the present work is the development of the capability for the random response analysis of naval structures travelling in rough seas so that more accurate and realistic predictions of the integrity and safety of such structures can be made by the scientific authority. Accordingly, the main source of loading that must be dealt with is the random pressure loading imparted onto the hull structure due to the action of the random ocean waves. This form of loading represents the most significant time-varying loads experienced by marine structures [15]. Since the adequate description of the loading is one of the fundamental steps involved in the analysis of any engineering structure, the development of a procedure to appropriately describe the loading in the framework of a probabilistic finite element methodology is a very important component of the work presented in this report.

3.1 Wave Loads on Marine Structures

The computation of hydrodynamic wave forces on marine structures is a difficult task because it involves the complexity of the interaction of waves with the structure. The two approaches commonly used may be

broadly classified into deterministic and statistical. Although the statistical approach is the one of interest in this work, it is quite appropriate to give a brief overview of the essential ingredients of each of the two approaches because the statistical approach is not completely independent of the deterministic one. This interdependence will become evident as we progress in this report.

In a deterministic approach, an appropriate wave theory for describing the water particle kinematics for the given wave condition is selected and the hydrodynamic forces are determined. The three different methods for this class of approach include the Morison equation, the Froude-Krylov theory, and the diffraction (or potential flow) theory [16]. The Morison equation assumes the force to be a linear combination of inertia and drag forces. The inertia and drag components of the force involve coefficients which are determined experimentally. The Morison equation is very suitable for describing the hydrodynamic loading on slender structures since the drag force is significant for such applications. For example, the in-line force per unit length (p) on a vertical slender cylinder in unsteady flow may be represented in the form [16]:

$$p = C_d \rho \frac{D}{2} u_n |u_n| + C_m \rho \pi \frac{D^2}{4} \dot{u}_n \qquad (3.1)$$

where ρ is the water density, D is the diameter, u_n and $\dot{u}_n$ are the water particle velocity and acceleration, respectively, and C_d and C_m are the drag and inertia coefficients, respectively.

For situations in which the drag force is small and the inertia force predominates, but the structure is still relatively small compared to the water wave length, the Froude-Krylov theory may be applied. This method utilizes the incident wave pressure and the pressure-area method on the surface of the structure to compute the force. Because the calculation of the force on the structure is performed assuming that the structure is not there as far as the waves are concerned, this approach

has limited practical applications. The merit of the method lies in its simplicity and the possibility of closed-form force solutions for some symmetric structures.

For large structures, the characteristic dimension of the structure becomes comparable to the wave length and so the presence of the structure is expected to alter the wave field in the vicinity of the structure. If the structure spans a significant portion of a wave length, the incident waves upon arriving at the structure undergo significant scattering or diffraction. Therefore, the diffraction of the waves from the surface of the structure should be taken into account in the evaluation of the wave forces. This method is generally known as the diffraction theory. The solution involves the numerical solution of the Laplace equation together with the associated boundary conditions, namely:

$$\nabla^2\Phi = \frac{\partial^2\Phi}{\partial x^2} + \frac{\partial^2\Phi}{\partial y^2} + \frac{\partial^2\Phi}{\partial z^2} = 0 \qquad (3.2)$$

Equation (3.2) assumes the basic flow to be oscillatory, incompressible, and irrotational so that the fluid velocity may be represented as the gradient of a scalar potential, $\Phi = \Phi(x,y,z,t)$. Details of this and other theories are very well elaborated upon in the monograph by Chakrabarti [16].

The second approach to the characterization of loads induced by ocean waves is the utilization of statistical description techniques. This approach is considered more realistic in view of the fact that real sea surface profiles are, more often than not, highly irregular and confused in nature, and nonrepeatable in time and space. In this approach, the ocean waves and hence the associated sea surface profiles are considered to be random. The surface elevation, η, is considered to be a random process which is described by either its probabilistic properties

(such as the cummulative distribution function, $P(\eta)$, and the probability density function, $p(\eta)$), or the power spectral density $S_{\eta\eta}(k,\omega)$ usually referred to simply as the spectrum. Unlike the probabilistic-function description, the spectral description method preserves the frequency content of the wave field or surface elevation profile and the relative distribution of energies at different frequencies. Furthermore, it is naturally compatible with the frequency domain method for response analysis which was discussed extensively in Chapter 2. As such, it has found wide applications in engineering analysis. Thus, the wavy sea surface profile, η, is in general modelled as a stochastic field, which for simplicity, is usually considered to be stationary in time and homogeneous in space.

3.2 Ocean Wave Spectra

The most appropriate procedure for obtaining a spectrum is by measurement at the site under consideration. Unfortunately, such a spectrum is seldom available, especially when directional spectra are required. As an alternative, the usual procedure is to choose one of the theoretical spectrum models available. This theoretical wave spectrum describes short term wave conditions, since spectrum models depend on fetch, wind, and other meteorological conditions of the site.

Several mathematical spectrum models are available. These models are generally based on one or more parameters, for example, significant wave height and wave period. A few of these spectrum models that have been applied to marine structures include the Pierson-Moskowitz spectrum, the ISSC spectrum, the ITTC spectrum, and the JONSWAP spectrum. A brief description of each of the above spectra is given below.

The Pierson-Moskowitz spectrum (usually referred to as the P-M model) is a single-parameter spectrum based on the significant wave height or wind speed. It was developed in 1964 from the results of

analysis of wave spectra in the North Atlantic. It has since been extensively used by ocean engineers as one of the most representative for waters all over the world [16,17]. The P-M spectral model describes a fully-developed sea determined by the wind speed. The fetch and duration are considered infinite. The model is applicable to wave records obtained after the wind has blown over a large area at a nearly constant speed and direction for many hours prior to the time of taking the wave record. It is mathematically represented as:

$$S(\omega) = \alpha g^2 \omega^{-5} \exp\left[-0.74 \left(\frac{\omega U_w}{g}\right)^{-4}\right] \tag{3.3}$$

where α=0.0081, g is the acceleration due to gravity, and U_w is the wind speed. Equation (3.3) may also be written in terms of the frequency of the spectral peak, ω_o, namely:

$$S(\omega) = \alpha g^2 \omega^{-5} \exp\left[-1.25 \left(\frac{\omega}{\omega_o}\right)^{-4}\right] \tag{3.4}$$

Karadeniz et al [13], used a multi-directional P-M spectrum to characterize the sea state in their analysis of gravity and jacket-type structures. Their model has the form:

$$S_{\eta\eta}(\omega,\Phi) = \left[\frac{2}{\pi} \cos^2(\Phi-\Phi_s)\right]\left[\alpha g^2 \omega^{-5} \exp\{4\alpha g^2 H_s^{-2} \omega^{-4}\}\right] \tag{3.5}$$

In equation (3.5), Φ_s is the principal direction of the sea state in which individual waves with direction Φ simultaneously occur, ω is the frequency of wave motion, H_s is the significant wave height, g is the acceleration due to gravity, and α is a constant (0.008).

In 1964, the International Ship Structures Congress (ISSC) suggested a slight modification to the Bretschneider spectrum [16] in the form:

$$S(\omega) = 0.1107\ H_s^2\ \frac{\bar{\omega}^4}{\omega^5}\ \exp[-0.4427(\frac{\bar{\omega}}{\omega})^4] \tag{3.6}$$

in which the peak frequency, ω_o, is related to $\bar{\omega}$ through:

$$\bar{\omega} = 1.296\omega_o \tag{3.7}$$

The International Towing Tank Conference (ITTC) proposed (in 1966, 1969, 1972) a modification of the P-M spectrum in terms of the significant wave height and zero crossing frequency, ω_z. The mathematical representation of the ITTC spectrum is in the form:

$$S(\omega) = \alpha g^2 \omega^{-5}\ \exp[-\frac{4\alpha g^2 \omega^{-4}}{H_s^2}] \tag{3.8}$$

$$\text{where } \alpha = \frac{0.0081}{k^4} \tag{3.9}$$

$$\text{and} \quad k = \frac{\sqrt{g/\sigma}}{3.54\omega_z} \tag{3.10}$$

$$\text{in which } \sigma = \sqrt{m_o} = \frac{1}{4} H_s \tag{3.11}$$

In the above, σ is the standard deviation (r.m.s. value) of the water surface elevation, m_n is the nth moment of the spectrum defined as

$$m_n = \int_0^\infty \omega^n S(\omega) d\omega \tag{3.12}$$

and the average zero crossing frequency or apparent frequency (defined in Chapter 2), ω_z is:

$$\omega_z = \left\{ \frac{m_2}{m_0} \right\}^{1/2} \tag{3.13}$$

The JONSWAP spectrum was developed during a joint North Sea Wave Project from which its name is derived. The formula for this spectrum is given in [16] as:

$$S(\omega) = \alpha g^2 \omega^{-5} \exp\left[-1.25 \left(\frac{\omega}{\omega_o}\right)^{-4}\right] \gamma^{\exp\left[-\frac{(\omega-\omega_o)^2}{2\tau^2\omega_o^2}\right]} \tag{3.14}$$

in which γ = peakedness parameter, τ = shape parameter (τ_a for $\omega \leq \omega_o$ and τ_b for $\omega > \omega_o$). In terms of the significant wave height, H_s, and the peak frequency, ω_o, an approximate expression for the JONSWAP spectrum is:

$$S(\omega) = \alpha^* H_s^2 \frac{\omega^{-5}}{\omega_o^{-4}} \exp\left[-1.25\left(\frac{\omega}{\omega_o}\right)^{-4}\right] \gamma^{\exp\left[\frac{-(\omega-\omega_o)^2}{2\tau^2\omega_o^2}\right]} \tag{3.15}$$

where

$$\alpha^* = \frac{0.0624}{0.230 + 0.0336\gamma - 0.185\,(1.9+\gamma)^{-1}} \tag{3.16}$$

For γ=1, the value for α^* is 0.312, and Equation (3.15) reduces to the P-M spectrum. The JONSWAP spectrum applies to wind generated waves under conditions of limited fetch and homogeneous wind fields.

A host of other spectrum models are available and Chakrabarti [16] has a quite elaborate description of these models. The choice of a spectrum model in the design or analysis of marine structures is up to the designer or analyst and depends on the particular application.

All the spectrum models described above are unidirectional frequency spectra which do not account for the directional distribution of wave energy. Since ocean waves are multi-directional in practice, a more

accurate description of random seas, and hence sea surface elevation profiles, requires information on the directional dispersion of wave energy. In other words, the sea surface elevation is a random function of both space and time thereby making it necessary to describe the power spectrum in terms of both frequency (ω) and wave number (k). Measurements of directional wave spectra (or wave number spectra) are considerably more difficult than those of frequency spectra. While frequency spectra can be obtained from a wave record at a single point, directional wave spectra require simultaneous recording of several wave components [18]. A few measuring techniques in respect of the latter case are discussed in [18], but sources of measured directional spectra are considered to be rare [17].

Some methods for obtaining directional wave spectra discussed by Ochi [19] include:

(i) obtaining the sea surface elevation over an area by means of stereophotographs;

(ii) analyzing data obtained from one-dimensional arrays, two-dimensional arrays, and multielement arrays;

(iii) obtaining the directional information from wave elevations, slope, and curvature, as recorded by a floating buoy.

Nwogu [20] also presented a procedure for estimating directional wave spectra from an array of wave probes based on the Maximum Entropy Method (MEM).

Information on wave directionality is especially important for predicting wave-induced forces on ships and floating structures because the forces are associated with coupled motions induced by waves travelling in various directions [19]. However, because of the difficulty in

measuring directional spectra, it is usual to evaluate directional wave spectra by applying a formulation representing the energy spreading function to a point (i.e. unidirectional) spectrum. This is considered to be particularly convenient for evaluating the responses of ships and marine structures in a seaway [19], for which correlations among the six degrees of freedom have to be considered.

According to Nwogu [20], the concept of a directional spreading function to characterize a wave field should only be applicable to a spatially homogeneous wave field with no correlation of the wave components travelling in different directions. In [19], the MEM was reported to have yielded a spreading function of each frequency band which is consistent with cross-spectra of the measured water surface elevation time series.

A directional wave spectrum is usually represented in the form:

$$S(\omega,\theta) = S(\omega)D(\omega,\theta) \tag{3.17}$$

in which $D(\omega,\theta)$ is a nonnegative angular spreading function describing the distribution of wave energy over direction, and has to satisfy:

$$\int_{-\pi}^{\pi} D(\omega,\theta)d\theta = 1 \tag{3.18}$$

In Equation (3.17), the wave frequency (ω) is related to the wave number (k) by the linear dispersion relation, and $S(\omega)$ is the conventional unidirectional frequency spectrum.

Available idealized spreading function formulations include [19] the cosine-square formulation, the SWOP formulation, the Mitsuyoisu formulation, and the Hasselmann formulation. The SWOP energy spreading function, for example, was derived from analysis of data obtained during the Stereo Wave Observation Project (SWOP), and has the form:

$$D(\bar{\omega},\theta) = \begin{cases} \frac{1}{\pi}\,(1 + a\cos 2\theta + b\cos 4\theta) \text{ for } \frac{-\pi}{2} < \theta < \frac{\pi}{2} \\ 0 \quad \text{otherwise} \end{cases} \tag{3.19}$$

where

$$a = 0.50 + 0.82 \exp\left(-\frac{1}{2}\,\bar{\omega}^4\right) \tag{3.20a}$$

$$b = 0.32 \exp\left(-\frac{1}{2}\,\bar{\omega}^4\right) \tag{3.20b}$$

$$\bar{\omega} = \text{dimensionless frequency} = \frac{U\omega}{g} \tag{3.20c}$$

and U is the wind speed at 19.5 m above the sea surface. It may be noted that the multi-directional version of the P-M spectrum used by Karadeniz et al. [13], that is Equation [3.5], is a cosine-square formulation of the spreading function. This is extremely simple to use but it is a function of neither frequency nor wind speed.

Recently, Juszko [21] employed various directional parameterizations for modelling high-resolution directional wave spectra under contract to the scientific authority. These wave spectra were obtained from a WAVEC buoy moored on the Grand Banks in 1984. The ten-parameter directional spectum presented has the form:

$$S_{\eta\eta}(\omega,\theta) = \frac{1}{4} \sum_{i=1}^{2} \frac{\left(\frac{(4\lambda_i+1}{4}\,\omega_{m_i}{}^4\right)^{\lambda_i}\delta_i{}^2\, e^{-\left[\frac{4\lambda_i+1}{4}\right]\left[\frac{\omega_{m_i}}{\omega}\right]^4} * \cos^{2p_i}\frac{(\theta-\theta_{m_i})}{2}}{\Gamma(\lambda_i)\,\omega^{4\lambda_i+1}} \tag{3.21}$$

The approach taken in the work of Reference [21] was to extend the Ochi and Hubble [22] six-parameter amplitude model to include various representations of the directional component through the use of a mean direction and a directional spread parameter. The model was reported to be capable of reproducing over 90% of the data records and so will be the

top candidate for consideration as a suitable choice of the sea surface profile in this work. Further discussions on directional wave spectra can be found in the monograph by Price and Bishop [23].

3.3 Determination of Random Pressure Loads

An important step regarding the probabilistic descriptions of the loading of marine structures is the selection of an appropriate power spectrum model for the ocean waves as discussed in the preceding section. The next critical step is the utilization of this information for the determination of the corresponding random pressure loads experienced by such structures. The general procedure is to consider the spectrum of the sea waves or sea surface elevation as the input process and seek to determine the corresponding force cross or auto spectra densities output with the aid of the classical relations:

$$S_{pp}(\omega) = \int_0^{2\pi} H^*_{p\eta}(i\omega,\theta) H_{p\eta}(i\omega,\theta) S_{\eta\eta}(\omega,\theta)\, d\theta \qquad (3.22)$$

in which Spp is the spectral density of the pressure, θ represents the direction of the individual waves making up the sea state, $H_{p\eta}$ represents the transfer function (or frequency response function) from sea surface elevation to wave pressure, and $H^*_{p\eta}$ denotes the complex conjugate of $H_{p\eta}$. This approach has been used by Karadeniz et al [13], for example, in the spectral fatigue analysis of offshore platforms. In their work, the linear wave theory and Morison's formula were applied to the undisturbed wave to determine these transfer functions. They also applied a correction based on diffraction theory for the higher wave frequencies. It is in the determination of these transfer functions, either experimentally or computationally, that the classical theories of deterministic hydrodynamic wave analysis become important and relevant in a probabilistic approach.

The determination of the transfer functions $H_{p\eta}(i\omega,\theta)$ whose magnitude, in the terminology of hydrodynamcs, is more popularly referred to as the response amplitude operator (RAO) is needed in the application of Equation (3.22) which is valid for all linear or linearized systems. For pressure loads which are of interest here, the RAO is formally defined as the response amplitude per unit wave height. However, it is usually more convenient in hydrodynamics to describe the RAO as the response amplitude per unit wave amplitude. In the computation of RAO, the waves are considered regular and a sufficient number of frequencies (and directions in case of directional wave spectra) are chosen to cover the entire range of frequencies (and directions or wave headings) covered by the ocean wave spectrum.

In the current work, a program called PRECAL is used for the computation of the transfer functions. This program is one of the three HPCFEM (acronym for Hydrodynamic Pressure Calculation for a Finite Element Model) suite of programs that is available to the scientific authority as a member organization of the NSMB Co-Operative Research. The purpose of this suite of programs is the calculation of the hydrodynamic pressure on the wetted surface of a ship moving in regular sinusoidal waves for input into a finite element model. The first program in the suite called HYDMES is used for the generation of the hydrodynamic mesh data from a given ship geometry database. The second program PRECAL then uses the hydrodynamic mesh data to calculate the hydrodynamic pressure acting on the wetted surface of the ship caused by:

i. Oscillatory motion in regular sinusoidal waves for infinite depth;

ii. Forward motion in regular sinusoidal waves for infinite depth.

The hydrodynamic pressure at a point on the wetted hull surface per unit wave amplitude is derived based on a three-dimensional linear potential

theory in which the effects of the incident wave, diffracted wave, radiated wave, and the resultant vertical displacement of that point are all accounted for. The fluid is assumed to be inviscid and incompressible while the flow is taken to be irrotational. The third program in the suite, FINMES, is the Finite Element Mesh program which provides the user with the hydrodynamic pressure values, interpolated from the values calculated in PRECAL, for either a finite element model or for user specified points. It must be pointed out that the analytical basis of all computations performed in the entire HPCFEM suite of programs is completely deterministic and as such has no element of randomness whatsoever. Further details of the theoretical basis and the operation of the HPCFEM suite of programs can be found in the publications of the Research and Development Division of the American Bureau of Shipping and allied publications for NSMB Research Group [24-30].

Since the use of PRECAL is solely for the determination of the transfer functions (RAOs) in (3.22), it is important to recognize that any similar deterministic hydrodynamic analysis program may be utilized for computing these transfer functions.

In the context of PRECAL, the pressure amplitude per unit wave amplitude, P_A, together with the phase angle, ϕ, are given for each specified point for every frequency of encounter (ω) and wave heading (θ). Then the $H_{p\eta}(i\omega,\theta)$ is calculated from the expression

$$H_{p\eta}(i\omega,\theta) = P_A(\omega,\theta)e^{i\phi(\omega,\theta)} \tag{3.23a}$$

or in the expanded form,

$$H_{p\eta}(i\omega,\theta) = P_A(\omega,\theta)\cos\phi(\omega,\theta) + iP_A(\omega,\theta)\sin\phi(\omega,\theta) \tag{3.23b}$$

Thus, the power spectrum of the random pressure loading may now be computed using Equation (3.22).

3.4 Determination of the Cross Spectral Density Matrix of the Applied Loads

The power spectrum of the random pressure load computed in the preceding section is a suitable and acceptable input for a finite element program to be used for random response analysis. However, it cannot be directly utilized in its raw form because of the distributed nature of this pressure load. A procedure is required to convert this distributed loading to the loads at nodal (global) degrees of freedom of the finite element model. In other words, a consistent finite element representation of the assembled cross spectral density of nodal forces corresponding to the distributed random pressure field must be determined. It is only this form of description that can be used in the representation of the discretized equations of motion (2.21) and the subsequent solution process discussed in the third section of Chapter 2.

The formulation of a consistent finite element representation of a distributed random load is quite involved. The most rigorous approach is the development and application of special elements for the modelling and discretization of these random distributed loads considered as random fields. These elements, popularly referred to as Stochastic Finite Elements (SFEM) or Random Field Finite Elements have been used quite a bit, especially in applications involving uncertain (i.e. stochastic) parameters; see, for example, the works of Contreras [31], Liu et al. [32], and Vanmarcke et al. [33]. Stochastic finite elements are the most suited for the discretization of random fields because their mathematical formulation accounts for the resolution of stochastic inhomogenities and the extent of spatial correlations. In practical finite element analysis, the implication is that two types of elements or discretizations are required: one for the structure or the governing equations of motions and another for the random fields present. Thus, the use of SFEM may be computationally expensive and inconvenient. As a result, there-

fore, less rigorous but acceptably reliable methods of obtaining the consistent finite element representations of distributed loadings are preferred for applications in which only the externally applied load is stochastic. These latter methods are able to utilize conventional finite elements used in deterministic analysis for the discretization of the random pressure fields to a reasonable level of accuracy.

In deterministic analysis, if the dynamic surface pressure acting on an element at time t is denoted as $p(\underline{s},t)$ where $\underline{s}$ is the position on the element, then it is well known that the consistent finite element representation of the nodal forces at time t, $\{F_e(t)\}$ corresponding to this distributed load is given by

$$\{F_e(t)\} = \int_{A^e} [N]^T p(\underline{s},t)\, dA^e \tag{3.24}$$

where A^e is the area of the element and [N] is the matrix of element shape functions relating the displacements at any point to the element nodal displacements. Let $[a]_i$ denote the Boolean matrix which relates the nodal degrees of freedom of element i to the nodal degrees of freedom of the complete structure. If this pressure field acts over a number of elements NE of the structure, the consistent load vector corresponding to the complete global degrees of freedom is then given by [9]

$$\{F(t)\} = \sum_{i=1}^{NE} [a]_i^T \int_{A_i} [N]_i^T p(\underline{s},t)\, dA_i \tag{3.25}$$

where $[N]_i$ is the shape function for element i and A_i is the area of the element.

Now let us consider the case in which $p(\underline{s},t)$ is random. Using the definition of the cross spectral density given in Equation (2.14) of Chapter 2, it can be readily shown that the cross spectral density of the nodal forces in Equation (3.25) is given by

$$[S_{FF}(\omega)] = \sum_{i=1}^{NE} \sum_{j=1}^{NE} [a]_i^T \int_{A_i A_j} [N(\underline{s}_i)]_i^T S_{PP}(\underline{s}_i, \underline{s}_j, \omega) [N(\underline{s}_j)]_j dA_i dA_j [a]_j \quad (3.26)$$

where $S_{PP}(\underline{s}_i, \underline{s}_j, \omega)$ is the cross spectral density of the random pressure field, and A_i, A_j represent the surface area of elements i,j. Equation (3.26) gives the consistent finite element representation of the assembled cross spectral density matrix for the random pressure load.

It can be seen that the evaluation of Equation (3.26) is computationally intensive. First, the double product (area integration) over pairs of elements has to be performed and secondly the double summation also must be performed. Considering that this procedure has to be performed for every applied (forcing) frequency of interest to the user, the computation costs could be phenomenal! This is why the first attempts at calculating $[S_{FF}(\omega)]$ for distributed surface pressures used ad-hoc approximations to represent the continuous field by concentrated transverse shear loads acting at the node points.

The works of Olson [34] and Olson and Lindberg [35] represent the pioneering efforts directed toward the calculation of the consistent finite element representation of distributed random loads. These works are based on the standard modal approach using the mode shapes obtained from a finite element representation of the continuum under study. A polynomial representation over each finite element of the excitation cross spectral is then introduced. This permits a closed-form evaluation of the spatial integrations involved in the determination of the force cross spectral density matrix. The method was applied for a four-degree-of-freedom beam element in [34] and a twenty-degree-of-freedom triangular plate element in [35]. In [34], for example, it was assumed that $S_{PP}(x_i, x_j, \omega)$ acting on a uniform beam could be represented as:

$$S_{PP}(x_i, x_j, \omega) = e_1 + e_2 x_i + e_3 x_j + e_4 x_i x_j \quad (3.27)$$

where the parameters e_1-e_4 are evaluated in terms of the values of Spp for the four node points of the two elements i and j, taking them two at a time. This bilinear approximation gives

$$[S_{FF}(\omega)] = \sum_{i=j}^{NE} \sum_{j=1}^{NE} [a]_i^T [e_1\{f_0\}_i\{f_0\}_j^T + e_2\{f_1\}_i\{f_1\}_j^T + e_3\{f_0\}_i\{f_1\}_j^T + e_4\{f_1\}_i\{f_1\}_j^T] [a]_j \quad (3.28)$$

where

$$\{f_0\} = \int_0^{\ell} [N(x)]^T \, dx \quad (3.29a)$$

$$\{f_1\} = \int_0^{\ell} [N(x)]^T \, x \, dx \quad (3.29b)$$

are the consistent load vectors for uniform and linearly varying loads. Note that e_1-e_4 are functions of frequency and $\{f_0\}$, $\{f_1\}$ are independent of frequency.

Dey [36] employed a lumped-load method to convert the pressure cross-spectral density of the nodal forces. In this approach, it was assumed that the random nodal loads can be obtained by multiplying the random forces by the area allocated at the nodal points. In other words, it is assumed that the same random force acts on the entire area with full correlation. This formulation gives the consistent finite element cross spectral density matrix as

$$[S_{FF}(\omega)] = [A] [S_{PP}(\underline{s},\omega\_)] [A]^T \quad (3.30)$$

in which [A] is a diagonal matrix of the areas associated with each global degree-of-freedom.

In a more recent study, Yang and Kapania [37] presented a consistent finite element formulation for a 48 degree-of-freedom quadrilateral shell element with bi-cubic Hermitian polynomial interpolation functions as the displacment shape functions. These shape functions are used to form the matrix of cross spectral densities of the generalized nodal forces for distributed loads which, unlike the work of [36], are not assumed to be fully correlated. The use of Gaussian quadrature in this work allows the spectral density function to be used directly in its original form rather than in an approximate polynomial form as was done in [34,35]. Another interesting feature of the work in [37] is that the element shape functions are also used to interpolate the spectral density values of an arbitrary pair of points within two separate shell elements from the element nodal values. The formulation was used to predict the stationary random response of cooling tower type shells in which the random distributed loads were assumed as stationary in time but permitted to be non-homogeneous in space. It can be seen that this formulation is actually an implementation of Equation (3.26) for the particular case of the shell element used in their study.

3.4.1 Procedure Implemented in this Work for Random Load Description

Rather than attempt to implement one of the above procedures, a different approach has been devised during the course of this work. The pressure transfer functions are converted to the nodal force transfer functions referred to global degrees-of-freedom of the finite element model. The procedure consists of calculating the resultant force acting on an element by multiplying the pressure by the area of the element. Then the portion of this resultant force that is allocated to each node is determined on the basis of the consistent finite element representation corresponding to a unit pressure load acting uniformly over the surface of the element. The direction cosines of the normal at the element centroids are used to compute the components of the nodal

forces at each node with respect to the global coordinate axes. While this procedure is short of an exact consistent finite element representation (since it will not induce forces in the rotational degrees-of-freedom), it is believed to be capable of giving very good approximations, while being more computationally efficient. Indeed, for planar elements, the procedure yields exact results for the three elements implemented, and in any case should always give better results than lumped-load method of Dey [36] described above.

Once the transformation from pressure transfer functions to nodal force transfer functions has been accomplished, the relation:

$$S_{FF}^{ij}(\omega) = \int_0^{2\pi} H_{F_i\eta}^*(i\omega,\theta) H_{F_j\eta}(i\omega,\theta) S_{\eta\eta}(\omega,\theta) d\theta \quad (i, j=1, \ldots, NS) \tag{3.31}$$

is used to directly compute the required assembled cross-spectral density matrix corresponding to the global degrees-of-freedom. It may be noted that the right hand side of Equation (3.31) is identical to that of Equation (3.22) except that the nodal force transfer function $H_{F\eta}(i\omega,\theta)$ has replaced the pressure transfer function $H_{p\eta}(i\omega,\theta)$.

It is fortunate that this approach could be devised and adopted in this work as the applications are specifically aimed at ship structures in random seas. We believe it is still desirable, however, to provide a more generalized capability for modelling distributed random loads in VAST.

4.0 COMPUTER PROGRAMS FOR RANDOM RESPONSE ANALYSIS

4.1 Program RANVIB

A random vibration analysis module called RANVIB has been developed to provide a random response capability in the finite element program VAST. The program has been developed on the basis of the modal frequency response method that was extensively discussed in Chapter 2. In this chapter, a description of the flow and manner of operation of the program and its subprograms is presented. The main features of the capabilities of the program are highlighted and the few limitations are noted.

To perform a finite element analysis using VAST, appropriate Master Control Codes must be selected and the random vibration analysis is no exception. The Master Control Code that triggers a random response analysis is the newly introduced (eleventh) code IPOSTP which should be set equal to 1, together with a header "RANRES" in the PREFX.USE file. If random stress and/or strain responses are of interest, then additionally the header "NODSTR" should also be present in the PREFX.USE file. This is because the statistical properties of random stresses and strains are computed at the nodes using the averaged modal stresses or strains at the nodal points computed by POSTV2. It should be noted that all other ten Master Control codes must be selected to perform operations that are required before the random response analysis is performed. For a virgin VAST run for the purpose of performing random response analysis, for example, the control codes IELEMS, IASSEM, ISTIFM, IMASSM, IDECOM, IEIGEN, ILOADS, IDISPS should be set to 1. If either random stresses or strains are also of interest, then the Master Control Code ISTRES should also be set to 1. Finally, IPOSTP must be set to 1 and appropriate headers provided in the PREFX.USE file as described above. Figure 4.1 illustrates the various VAST modules required for a virgin random vibration analysis. Data preparation for the modules shown in this diagram follow,

of course, exactly the procedures described in the VAST User's Manual [38]. The minor differences are discussed below.

The difference in data preparation starts with the module DISP5 (see Figure 4.1). For this module, LTYPE is set to -1 instead of 1 (for steady state displacements due to sinusoidal loading) or 2 (for steady state displacements due to a Fourier series representation of a periodic loading). Furthermore, for the damping, the modal damping (IDAMP = 1) follows the same procedure as for a frequency response analysis. However, the random vibration analysis also permits the specification of proportional damping (IDAMP = 2) in which only two parameters α_M and α_K (instead of NM modal damping ratios) are required to describe the damping in the manner described in Chapter 2. For this type of damping, the user must still specify NM values of modal damping ratios but must ensure that the first two damping ratios are α_M and α_K respectively, so that

$$\alpha_M = \text{DAMP}(1) \tag{4.1a}$$

$$\alpha_K = \text{DAMP}(2) \tag{4.1b}$$

All other modal damping ratios are ignored for this type of damping because they are not needed in the computation of the complex frequency response functions. Similarily, for structural damping, (IDAMP = 3), the user inputs the structural damping factor (g) as DAMP (1) while DAMP(2, ... NM) values are entered as zero. All other data for the DISP5 module is prepared as if LTYPE=1 as described in the VAST user manual.

The load module for a random response analysis is different from that of a deterministic analysis in that the function of the random load module is to generate the consistent cross spectral density matrix (and not a consistent load vector) of the nodal forces from the user specified power spectra of point loads and/or distributed loads. A new load module

called RANLOD has been developed during the course of this work to perform this function. A random load data file called PREFX.RLD which describes the point loads and/or distributed loads for the various forcing frequencies to be used in the analysis must be prepared by the user. This data file is then used by RANLOD to generate the assembled consistent cross spectral density matrix of the applied loads which are written on a binary file PREFX.PSD for each forcing frequency. This file must be created by running RANLOD before a random vibration analysis can be performed. A description of the random load generation programs is given in Section 4.2.

Next, if either the random stresses or strains are of interest to the user, then the modal stresses are computed and written on the binary file PREFX.T53. Modifications have been made to the STRESS module to permit the computation of these modal stresses. Modifications are also to be made to the postprocessing program POSTV2 to allow for the processing of the PREFX.T53 containing modal stresses so that averaged modal stresses and/or strains at the nodes can be made available on PREFS.P21 and PREFS.P22 files.

Finally, the random vibration analysis module (RANVIB) is run to compute the random dynamic responses of interest to the user as specified in the PREFX.RIN file which is the input data file for this program. A description of this data file is given in Appendix A.

Program RANVIB is the main driver for the random response analysis subprograms. It consists of four main subprograms: PRERDM, MODRES, RANRES, and PRNTRR. At the beginning of a RANVIB run, all temporary files to be used for storing intermediate results and all permanent files to be used for saving the computations (and which will be used for graphics post processing) are opened and named.

Briefly, the functions of the above named subprograms are as follows. Subroutine PRERDM prepares information necessary for the computations to be performed; subroutine MODRES computes the random modal response; subroutine RANRES directs and controls the computation of the statistical properties of the quantities of interest; and subroutine PRNTRR prints out the random response results. A simplified flow diagram of program RANVIB is shown in Figure 4.2.

Subroutine PRERDM first reads the PREFX.RIN input data file for user information. This user information consists of the physical processes and statistical properties of interest to the user. As described in Appendix A, the first card on the PREFX.RIN files contains the parameters IRESP and IDAMP. If IRESP=0, only the modal response will be computed and saved on the PREFX.RMR file which may be used in a future run. This modal response consists of the cross spectral density matrix of the modal displacements $[S_{qq}(\omega)]$ for all forcing frequencies and the covariance matrix of modal displacements $[C_{qq}]$. Both of these quantities are very important for random response computations. If IRESP=1, the modal response will be freshly computed (i.e. in the current run) and will be used for random response computations. If IRESP=2, a modal response computed during a previous run and saved on PREFX.RMR file is used for the response computations. This is like a restart and saves a lot of computation time. The parameter IDAMP specifies the type of damping. Other user information on the PREFX.RIN file includes the physical processes and statistical properties of interest, whether cross statistics or only auto-statistics are of interest, and whether responses for all nodes or only a selected number of nodes are to be computed. Subroutine PRERDM extracts the relevant natural frequencies and orthonormalized mode shapes from the PREFX.T51 file to form the modal matrix [R] which is written columnwise on tape. The PREFX.T52 file is read for information concerning additional forcing frequencies and damping.

The random physical processes are divided into two groups. The first group consists of displacements, velocities, and accelerations and are referred to as primary responses. The second group which consists of stresses and strains are called secondary responses. The computation of the statistical properties of secondary response processes has not yet been implemented. If primary random responses are needed only at a selected number of nodes, a reduced modal transformation matrix [P] corresponding to these nodes is formed and written columnwise on tape NTPR1. If stresses are of interest, the transformation matrix [T] for the stresses at the selected nodes or all the nodes of the finite element model is determined from the PREFS.P21 file and written columnwise on tape NTPR2. Similarly, the transformation matrix [W] for the strains is determined from the PREFS.P22 file and written columnwise on tape NTPR3. It should be noted that while different statistical properties of processes within a group may be of interest, the locations at which properties of processes within a group are to be computed must be the same for the processes. This is to facilitate the use of the same [P] for primary responses. For secondary responses, this allows the use of the same information to be communicated to POSTV2 for the generation of PREFS.P21 and PREFS.P22 files and the possibility of generating both files in a single program run, to be used in the determination of [T] and [W]. Furthermore, this permits the use of the same number of computational degrees-of-freedom (NSPRIM) for all primary response processes and the same number of computational degrees- of-freedom (NSECND) for both stresses and strains. Another advantage of performing computations at the same locations for all primary responses is that the computation of the spectral densities of one primary response process from another is straightforward.

The last operation performed by subroutine PRERDM is the checking of the user requests to determine additional statistical properties that will be needed internally by the program but have not been explicitly requested by the user in the input file. For example, if the user does

not request the power spectrum of velocities but wants the correlation functions of velocities to be computed, subroutine PRERDM will inform RANVIB that the power spectrum of velocities will be computed by setting IVV(1) (see Appendix A) equal to 2 instead of the zero value assigned by the user. In this case, however, the results of the velocity power spectra will neither be saved in the response file nor printed in the VAST output file (PREFX.LPT). The flow diagram of subroutine PRERDM is shown in Figure 4.3.

The next subprogram that is run after PRERDM is subroutine MODRES which performs the computation of the modal responses according to the value of IRESP as described above. The first operation within MODRES is the arrangement of the forcing frequencies in ascending order of magnitude. This is because random response computations involves numerical integrations with respect to frequency and so it is important that the frequencies are in order so that the numerical algorithm can be applied in order at the different steps. It should be noted that the arrangement of the cross spectral density of the loading on the PREFX.PSD file is also in ascending order of magnitude of each forcing frequency (including the natural frequencies of interest to the user). The natural frequencies are usually included in the response computations so as to be able to predict the peak responses accurately at these resonant frequencies. This is why the natural frequencies must be known to the user before RANLOD is run, as is shown in Figure 4.1.

If IRESP is not equal to 2, MODRES loops over all forcing frequencies to perform the following computations. First, the cross spectral density of the applied loads $[S_{FF}(\omega)]$ for the current frequency (ω) is read from the PREFX.PSD file. Then the cross spectral density of the modal force $[S_{ff}(\omega)]$ is computed using Equation (2.26). Next, the complex frequency response function for the current frequency is computed for all the NM modes. This computation is based on Equation (2.29a) for IDAMP=1, Equation (2.29c) for IDAMP=2, and Equation (2.29e) for IDAMP=3.

Next, the cross spectral density matrix of the modal displacement $[S_{qq}(\omega)]$ for the current frequency is computed using Equation (2.28), and written on tape NTMODS. After the end of the forcing frequencies loop, the covariance matrix of the modal displacements $[C_{qq}]$ is computed using Equation (2.49) and also written on NTMODS (i.e. the PREFX.RMR file). This function is provided by subroutine MODCOV which is also capable of computing other modal covariances such as modal velocities, modal accelerations, modal acceleration-rates or any other modal rates through a parameter JFACT. This subroutine has been designed with the objective that it will be useful for the computation of higher-order spectral moments (of any order) that may be used in spectral fatigue analysis in future. A simplified diagram of the flow of subroutine MODRES is illustrated in Figure 4.4.

As can be seen in Equation (2.26) or its indicial representation in Figure 4.4, the computation of the cross spectral density matrix of the modal force from that of the applied force and the modal matrix is very intensive since the evaluation of a triple matrix product has to be performed at every forcing frequency of interest. This is even more so since neither the (NSxNM) modal transformation matrix [R] nor the NAF (NSxNS) cross spectral density matrices $[S_{FF}(\omega)]$ can be stored in-core in the computer for large values of NM, NAF, or NS thereby necessitating a lot of input-output operations. With the exception of modal matrices, all cross spectral density matrices are stored on tape as vectors (either rowwise or columnwise) and only two complex vectors are stored in-core at any given time during the analysis. Even for frequency-dependent modal matrices, only one matrix at a particular frequency is stored in-core at any given time. This is why the results of the modal response quantities (even though usually not of interest to the user) are saved on PREFX.RMR so that it can be used in future runs when additional statistical properties or properties of other random processes are required. Indeed, in a typical run, the computation of the modal responses may consume more CPU time than the computation of the statistical properties of the processes.

An approximation may be employed to reduce the computations involved in the evaluation of $[S_{ff}(\omega)]$. This approximation assumes that $[S_{ff}(\omega)]$ is a diagonal matrix whose diagonal terms are computed as

$$S_{ff}^{rr}(\omega) = \{\phi\}_r^T [S_{FF}(\omega)] \{\phi\}_r \qquad (4.2)$$

where $S_{ff}^{rr}(\omega)$ is the diagonal term corresponding to the rth mode, and $\{\phi\}$ is the eigenvector for mode r. However, this approximation is known to be valid only for lightly damped structures whose natural frequencies are also widely separated [9]. This approximation is not used in RANVIB.

The next subprogram run after MODRES is subroutine RANRES. This subprogram directs the computation of the statistical properties of the random responses in the manner illustrated in Figure 4.5. First, the modal displacement covariance matrix $[C_{qq}]$ is read from the PREFX.RMR binary file on tape NTMODS. Then, the spectral density of the primary responses are computed as required by the user. This is performed first for displacements, then for velocities and lastly for accelerations. The other statistical properties of the primary responses are then computed. Again, the order of computation is: displacements, velocities, accelerations. The order of computation of statistical properties is: covariances, correlations, apparent frequencies. For the secondary responses, stresses are treated first, then strains follow as needed. The order of computations of the statistics of the responses in both cases is spectral densities, covariances, correlations, apparent frequencies. Finally the statistical properties of nodal forces are computed following the same order as for the secondary responses. It will be noted that in all cases the spectral densities are computed first when needed. This is because they may be required in the calculation of other statistical properties. Similarly, the covariances are computed before the apparent frequencies because the former represent the denominator in the definition of the latter, Equation (2.60).

Figures 4.6a and 4.6b give the flow diagrams of the procedures for computing the spectral densities of primary responses and secondary responses respectively. Both procedures form subroutine POWERS which proceeds in the form of Figure 4.6a or 4.6b depending on the value of the parameter ICODE. For primary responses, ICODE=2, for stresses ICODE=3 while for strains, ICODE=4. Provision has been made for nodal forces (ICODE=1) which will be implemented in the future. It can be seen from Figures 4.6a and 4.6b that the major operation involved in the computation of the cross spectral densities is the evaluation of the triple matrix products for each of the forcing frequencies, namely,

$$[S_{XX}(\omega)] = [P][S_{qq}(\omega)][P]^T \tag{4.3}$$

for displacements for example. Thus, computation time can be saved if the size of [P] (i.e. NSPRIM) is very small and this is accomplished by requesting only a selected number of nodes instead of asking for responses at all nodes of the model. The same also applies to other responses including stresses and strains when the computation of secondary responses becomes operational.

The flow diagrams illustrating the procedures for the computation of covariances are shown in Figures 4.7a-4.7e. Different flow diagrams have been provided for displacements, velocities, accelerations, stresses, and strains since the procedures depend (slightly) on the response quantity of interest as decided by the parameter ICODE. A value of ICODE=1 is for nodal forces, ICODE=2 is for displacements, ICODE=3 is for velocities, ICODE=4 is for accelerations, ICODE=5 is for stresses, and ICODE=6 is for strains. All procedures are performed by subroutine COVARC. An important issue in the computation of covariances is the decision about whether the covariances will be computed from the corresponding (or related) spectral densities or from an appropriate modal covariance matrix. As was discussed in Chapter 2, it is preferable to compute the covariance

matrix of a response process from the modal covariance matrix if the spectral densities of the process have not been previously computed because of the savings in computation time. The triple matrix product involved in this is performed by subroutine COVMUL. However, if the spectral densities are available, it is better to use them in the computation of the covariances because the computations required are considerably reduced and they should also give more accurate values since the spectral densities are directly integrated. This philosophy is the basis for the flow diagrams presented in Figures 4.7a-4.7e. It will be noted in Figures 4.7a-c that in the cases concerning primary responses, even if the spectral densities of the particular process of interest is not available but those of another primary response process are available, then the required spectral densities are first readily computed from those available and then used for determining the required covariances. Note that in Figures 4.7a-c, C_{qq}^{kl}, C_{qV}^{kl}, C_{qA}^{kl} denote the elements of the covariance matrices of modal displacements, modal velocities, and modal accelerations respectively. The diagonal terms of the covariance matrix give the mean square responses and the square roots of those mean squares gives the root mean square responses commonly referred to as rms responses. In RANVIB, the mean square responses (and not rms values) are saved on results files and printed out in the VAST output file.

The computation of autocorrelation functions is performed by subroutine CORELA described in Figure 4.8. This is essentially a straight forward implementation of Equations (2.41), which in numerical form has the form:

$$R_{XX}(\tau) = \frac{1}{2\pi\tau} \sum_{i=1}^{NAF-1} \left\{ \frac{S_{XX}(\omega_{i+1}) - S_{XX}(\omega_i)}{(\omega_{i+1} - \omega_i)\tau} \left[\cos(\omega_{i+1}\tau) - \cos(\omega_i\tau)\right] \right.$$

$$\left. + S_{XX}(\omega_{i+1})\sin(\omega_{i+1}\tau) - S_{XX}(\omega_i)\sin(\omega_i\tau) \right\} \quad (4.4)$$

The sequence of NTAU values of τ of interest to the user are indicated either explicitly or otherwise in the input data file as described in Appendix A. This numerical approximation assumes a linear variation of $S_{XX}(\omega)$ between the discrete frequencies ω_i and ω_{i+1}. This is the same approximation assumed when the mean square response is computed from the power spectrum using:

$$E[X^2] = \frac{1}{4\pi} \sum_{i=1}^{NAF-1} [S_{XX}(\omega_{i+1}) + S_{XX}(\omega_i)](\omega_{i+1} - \omega_i) \qquad (4.5)$$

as an approximation to Equation (2.42).

Thus, it is important that a sufficient number of frequencies are selected in the frequency range of interest in order that accurate values of correlation functions and covariances be computed with the above trapezoidal schemes.

Subroutine APFREQ computes the apparent frequencies as shown in Figure 4.9. As discussed in Chapter 2, the denominator in the definition of the apparent frequency is simply the mean square response while the numerator is the mean square response of the corresponding rate process. Covariances required are computed in the manner described earlier. Since only autostatistics are required for apparent frequencies, a special subroutine COVINT is available for numerically integrating autospectra (if previously computed) using Equation (4.5) for determining mean square responses. This subroutine is especially designed for use by subroutine APFREQ but is also used by subroutine COVARC if cross statistics are not of interest and autospectra have been previously computed.

All random response results requested explicitly by the user are saved in the appropriate files. In addition to the PREFX.RMR file for saving the modal responses, six additional permanent binary files are used to save responses. These are PREFX.RFC for forces, PREFX.RDP for

displacements, PREFX.RVL for velocities, PREFX.RAC for accelerations, PREFX.RSS for stresses, and PREFX.RSN for strains. Separate files are used for saving these results because the volume of output data written on any of the files may be large, especially if cross statistics are requested. These files are later used for plotting.

The final subprogram run in RANVIB is subroutine PRNTRR which directs the printout of the random response results in the VAST output file (PREFX.LPT). This subroutine consists of subroutines PRNTPS for printing the autospectra, PRNTMS for printing mean square responses, PRNTCR for printing autocorrelation functions, and PRNTAF for printing the apparent frequencies. The cross statistical properties of responses are not printed out but are available in the permanent files to be used for post processing as needed. A description of how to request the printouts of the random response results is included in Appendix A. Figure 4.10a illustrates the order in which the processes are printed out while Figure 4.10b shows the order in which the response statistics of a given process are printed out.

4.2 Computer Programs for Random Load Generation

A set of computer programs for generating the consistent finite element cross spectral density matrix of the random load for a ship whose hydrodynamic pressure transfer functions are computed by the HPCFEM suite of programs were developed to meet the requirements of Section 2.0 of this contract. Figure 4.11 shows the skeletal flow diagram of the procedure for generating the PREFX.PSD file which is essentially the random load information required by program RANVIB for random response analysis.

The three programs developed during the course of this work are referred to as PREHPC, POSHPC, and RANLOD.

Program PREHPC is a pre-interface program to the HPCFEM suite of programs. The main function of this program is to utilize information from the VAST input data files and its own input data file called PREFX.HPC for the generation of the input data files required to run the HPCFEM programs. These input data files include HYDMES_SHIP_INPUT.DAT, HYDMES_SHIP_GEOMETRY_INPUT.DATA, PRECAL_INPUT.DAT, and FINMES_INPUT.DAT. The procedure for creating the input data file (PREFX.HPC) for running PREHPC is described in Appendix B. Subprogram HGLWD in module HVAST may be used for generating a PREFX.LWD which contains the sectional mass distribution along the ship longitudinal direction. The procedure for running program HVAST can be found in [39]. Similarly, subprogram DIGHLL in module HLLFLO may be used for generating the offset table for the ship lines of form if the offsets of the two-dimensional sections of the ship is not otherwise known. Program DIGHLL uses a digitizing tablet to create an offset table from an offset diagram and the offset table is stored in a file PREFX.DGH for use by program PREHPC. Of course, there are user options to manually provide the sectional masses and the offsets in the input data file PREFX.HPC if they are known. Further details on the procedure and requirements for running DIGHLL are given in [40].

Program PREHPC also generates an output file PREFX.PRE which contains information about the ocean environment in which the ship is travelling. Such information includes the type of ocean (as identified by a suitable ocean wave spectrum), the number of encounter frequencies, the number of wetted elements, the element type, the element connectivities, and the direction cosines of the normals of the elements.

Next, the HPCFEM suite of programs are run in the order HYDMES, PRECAL, and FINMES. The most relevant output file is the file called FINMES_PRESSURE.OUT which contains the pressure transfer functions at points corresponding to the centroids of the elements.

The next program to be run is POSHPC which is the post-interface program between the HPCFEM and VAST programs. Program POSHPC extracts the pressure transfer functions contained in file FINMES_PRESSURE.OUT and utilizes this information together with the information on PREFX.PRE file for automatically generating a PREFX.LOD file. This PREFX.LOD file is like a load file containing point loads for use in a transient dynamic analysis. The number of time steps, NTIME is set equal to (NAF*NWH*2) in which NAF is the number of forcing (or encouter) frequencies and NWH is the number of wave headings. The factor 2 accounts for the fact that the pressure transfer function at any point is a complex number with non-zero real and imaginary parts so that the phase information is preserved. The procedure for generating the point loads used to create the PREFX.LOD file is an approximate procedure for computing the consistent nodal forces corresponding to a given distributed loading by using a nodal load-lumping technique derived from the knowledge of the exact consistent finite element load vector. In fact, the approximate procedure is exact for planar elements and was implemented for three elements in the VAST element library. These elements include the thick-thin shell element (IEC=1), the triangular plate element (IEC=4), and the quadrilateral shell element (IEC=5). In essence, therefore, the pressure transfer functions are converted into nodal force transfer functions corresponding to the global degrees of freedom of the finite element model. The PREFX.LOD file when used to run program LOAD1 module in VAST generates a binary load file (PREFX.T47) which contain the nodal force transfer functions to be later used by program RANLOD.

The subprogram RANLOD is responsible for the computation of the cross spectral density matrix corresponding to the given random loading. RANLOD utilizes information on the PREFX.PRE and PREFX.T47 files for computing the complex nodal force transfer functions for all the wave headings and forcing frequencies concerned. The cross spectral density matrix is then computed at each forcing frequency (ω) by using the expression:

$$S_{FF}^{ij}(\omega) = \int_0^{2\pi} H_{F_i\eta}^{*}(i\omega,\theta) H_{F_j\eta}(i\omega,\theta) S_{\eta\eta}(\omega,\theta) d\theta \quad (i,j=1,NS)$$

where $S_{FF}^{ij}(\omega)$ denotes the cross spectral density of the force for degrees-of-freedom i and j, $H_{F_i\eta}(i\omega,\theta)$ is the complex nodal force transfer function for i at wave heading (θ), $H_{F_i\eta}^{*}(i\omega,\theta)$, and $S_{\eta\eta}(\omega,\theta)$ is the value of the ocean wave spectrum evaluated at the current frequency and wave direction. The skeletal flow diagram for RANLOD is shown in Figure 4.12.

The program currently permits the use of nine types of ocean wave spectra which characterize the type of ocean in which the ship is travelling or stationed. These ocean wave spectra (identified by the parameter ISPEC) include the following:

ISPEC = 1 : TEN-PARAMETER JUSZKO SPECTRUM
= 2 : SIX-PARAMETER OCHI-HUBBLE SPECTRUM
= 3 : PIERSON-MOSKOWITZ SPECTRUM (W.R.T. WIND SPEED)
= 4 : PIERSON-MOSKOWITZ SPECTRUM (W.R.T. PEAK FREQUENCY)
= 5 : INTER. SHIP STRUCTURES CONGRESS (ISSC) SPECTRUM
= 6 : JONSWAP SPECTRUM (W.R.T. GRAVITATIONAL ACCLN.)
= 7 : JONSWAP SPECTRUM (W.R.T. SIGNIFICANT WAVE HEIGHT)
= 8 : INTER. TOWING TANK CONFERENCE (ITTC) SPECTRUM
= 9 : BRETSCHNEIDER SPECTRUM

Descriptions of these ocean wave spectra were given in Section 3.2 of Chapter 3. A summary of their mathematical expressions and the parameters required for their description is given in Appendix B, where the input data file PREFX.HPC is described.

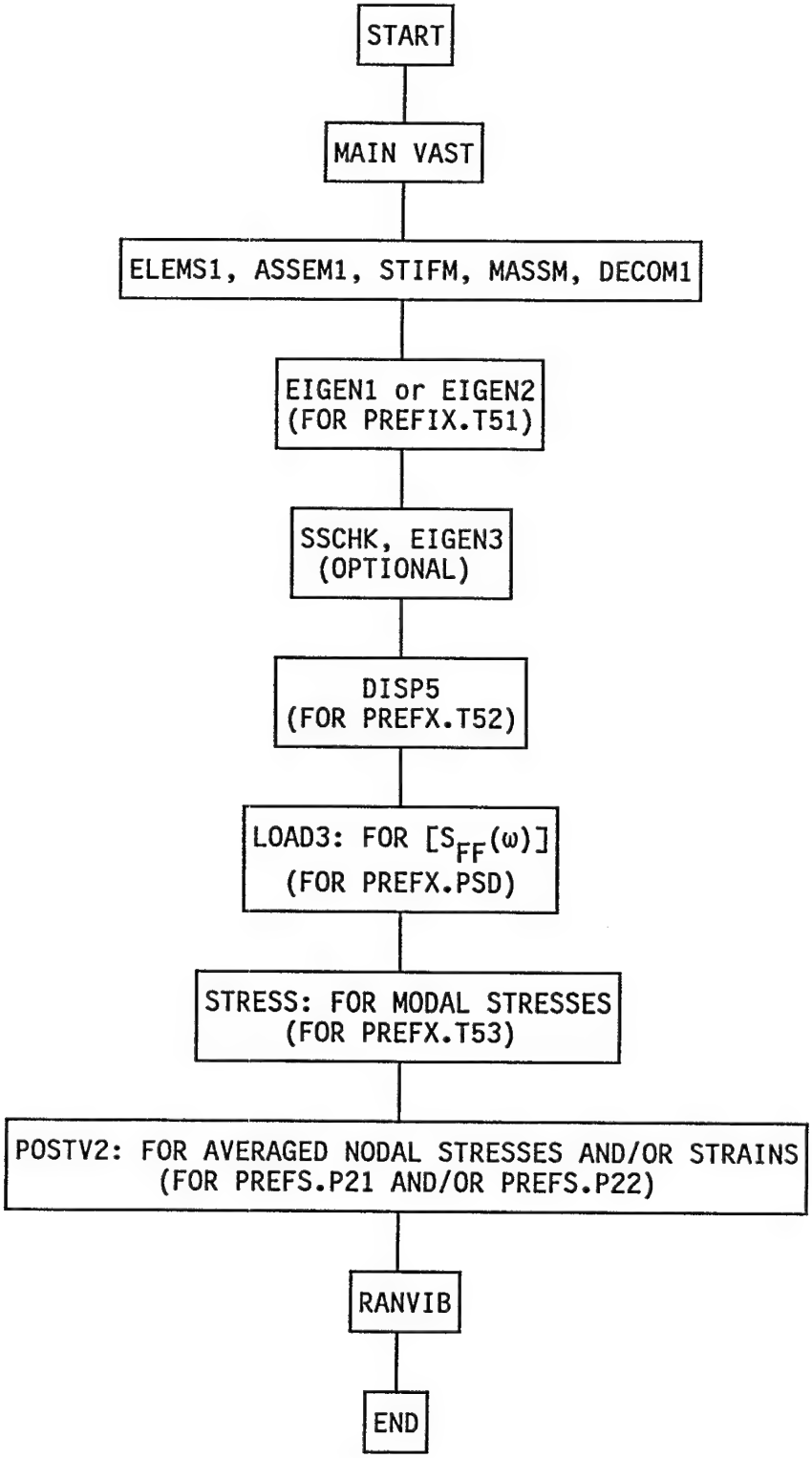

FIGURE 4.1. A Flow Diagram Showing Various VAST Modules Required for a Virgin Random Vibration Analysis

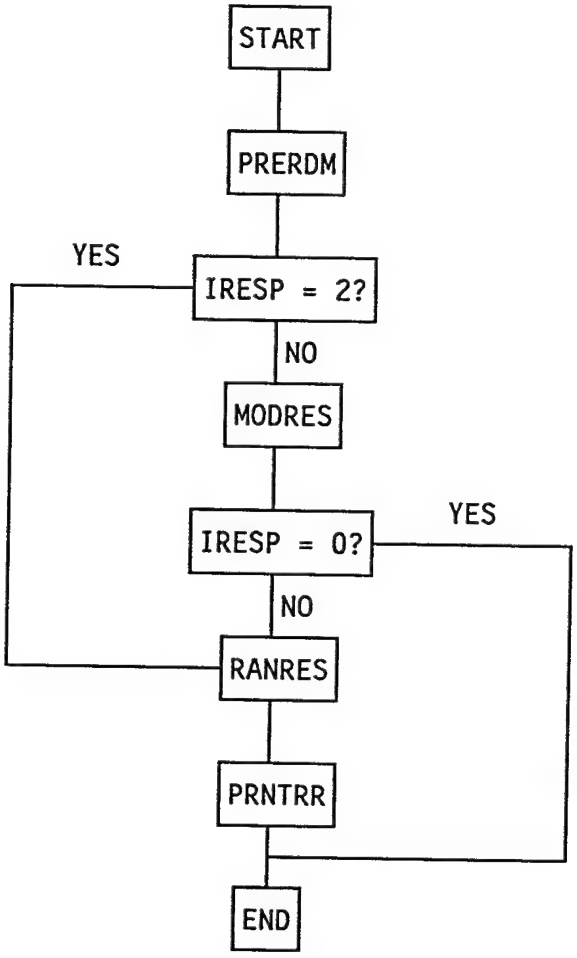

FIGURE 4.2. Simplified Flow Diagram of Program RANVIB

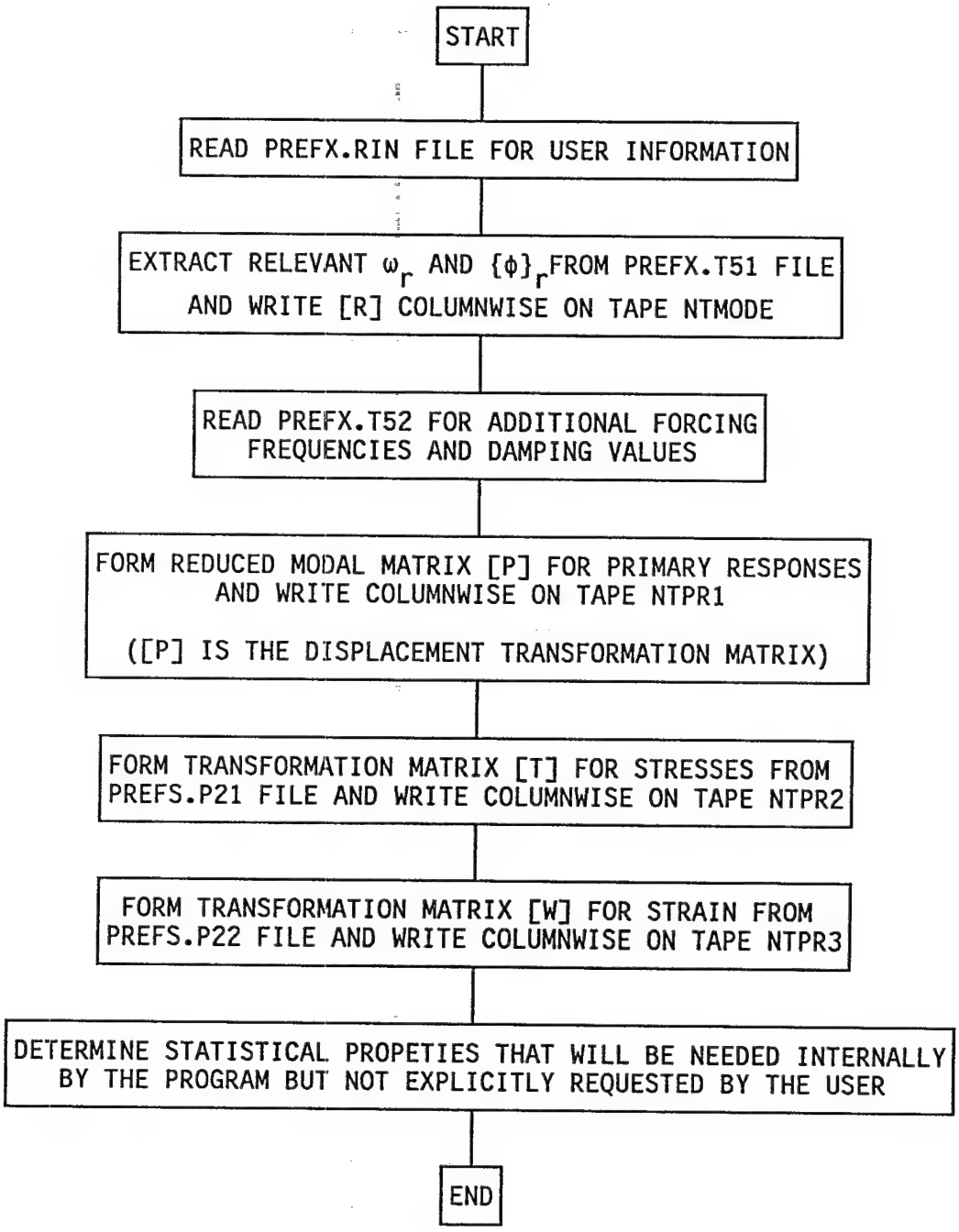

FIGURE 4.3. Flow Diagram of Subroutine PRERDM used for Preparing Information for Random Vibration Analysis

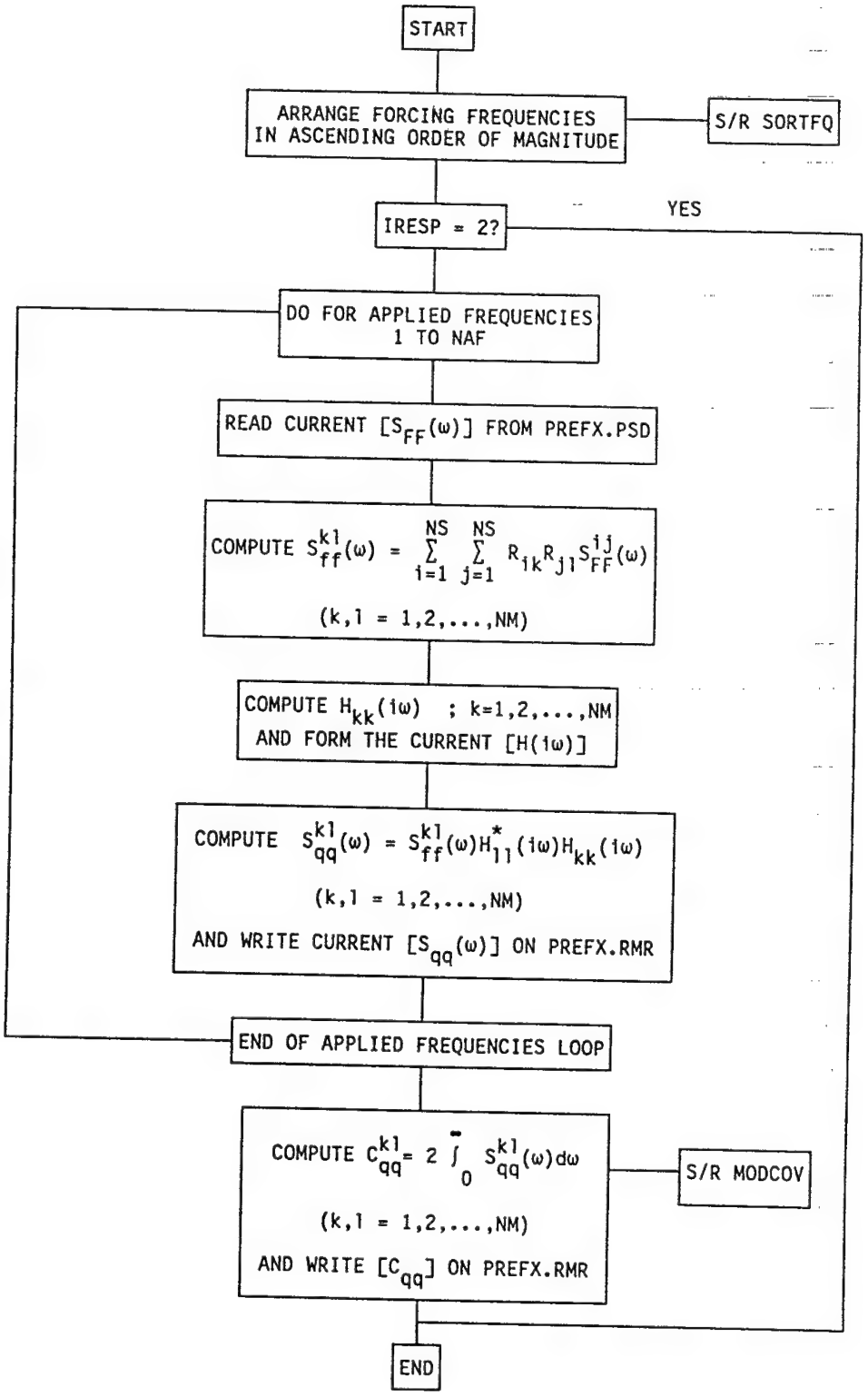

FIGURE 4.4. Flow Diagram of Subroutine MODRES for Computing the Cross Spectral Densities and Covariance Matrix of Modal Displacements

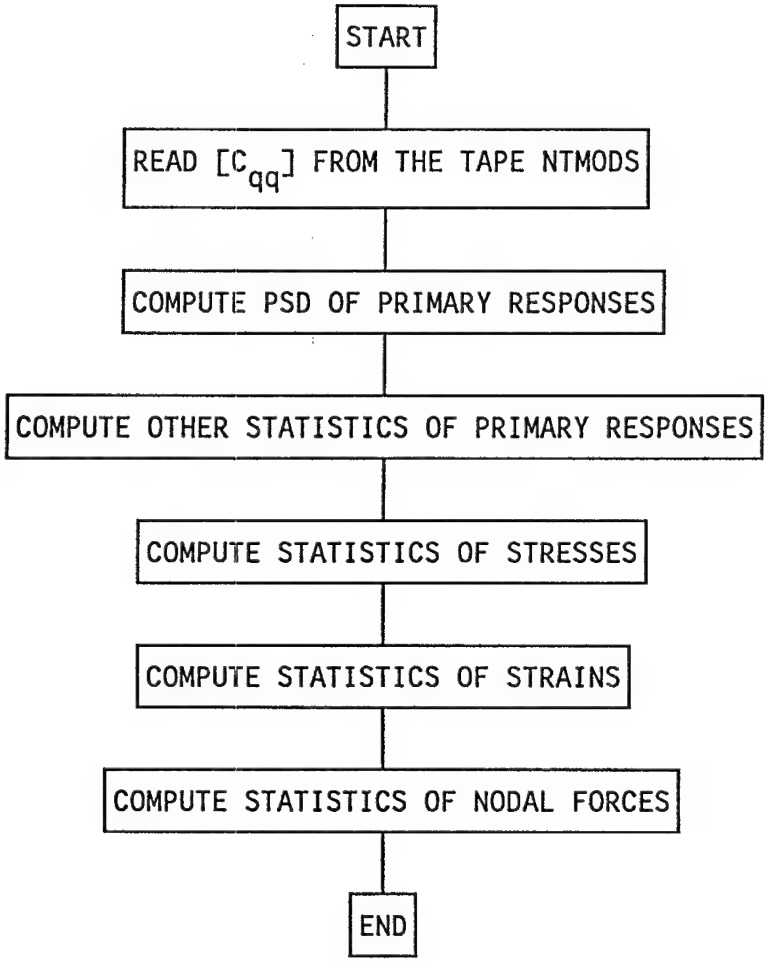

Note: Primary responses are computed in the order: DISPLACEMENTS, VELOCITIES, ACCELERATIONS

Statistics are computed in the order: PSD, COV, CORR., AP. FREQ.

FIGURE 4.5. Flow Diagram of Subroutine RANRES which Directs the Computation of the Response Statistics for all Processes

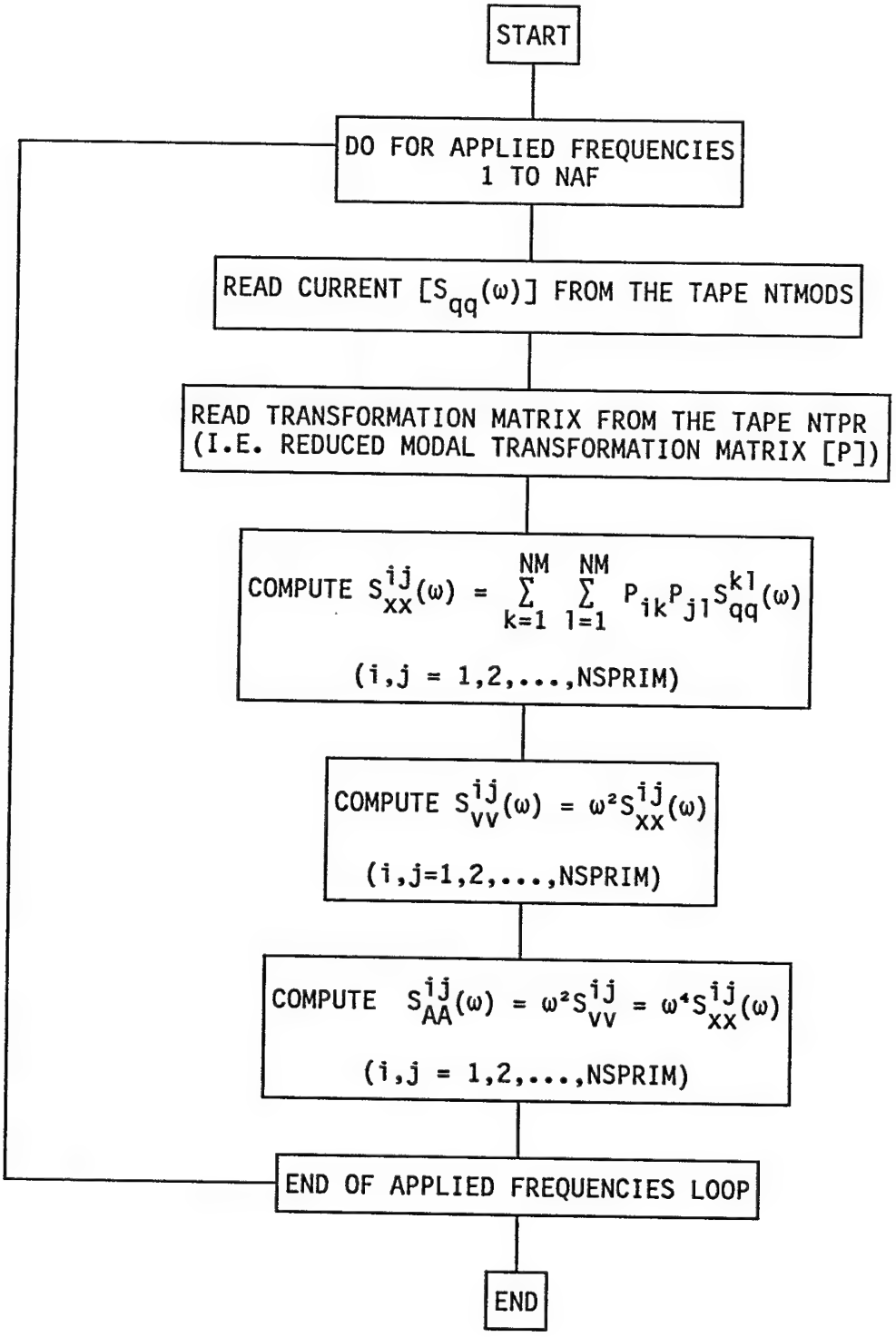

FIGURE 4.6a. Flow Diagram for the Computation of the Spectral Densities of Primary Responses in Subroutine POWERS

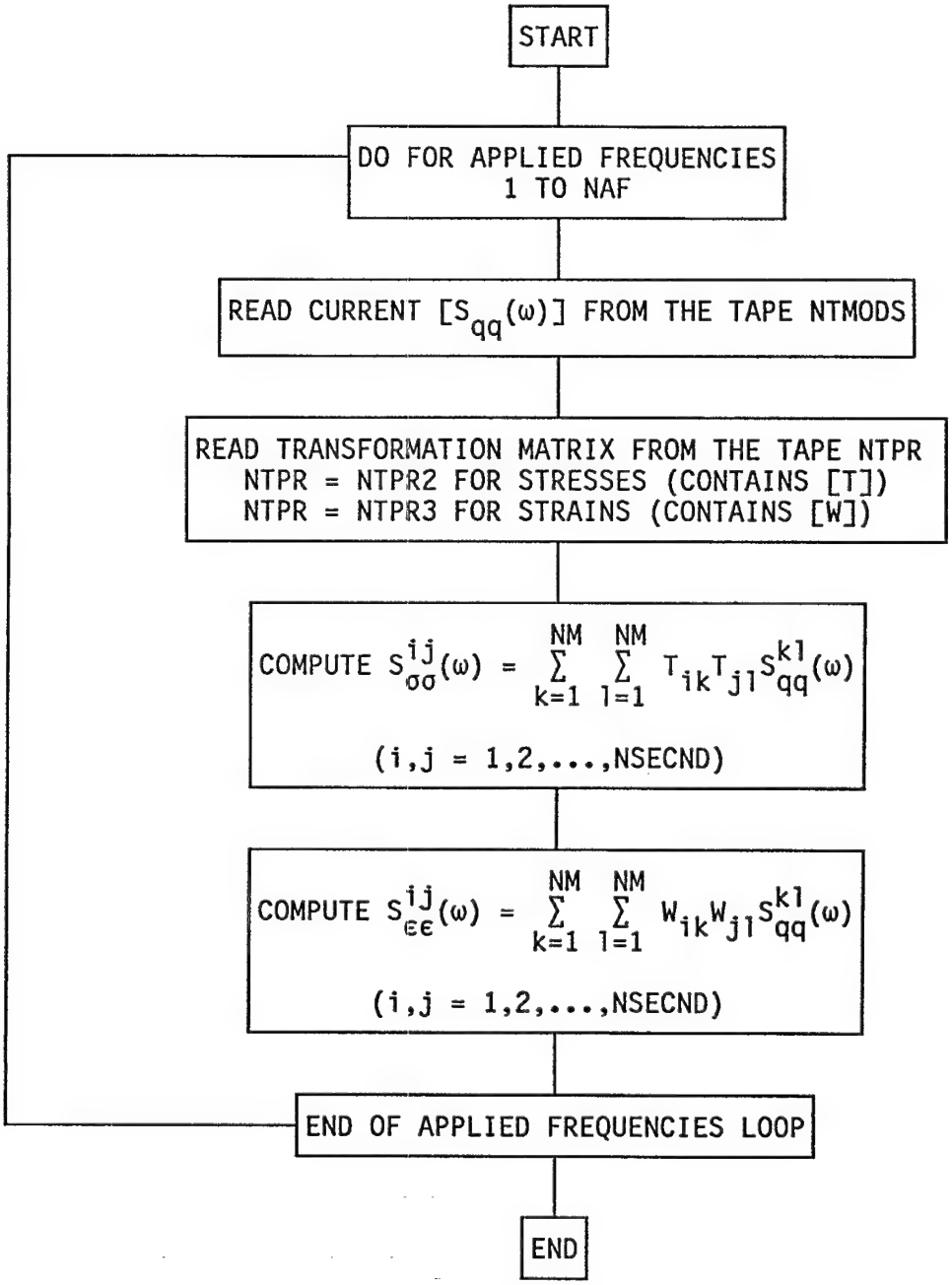

FIGURE 4.6b. Flow Diagram for the Computation of the Spectral Densities of Secondary Responses in Subroutine POWERS

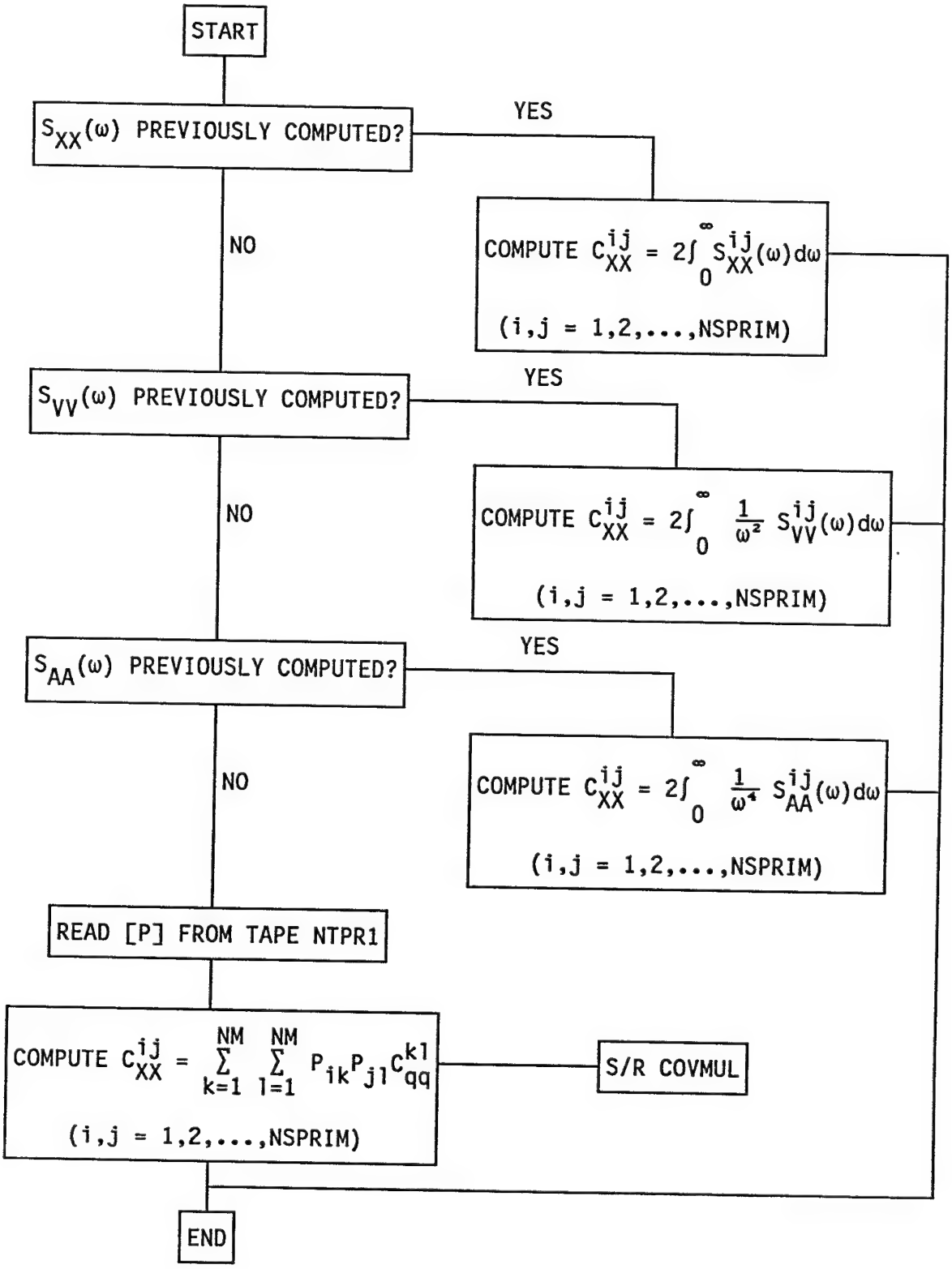

Figure 4.7a. Flow Diagram for the Computation of the Covariance Matrix of Displacements in Subroutine COVARC

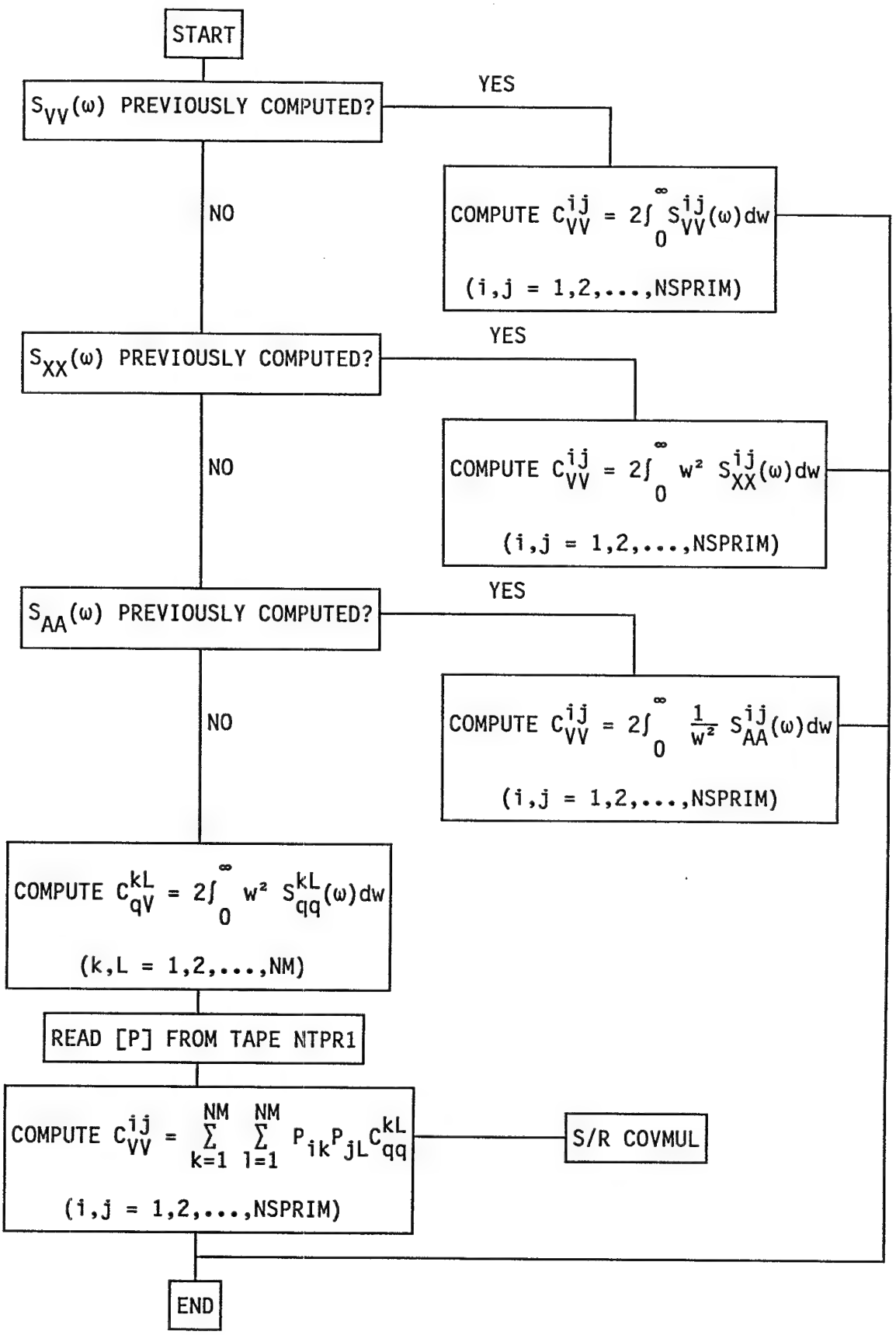

Figure 4.7b. Flow Diagram for the Computation of the Covariance Matrix of Velocities in Subroutine COVARC

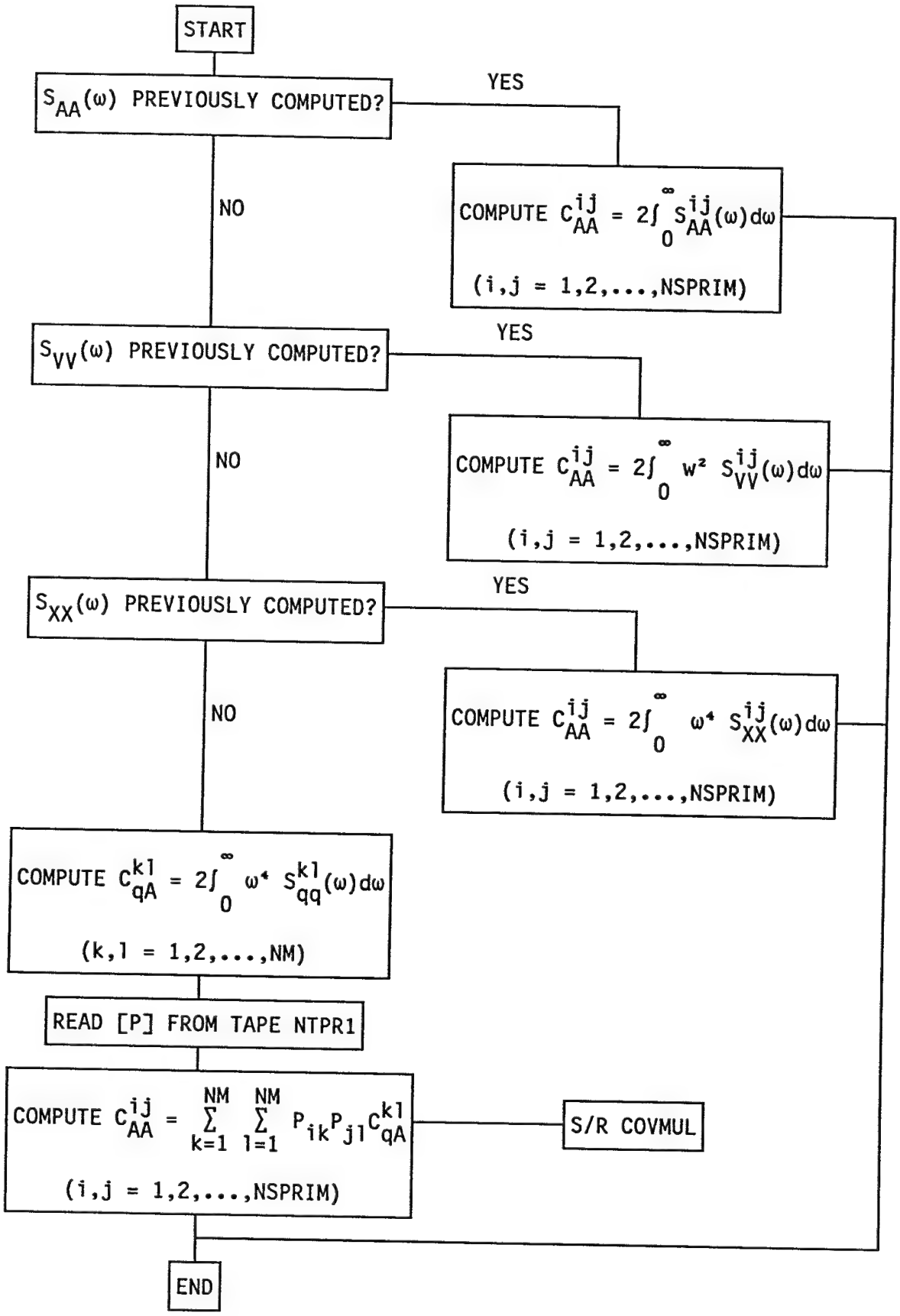

Figure 4.7c. Flow Diagram for the Computation of the Covariance Matrix of Accelerations in Subroutine COVARC

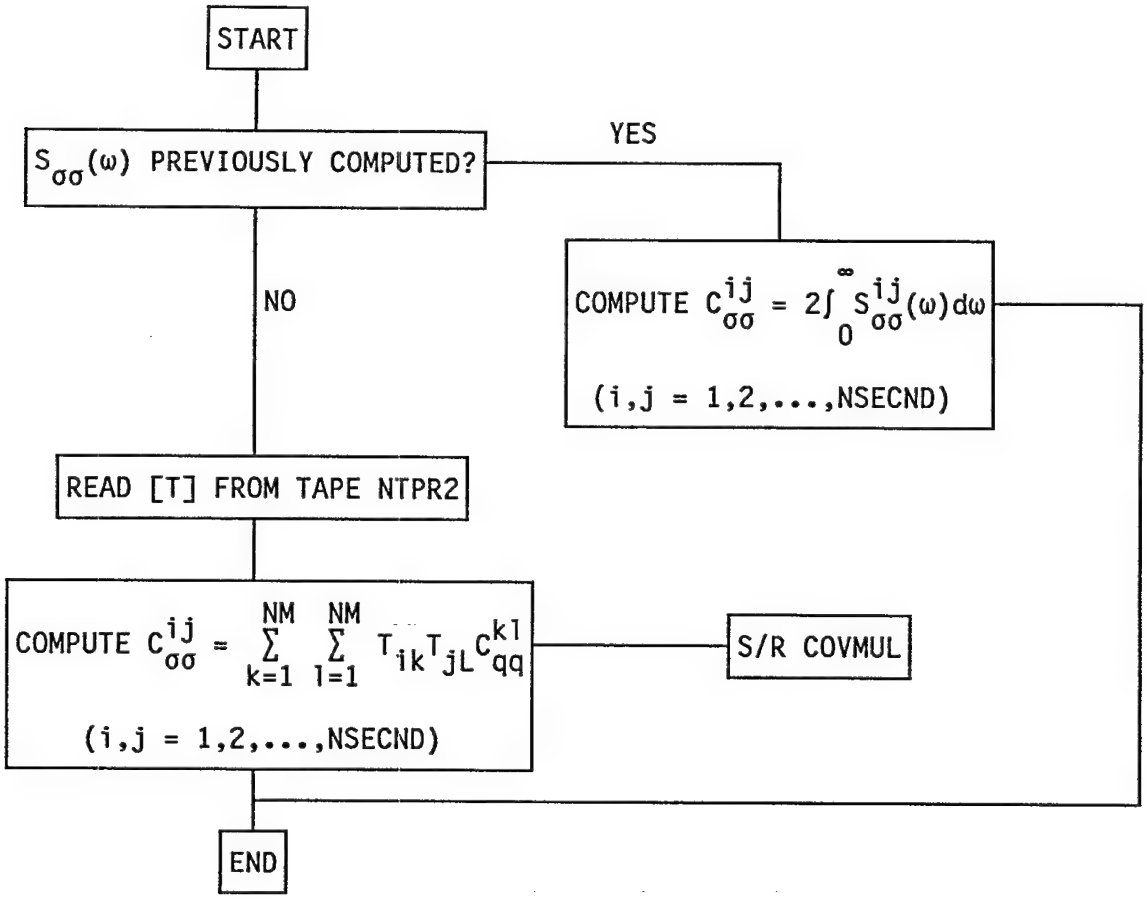

Figure 4.7d. Flow Diagram for the Computation of the Covariance Matrix of Stresses in Subroutine COVARC

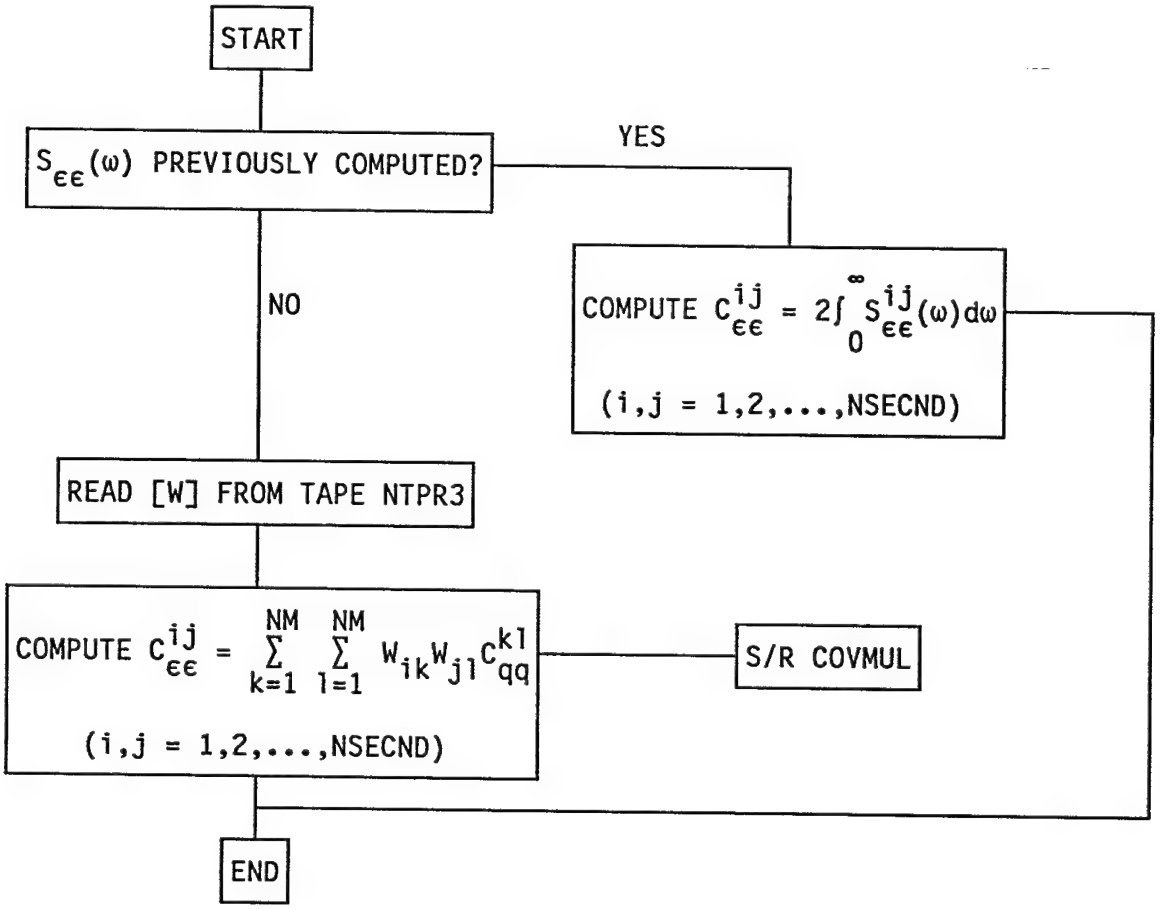

Figure 4.7e. Flow Diagram for the Computation of the Covariance Matrix of Strains in Subroutine COVARC

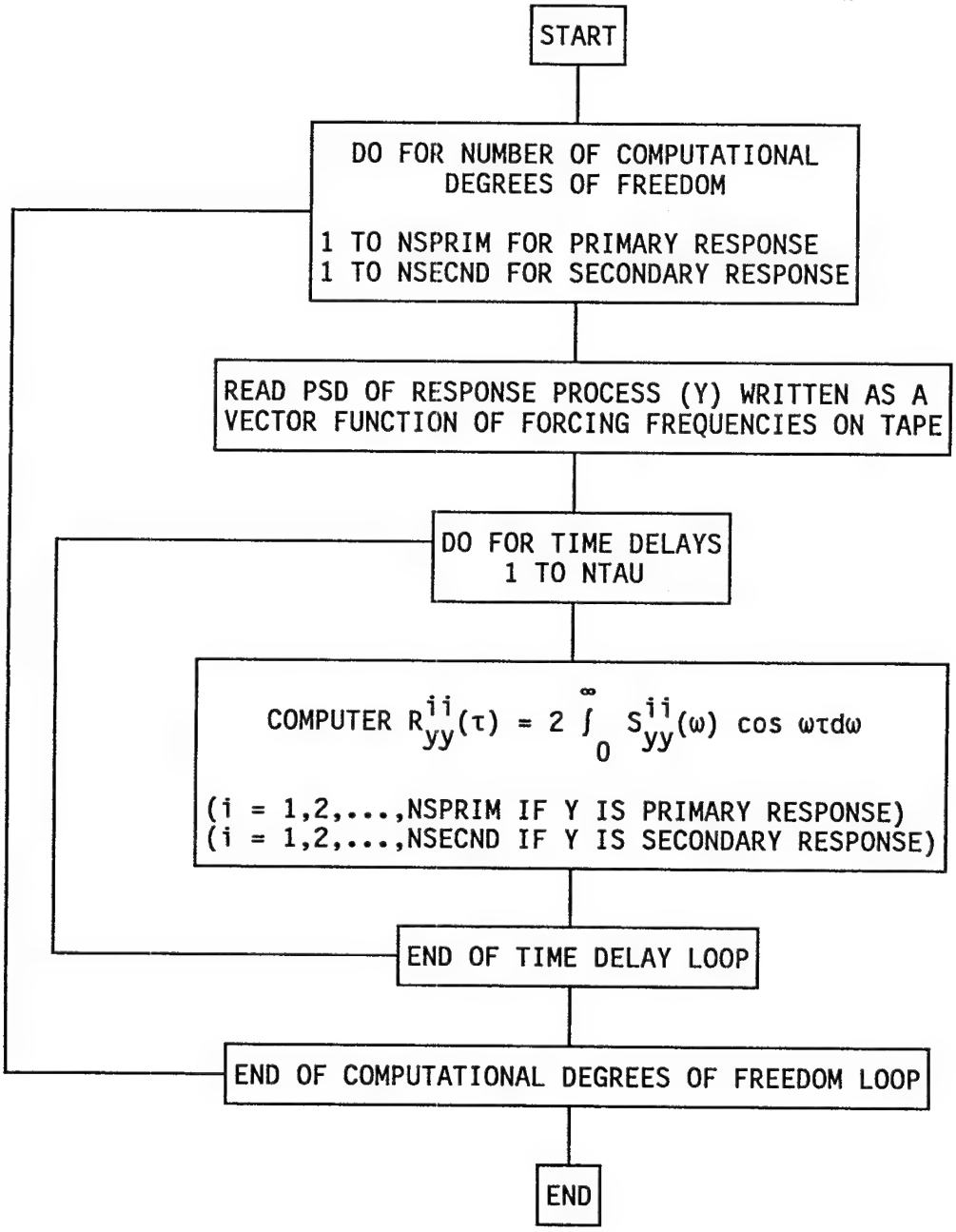

FIGURE 4.8. Flow Diagram of Subroutine CORELA for the Computation of Correlation Functions

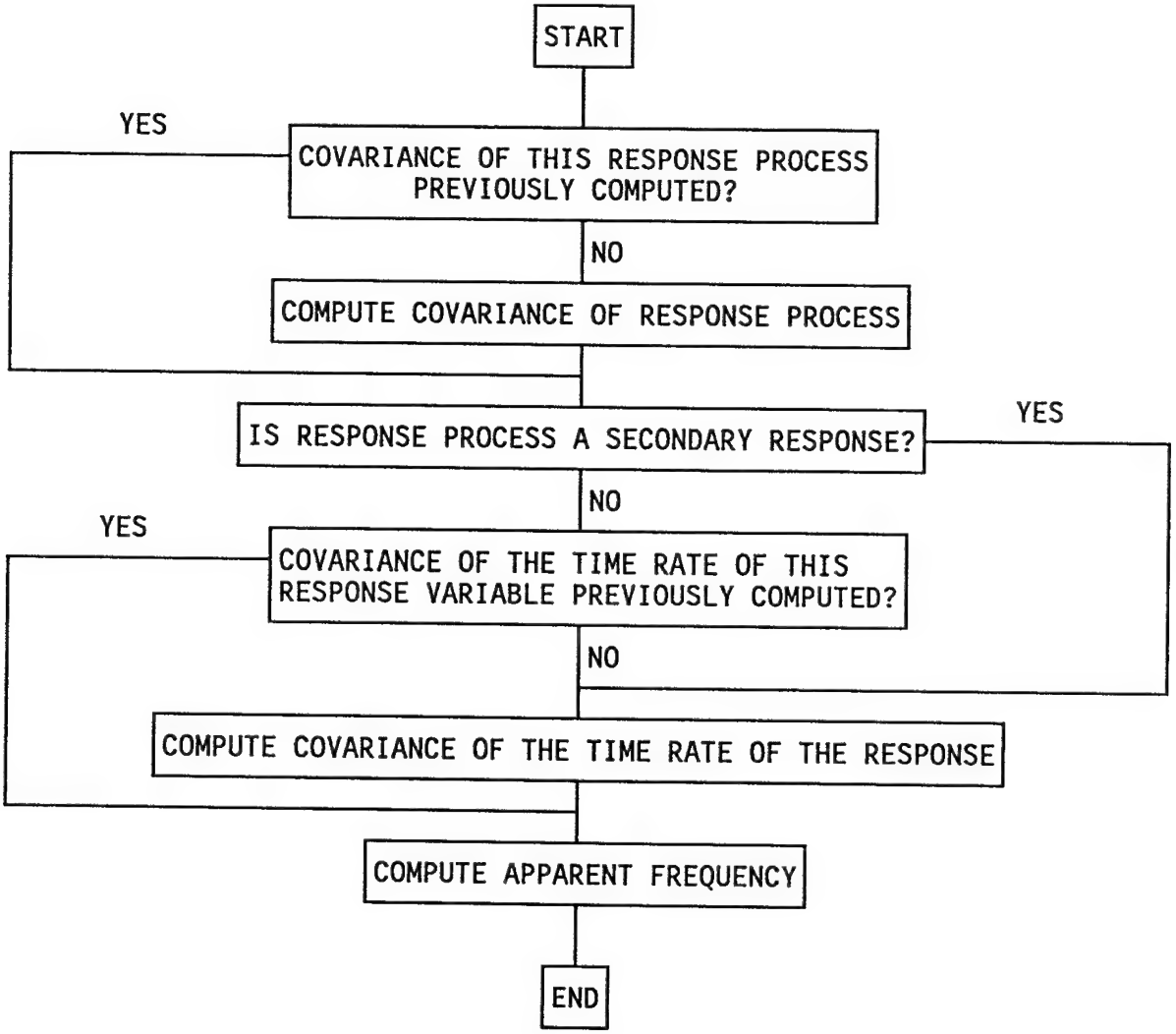

FIGURE 4.9. Flow Diagram of Subroutine APFREQ for the Computation of Apparent Frequencies

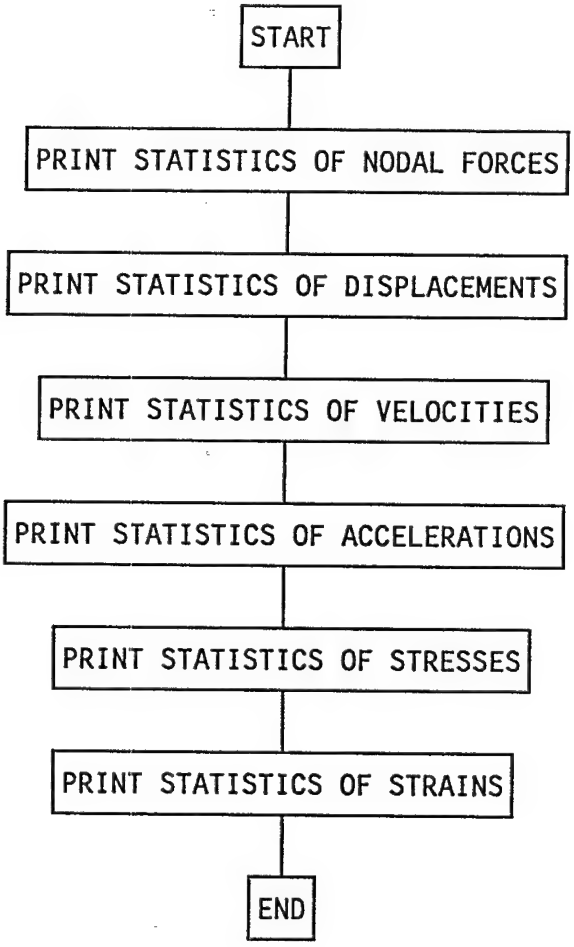

FIGURE 4.10a. Flow Diagram of Subroutine PRNTRR for Printing the Response Results in the VAST Output File (PREFX.LPT)

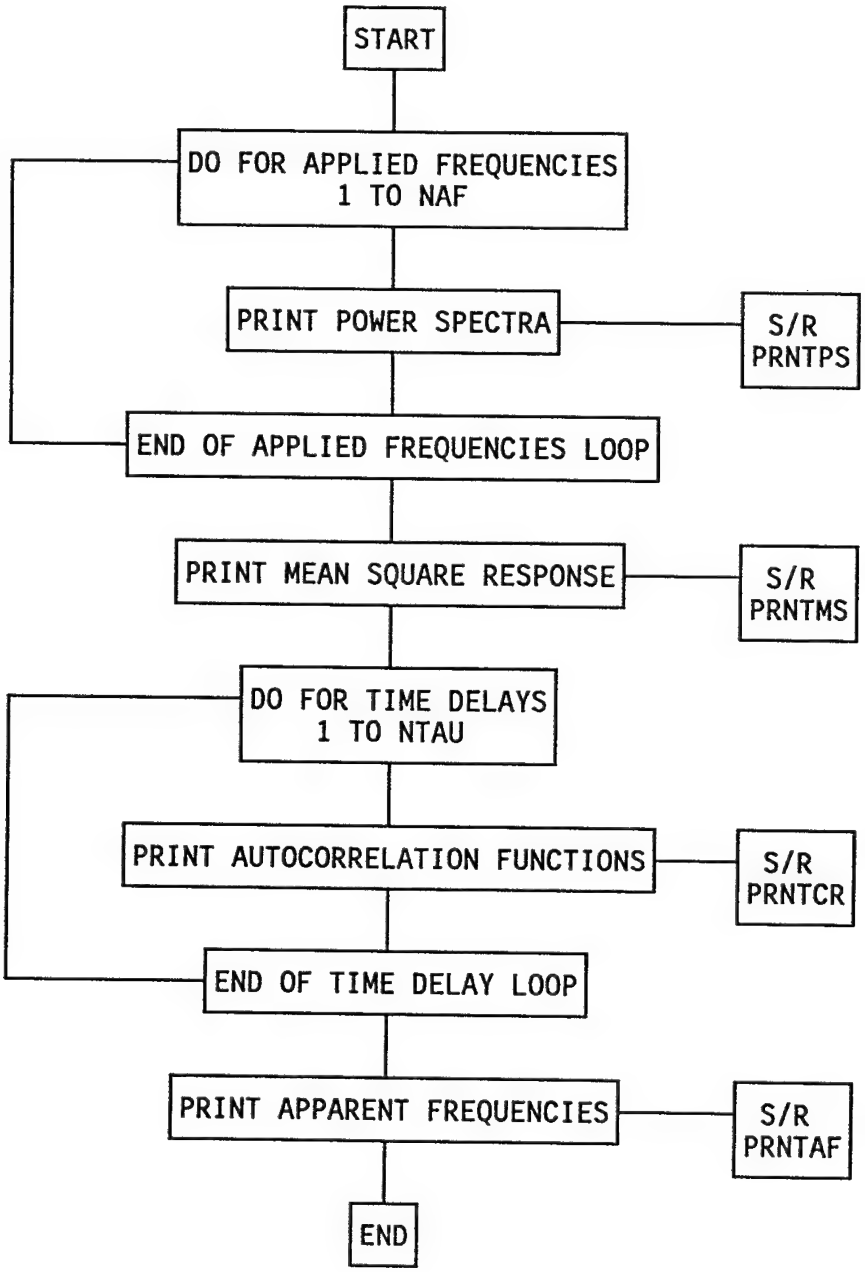

FIGURE 4.10b. Flow Diagram Illustrating the Order in which the Various Response Statistics are Printed out for Each Process

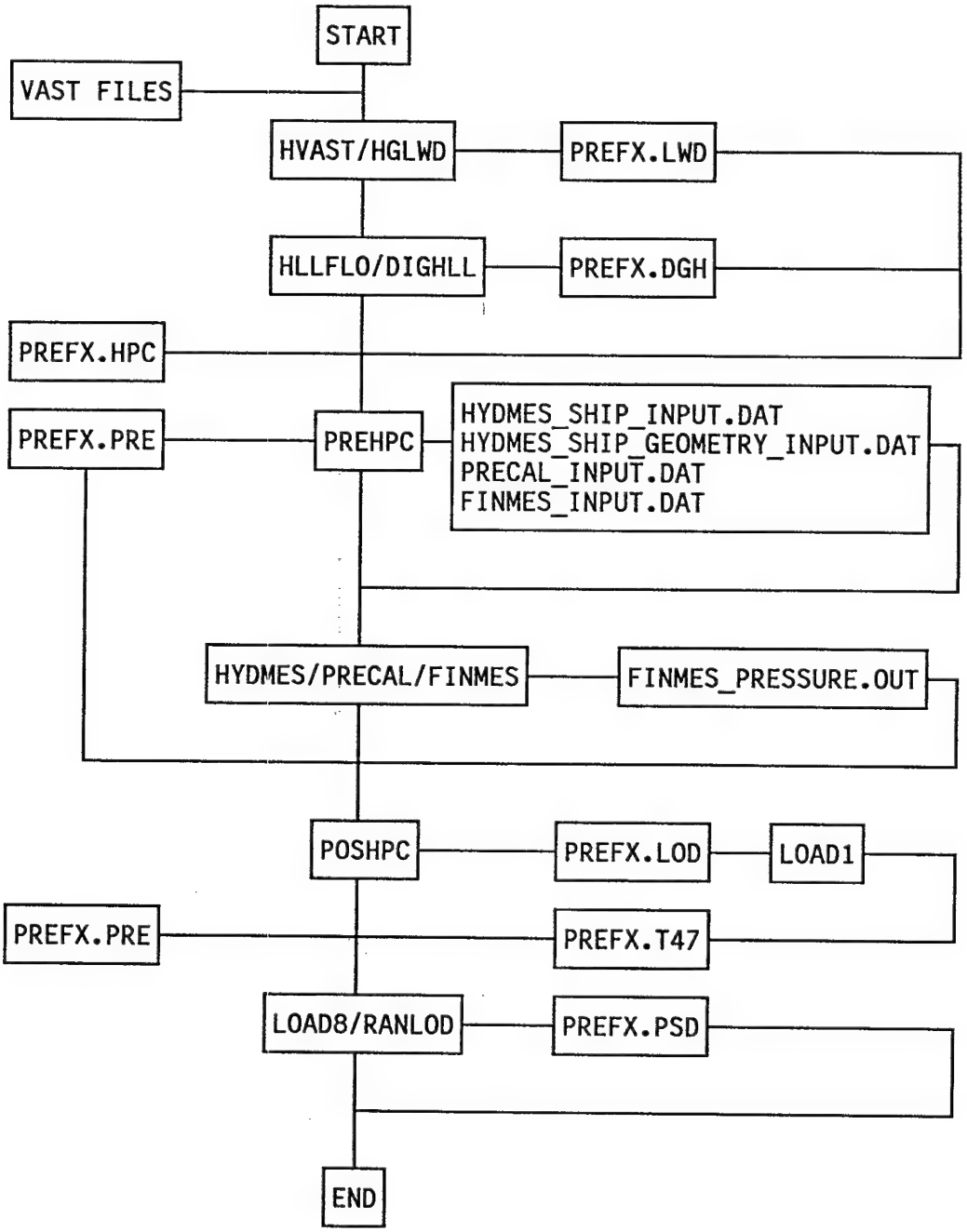

FIGURE 4.11. Procedure for Generating the Consistent Cross Spectral Density Matrix of the FEM of a Ship whose Hydrodynamic Pressure Transfer Functions are Computed by the HPCFEM Suite of Programs

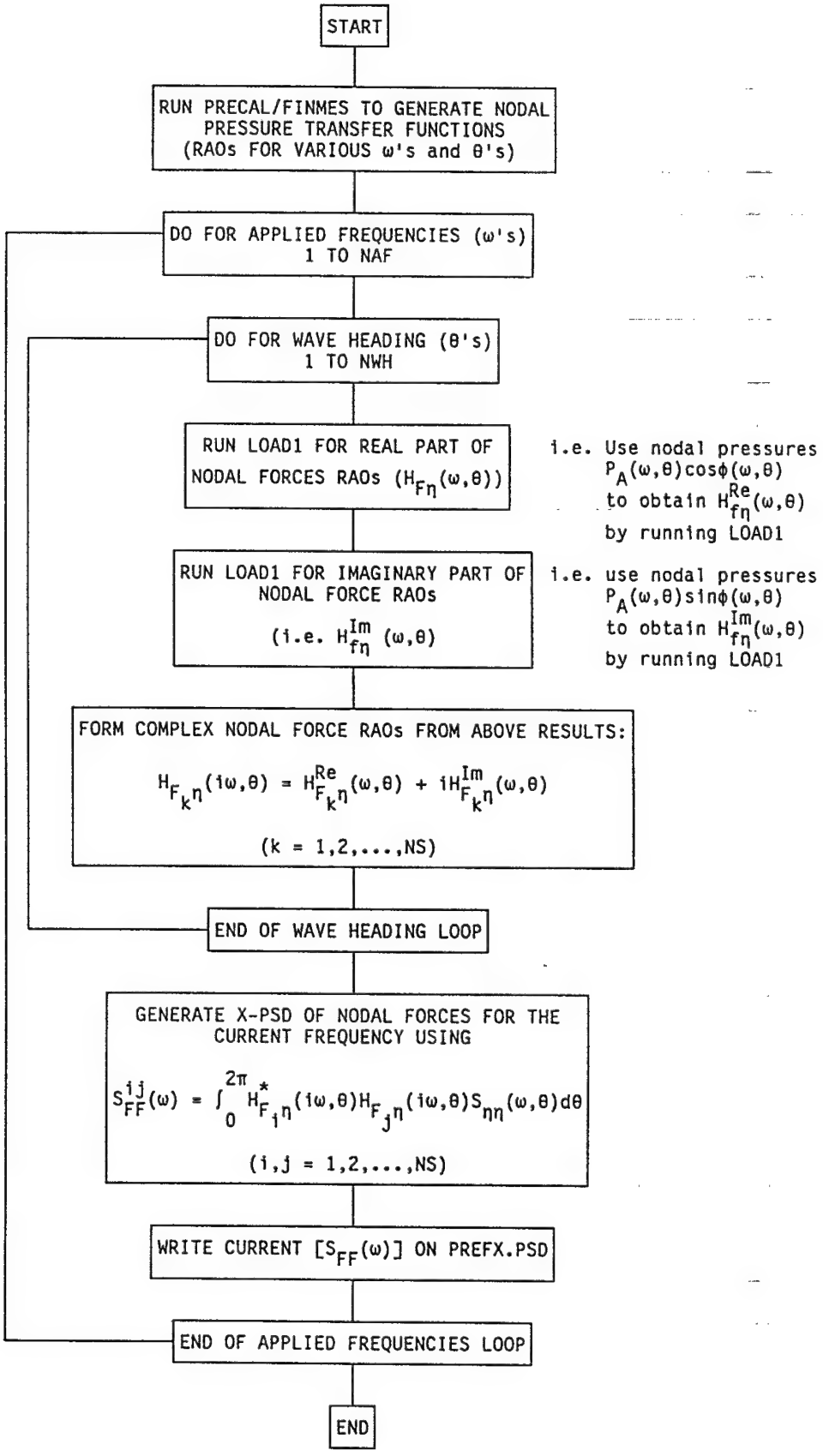

FIGURE 4.12. Procedure for Generating the PREFX.PSD File for Random Wave Loads

5.0 GRAPHICS SUPPORT FOR RANDOM VIBRATION ANALYSIS

This aspect of the contract has been deferred to the next fiscal year.

The graphics support capabilities that are planned are essentially "x-y" plots of input and output quantities. Such plots include the power spectral density of pressures, forces, displacements, velocities, accelerations, stresses, strains, versus frequency on linear, logarithmic, or semi-logarithmic scales. It is also intended to plot correlation functions of output quantities as functions of time delay.

Furthermore, in order to be able to convey a quick overall picture of the extent of deformation, it is planned to provide the capability of plotting stress and strain contours using the appropriate RMS values of the random responses.

6.0 EXAMPLE PROBLEMS

A simple example problem for the verification of the random vibration analysis program is the five span continuous beam exposed to jet noise excitation as shown in Figure 6.1. This problem has been analyzed by several workers including Olson [34]. This example was selected because it provides a rigorous verification of the computer program. First, there are non-zero off-diagonal terms in the cross-spectral density matrix of the applied load arising from the distributed nature of the random pressure field induced by the jet noise propagation. Secondly, for the five-bay beam, the natural frequencies are not widely separated as can be seen in Table 6.1. Thus, the inclusion of the cross-modal term contributions to the overall response is important.

The five span straight beam is simply supported at its ends and at the four intermediate supports as shown in Figure 6.1. Each span has unit length. The beam has a bending stiffness of unity, a mass per unit length of 10^{-4} units, and a cross-sectional area of 1000.0 units. Each span is modelled with four general beam elements (IEC=3). The damping is taken as 1% of critical damping for each of the 15 natural modes of vibration used for computing the random response.

The jet noise excitation popularly referred to as plane wave propagation of clipped white noise is assumed to propagate along the beam in the direction shown in Figure 6.1. Its power spectral density is:

$$S(\omega,\bar{X}) = \exp(-i\omega\bar{X}/C_0L) \qquad (6.1)$$

where $\bar{X} = X_2-X_1$ is the distance between the points of interest located at X_1 and X_2, C_0 is the nondimensional speed of propagation taken to be 6 (following Olson), and L is the length of a span of the beam which is taken to be 1.

The power spectral densities of displacements obtained in the VAST run agree very well with the results of Olson [34], ABAQUS [11] and Johnsen and Dey [11,36]. For nodes 3, 7, 11, 15, and 19, the power spectral densities of displacements are given in Table 6.2. Just as in ABAQUS and the paper by Johnsen and Dey, the VAST results in Table 6.2 were computed by a procedure in which the equivalent nodal forces corresponding to the distributed loading were approximated by lumping at the nodes. Although this procedure gives acceptably accurate final results for the power spectral densities and mean square responses, an examination of some intermediate modal force response results show that the use of a consistent finite element representation of the distributed random load gives more accurate results. This is because the consistent finite element representation ensures the inclusion of terms in the cross-spectral density matrix induced by loading at rotational degrees-of-freedom which are not accounted for in a load lumping approximation. Table 6.3 gives a comparison of the results of the first modal forces for the first ten forcing frequencings considered in this analysis. The exact results were given by Olson [34] as:

$$S_{ff}^{11}(\omega) = \frac{2\pi^2 A^2}{[\pi^2-(\omega/C_o)^2]^2}\,[1 + \cos(5\omega/C_o)] \qquad (6.2)$$

where A is the exact normalized amplitude of the first mode which is 0.63246 for this beam. It can be seen that the percentage errors associated with the lumping load procedure are considerably more than those obtained in a VAST analysis in which a consistent finite elelment representation of the cross-spectral density of the random loads is used. It can also be noted that the errors increase as the values of the forcing frequencies increase because the exact mathematical expression given in (6.2) is very sensitive to the value of ω. This demonstrates the importance of the capability to model distributed random loads, a capability which is lacking in ABAQUS and the ASKA II program used by Dey [36].

The mean square responses for the translational displacement degree-of-freedom and the rotational degree-of-freedom (i.e. slope) are shown in Tables 6.4A and 6.4B, respectively. It can be seen that the VAST analysis results agree very well with the results of Olson [34]. It is also interesting to note that the mean square responses obtained in VAST using the two different methods described in Chapter 4 gave exactly the same results. In other words, the mean square responses computed directly from the power spectral densities and those computed from the modal mean square response gave the same results. This is a further check on the program.

The tight budget did not permit the possibility of testing more example problems. However, a simple two-degree-of-freedom system given on Page 361 of the book by Elishakoff [7] was the first problem used for debugging and testing the program and the correct answers were obtained. It is hoped that more example problems will be run in the future.

TABLE 6.1

NATURAL FREQUENCIES OF FIVE BAY BEAM

Mode No.	Natural Frequency (rad/s)	
	Exact	Computed by VAST
1	9.8696	9.8671
2	10.9498	10.9478
3	13.6927	13.6917
4	17.2469	17.2505
5	20.764	20.7169
6	39.478	39.5564
7	41.731	41.8316
8	46.903	47.0642
9	53.124	53.3782
10	58.936	59.3007
11	88.826	90.0506
12	92.182	93.5441
13	99.798	101.4734
14	108.795	110.7851
15	117.056	119.1292

TABLE 6.2

POWER SPECTRAL DENSITIES OF DISPLACEMENTS (in distance²/HZ)

Node No.	FREQ = 1.57 HZ			FREQ = 1.74 HZ			FREQ = 2.18 HZ		
	Johnsen & Dey	ABAQUS	VAST	Johnsen & Dey	ABAQUS	VAST	Johnsen & Dey	ABAQUS	VAST
3	0.0989	0.0963	0.0968	0.8447	0.7911	0.7917	0.1127	0.0845	0.0848
7	0.0848	0.0879	0.0879	0.3251	0.3419	0.3412	0.0170	0.0229	0.0231
11	0.0609	0.0607	0.0610	0.0018	0.0021	0.0022	0.1696	0.1701	0.1709
15	0.0411	0.0375	0.0378	0.3115	0.3002	0.2991	0.0170	0.0110	0.0110
19	0.0318	0.0342	0.0344	0.8222	0.8882	0.8859	0.1127	0.1409	0.1414

TABLE 6.3

POWER SPECTRAL DENSITY OF MODAL FORCES
FOR THE FIRST MODE (SFM(1,1)) AT VARIOUS FORCING FREQUENCIES

Forcing Frequency (rad/s)	Exact	Consistent FE Load Representation		Load Lumping Approximation	
		Value	% Error	Value	% Error
0.0	0.162114E+00	0.161999E+00	0.07	0.145764E+00	10.08
0.986711E+01	0.983786E-01	0.983152E-01	0.06	0.911085E-01	7.39
0.109478E+02	0.833137E-02	0.833969E-02	0.10	0.778139E-02	6.60
0.136917E+02	0.509409E+00	0.508663E+00	0.15	0.484238E+00	4.94
0.172505E+02	0.234608E+01	0.234470E+01	0.06	0.230600E+01	1.71
0.207169E+02	0.184701E+01	0.184906E+01	0.11	0.188878E+01	2.26
0.395564E+02	0.715720E-02	0.759556E-02	6.12	0.103953E-01	45.24
0.418316E+02	0.238297E-03	0.257319E-03	7.98	0.36696E-03	53.99
0.470642E+02	0.310576E-02	0.354043E-02	14.00	0.555000E-02	78.74
0.533782E+02	0.308945E-02	0.388650E-02	25.80	0.678970E-02	119.77

TABLE 6.4A

ROOT MEAN SQUARE DISPLACEMENT RESPONSE

Node No.	RMS Displacement		
	Olson [34]	VAST	% Difference
1	0.0	0.0	0.00
2	0.1719	0.1702	0.99
3	0.2274	0.2257	0.75
4	0.1557	0.1535	1.41
5	0.0	0.0	0.0
6	0.1225	0.1197	2.29
7	0.1534	0.1517	1.11
8	0.1040	0.1029	1.06
9	0.0	0.0	0.0
10	0.0904	0.0944	4.42
11	0.1176	0.1246	5.95
12	0.0841	0.0879	4.52
13	0.0	0.0	0.0
14	0.0889	0.0878	1.24
15	0.1360	0.1341	1.40
16	0.1129	0.1107	1.95
17	0.0	0.0	0.0
18	0.1585	0.1581	0.25
19	0.2391	0.2399	0.33
20	0.1793	0.1800	0.39
21	0.0	0.0	0.0

TABLE 6.4B

ROOT MEAN SQUARE SLOPE RESPONSE

Node No.	RMS Displacement		
	Olson [34]	VAST	% Difference
1	0.7988	0.7894	1.18
2	0.5101	0.5062	0.76
3	0.2775	0.2628	5.30
4	0.5319	0.5300	0.36
5	0.6308	0.6116	3.05
6	0.3436	0.3409	0.79
7	0.2421	0.2280	5.82
8	0.3662	0.3613	1.34
9	0.4378	0.4388	0.23
10	0.2819	0.2986	5.92
11	0.2253	0.2241	0.53
12	0.2902	0.3064	5.58
13	0.3801	0.3827	0.68
14	0.3308	0.3265	1.30
15	0.2216	0.2143	3.29
16	0.3005	0.2972	1.10
17	0.6113	0.6004	1.78
18	0.5652	0.5684	0.57
19	0.2198	0.2159	1.77
20	0.5378	0.5397	0.35
21	0.8235	0.8263	0.34

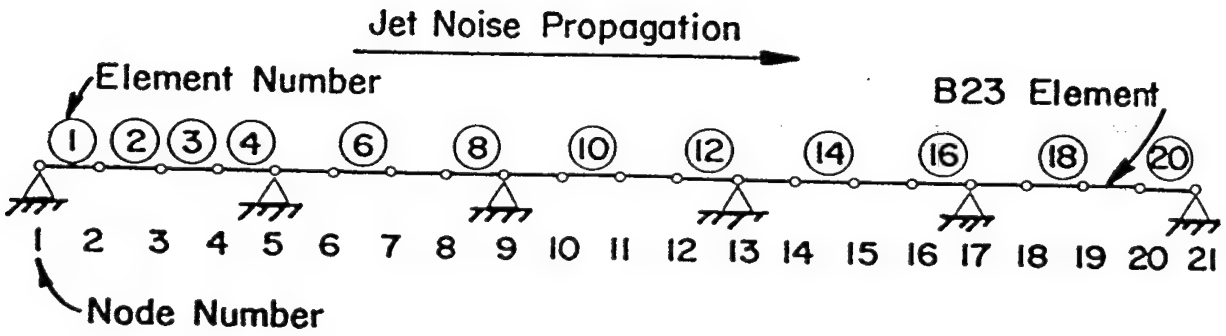

FIGURE 6.1. A Five Bay Beam Excited by Jet Noise

7.0 CONCLUSIONS AND RECOMMENDATIONS FOR FUTURE WORK

The integrity checks and verification problems in respect of the random vibration analysis program has been very encouraging. Overall, a quite respectable random vibration analysis capability has been provided for the VAST finite element program. The capability that has been provided surpasses that of most commercial finite element programs in that cross statistical properties are computed, a specialized distributed random load modelling capability has been implemented, and a variety of statistical properties of different processes may be requested by the user.

There are a few items that remain to be implemented to complete the first phase of the contract. First, the procedure for computing the statistical properties of stress and strain responses could not be implemented due to budget limitations. However, an elegant procedure has been designed to achieve this end in the near future. Secondly, the testing of the random load generation program using a real ship structure could not be performed because there was no provision made for that in the contract. Finally, the provision of a graphics support capability has been deferred to the next fiscal year.

In addition to the above, it is recommended that immediate enhancements to the RANVIB module should include the following:

(i) Capability for analysis involving the use of superelements;

(ii) Capability for response analysis of structures excited by support motion so that problems involving earthquake excitations (for example) can be dealt with;

(iii) Capability for dealing with models that make use of multipoint constraints;

(iv) Provision of a more generalized capability for computing the consistent cross spectral density matrix of distributed random loads as discussed in Chapter 3; and

(v) General algorithmic improvements to increase computation speeds.

On the long term, the development of RANVIB should be vigorously pursued because probabilistic analysis is gaining wider acceptance among designers and analysts. In the future other capabilities to be provided should include the ability to handle combined deterministic and random loading, situations involving initial stresses, and response to nonstationary and nonhomogeneous loads.

It should be noted that the main purpose of a probabilistic analysis of a structure is to be able to assess its integrity and, above all, make quantitative statements about the probability that it will perform its intended function satisfactorily. The subject that deals with this is referred to as structural reliability and so the ultimate objective should be the provision of a reliability analysis capability in VAST. A reliability analysis module would make use of the response statistics computed in the random vibration analysis module to make quantitative predictions about the probability of failure or safety of the structure. The scientific authority, recognizing that the issue of fatigue damage and reliability are very important to ship structures, included a provision in the second phase of the contract for conducting a state-of-the-art literature review and making appropriate recommendations. This aspect of the contract was also performed during this year and a separate report [41] on the literature review and recommendations has been prepared as called for in the contract.

It is hoped that the scientific authority maintains an interest in this project and continues to give it the dedicated commitment and support it truly deserves.

REFERENCES

1. A.E. MANSOUR, Probabilistic Design Concepts in Ship Structural Safety and Reliability, SNAME Transactions, Vol. 80, pp. 64-97 (1972).

2. J.A. PINKSTER et al., Stochastic Modelling, Report of Committee V.6, 10th International Ship & Offshore Structures Congress, Denmark, 1988, pp. 224-250 (1988).

3. P.D. SPANOS, Probabilistic Offshore Mechanics, CML Publications (1985).

4. T.T. SOONG, Random Differential Equations in Science and Engineering, Academic Press Inc., New York (1973).

5. D.E. NEWLAND, An Introduction to Random Vibrations and Spectral Analysis, Longman Inc., New York (1975).

6. Y.K. LIN, Probabilistic Theory of Structural Dynamics, Robert E. Krieger Publishing Company, Inc., Malabar, Florida (1976).

7. I. ELISHAKOFF, Probabilistic Methods in the Theory of Structures, John Wiley & Sons, Inc., New York (1983).

8. S.H. CRANDALL and W.Q. ZHU, Random Vibration: A Survey of Recent Developments, Transactions of the ASME, Journal of Applied Mechanics, Vol. 50, pp. 953-962 (1983).

9. M. PETYT, Finite Element Methods for the Response of Structures to Random Excitations, Internal Report, Institute of Sound and Vibration Research, University of Southampton, England (1975).

10. M. SHINOZUKA, T. KAKO, and A. TSURUI, Random Vibration Analysis in Finite Element Formulation, In: Random Vibration-Status and Recent Developments, I. Elishakoff and R.H. Lyon, Eds., Elsevier, Amsterdam (1986).

11. ABAQUS Theory Manual, Version 4.8, Section 3.11.6, Hibbitt, Karson & Sorensen, Inc., Providence, Rhode Island (1989).

12. MSC/NASTRAN Theory Manual, Section 12, The MacNeil-Schwendler Corporation, Los Angeles, California (1983).

13. H. KARADENIZ, S. VAN MANEN, and A. VROUWENVELDER, Probabilistic Reliablity Analysis for the Fatigue Limit State of Gravity and Jacket-Type Structures, In: Behaviour of Off-Shore Structures, C. Chryssostomidis and J.J. Connor, Eds., Proceedings of the Third International Conference, Volume 2, pp. 147-165 (1983).

14. N.C. NIGAM, Introduction to Random Vibrations, The MIT Press, Cambridge, Massachusetts (1983).

15. D.J. GRONIN, P.S. GODFREY, P.M. HOOK, and T.A. WYATT, Spectral Fatigue Analysis for Offshore Structures, In: Numerical Methods in Offshore Engineering, O.C. Zienkiewicz, R.W. Lewis, K.G. Stagg, Eds., John Wiley and Sons, New York (1978).

16. S.K. CHAKRABARTI, Hydrodynamics of Offshore Structures, Chapters 6 and 7, Computational Mechanics Publications, Boston, 1987.

17. F. KIRKEMO, Applications of Probabilistic Fracture Mechanics to Offshore Structures, Applied Mechanics Reviews, Vol. 41, No. 2, pp. 61-84 (1984).

18. Y. GODA, Random Seas and Design of Maritime Structures, Chapter 2, Page 27, Chapter 8, University of Tokyo Press (1985).

19. M.K. OCHI, Stochastic Analysis and Probabilistic Prediction of Random Seas, In: Advances in Hydroscience, Ven Te Chow, Ed., Vol. 3, pp. 217-375, Academic Press Inc. (1982).

20. O. NWOGU, Maximum Entropy Estimation of Directional Wave Spectra from an Array of Wave Probes, Applied Ocean Research, Vol. 11, No. 4, pp. 1976-182 (1989).

21. B.-A. JUSZKO, Parameterization of Directional Spectra, Contractor Report CR189/414 prepared for Defence Research Establishment Atlantic (DREA) by Juszko Scientific Services, Victoria, B.C., Canada (March 1989).

22. M.K. OCHI and E.N. HUBBLE, Six-Parameter Wave Spectra, In: Proceedings of the 15th Coastal Engineering Conference, Honolulu, Hawaii, pp. 301-328 (1976).

23. W.G. PRICE and R.E.D. BISHOP, Probabilistic Theory of Ship Dynamics, Chapter 9, Chapman and Hall, London (1974).

24. R.A. DAWKINS, NSMB Co-Operative Sea Loads Working Group - User's Manual for HPCFEM Suite of Programs, T.P.D.D. Report No. 88/7, Lloyd's Register of Shipping, London, U.K. (March 1989). LIMITED DISTRIBUTION.

25. R.A. DAWKINS, Specification of Hydrodynamic Pressure Calculation Program, Hull (N.C.) Division Report No. 85/27, Lloyd's Register of Shipping, London, U.K. (October 1985). LIMITED DISTRIBUTION.

26. D. COOPER and A.K. BROOK, Hydrodynamic Pressure Project : Correlation Between HPCFEM & Experiment, Report No. W1815 (Part 1, Rev. 1) for NSMB Co-Operative Research Ship Sea-Loads Working Group, British Marine Technology Report (November 1988). LIMITED DISTRIBUTION.

27. D. COOPER and A.K. BROOK, Hydrodynamic Pressure Project: Correlation Between HPCFEM & Experiment, Report No. W1815 (Part 2, Rev. 1) for NSMB Cooperative Research Ship Sea-Loads Working Group, British Marine Technology Report (November 1988). LIMITED DISTRIBUTION.

28. H.H. CHEN, J.M. TORNG, and Y.S. SHIN, Formulation, Method of Solution and Procedures for Hydrodynamic Pressure Project, Research and Development Division Technical Report No. RD-85026, prepared for NSMB Cooperative Research American Bureau of Shipping (ABS) (November 1985). LIMITED DISTRIBUTION.

29. H.H. CHEN, J.M. TORNG, and Y.S. SHIN, Appendix B of ABS Technical Report RD-85026 (December 1987). LIMITED DISTRIBUTION.

30. J.M. TORNG, Y.S. SHIN, and H.H. CHEN, Theoretical Manual for Three-Dimensional Hydrodynamic Pressure Calculation Program (PRECAL), Research and Development Disision Technical Report No. RD-88025, prepared for NSMB Cooperative Research Sea Loads Working Group, American Bureau of Shipping (December 1988). LIMITED DISTRIBUTION.

31. H. CONTRERAS, The Stochastic Finite-Element Method, Computers & Structures, Vol. 12, pp. 341-348 (1980).

32. W.K. LIU, T. BELYTSCHKO, and A. MANI, Random Field Finite Elements, International Journal for Numerical Methods in Engineering, Vol. 23, pp. 1831-1845 (1986).

33. E. VANMARCKE, M. SHINOZUKA, S. NAKAGIRI, G.I. SCHUELLER, and M. GRIGORIU, Random Fields and Stochastic Finite Elements, Structural Safety, Vol. 3, pp. 143-166 (1986).

34. M.D. OLSON, A Consistent Finite Element Method for Random Response Problems, Computers and Structures, Vol. 2, pp. 163-180 (1972).

35. M.D. OLSON and G.M. LINDBERG, Jet Noise Excitation of an Integrally Stiffened Panel, Journal of Aircraft, Vol. 8, No. 11, pp. 847-855 (1971).

36. S.S DEY, Finite Element Method for Random Response of Structures Due to Stochastic Excitation, Computer Methods in Applied Mechanics and Engineering, Vol. 20, pp. 173-194 (1979).

37. T.Y. YANG and R.K. KAPANIA, Finite Element Random Response Analysis of Cooling Tower, Transactions of the ASCE, Journal of Engineering Mechanics, Vol. 110, No. 4, pp. 589-609 (1984).

38. Vibration and Strength Analysis (VAST) User's Manual, Version #05, Martec Limited, Halifax, Nova Scotia (1989).

39. M. NORWOOD, M. CHERNUKA, G. NIGH, D. FANNING, and R. JATEGAONKAR, Vibration and Strength Analysis of Ship Hulls and Appendages by Finite Element Methods (HVAST), User's Manual - Version 2 (October 1984).

40. D. HALLY, HLLFLO User's Guide, Technical Communication 86/306, Defence Research Establishment Atlantic (DREA) (October 1986).

41. I.R. ORISAMOLU and M.W. CHERNUKA, Fatigue Analysis Under Random Loads and Structural Reliability : A State of the Art Review, Martec Technical Report No. 91-1 (March 1991).

APPENDIX A

DESCRIPTION OF INPUT DATA FILE PREPARATION FOR RUNNING PROGRAM RANVIB

The following is a description of the method for creating the PREFX.RIN file to be used as the input data file for running a random response analysis in VAST.

The user is advised to exercise caution in requesting the computations of the various statistical properties of the different possible random processes because a random response analysis is more expensive than a corresponding deterministic dynamic analysis. As such, it is recommended that only responses of interest should be selected by the user through the appropriate codes. Also, where possible, selective computations in which only a selected number of nodal locations are requested are recommended.

FORMAT OF INPUT FILE: PREFX.RIN

NOTE: STATS = Statistical Properties
Primary Responses = displacements, velocities, and accelerations
Secondary Responses = stresses and strains
(Computation of secondary responses not yet implemented.)

Card 1A (2I5)

IOPT	= 1	Modal frequency response method for analysis
	= 2	Direct frequency response method for analysis
IDAMP	= 1	Modal damping ratios used for describing damping (ξ_γ, γ=1,2,...,NM) (NOTE: Not applicable for IOPT=2)
	= 2	Proportional or Rayleigh Damping ($C = \alpha_m M + \alpha_k K$)
	= 3	Structural Damping ($C\dot{X} = igKX$)

Card 1B (I5) (Omit if IOPT≠1)

IRESP1	= 0	Only modal response to be computed during this run, i.e. for the sole purpose of creating PREFX.RMR
	= 1	Random response to be computed using the modal response computed during the current program run
	= 2	Random response to be computed using the modal response computed during a previous program run (PREFX.RMR must be available for this selection. This is like a restart and will usually reduce computation time significantly.)

Card 1C (I5) (Omit if IOPT≠2)

IRESP2	= 0	Only complex frequency response function to be computed during this run, i.e. for the sole purpose of creating PREFX.CFR
	= 1	Random response to be computed using the complex frequency response function computed during the current program run
	= 2	Random response to be computed using the complex frequency response function computed during a previous program run (PREFX.CFR must be available for this selection. This is like a restart and will usually reduce computation time significantly.)

Card 1D (2E10.3) (Omit if IDAMP ≠ 2)

ALFAM = α_M (constant in Rayleigh damping model)
ALFAK = α_K (constant in Rayleigh damping model)

Card 1E (E10.3) (Omit if IDAMP ≠ 3)

STRDMP = g (structural damping factor)

Card 1F (4I5)

IFORCE	= 0	Force STATS not required
	= 1	Force STATS wanted at all nodes
	= -1	Force STATS wanted only at selected nodes
IPRIMY	= 0	STATS of primary responses not required
	= 1	STATS of primary responses wanted at all nodes
	= -1	STATS of primary responses wanted at selected nodes
ISECND	= 0	STATS of secondary responses not required
	= 1	STATS of secondary responses wanted at all nodes
	= -1	STATS of primary responses wanted at selected nodes
NTAU	= 0	No correlation functions are required
	= NTAU	Correlation functions will be required in the analysis (maximum of 100)

where

NTAU = number of sequence of non-zero τ values for which the correlation functions are to be computed

(Note: If ISECND≠0, the user must have requested the computation of modal stresses by setting the master control code ISTRES to 1 so that the PREFX.T53 file containing modal stresses would have been generated and used in POSTV2 for the generation of averaged nodal stresses/strains. Of course, the user must also have appropriately requested a POSTV2 batch run.)

Card 2 Information for the calculation and printout of the statistical properties (i.e. STATS) of random nodal forces

(Omit if IFORCE=0)

Card 2A (I5)

IFX	= 1	Only AUTO-STATS of forces are of interest
	= 2	Both AUTO- and CROSS-STATS of forces are of interest

Card 2B (4I5)

IFST(1)	= 0	Power spectral densities of forces not of interest
	= 1	Power spectral densities of forces to be saved on random force file and printed in output file
	= -1	Power spectral densities of forces saved but not printed
IFST(2)	= 0	Covariance of forces not of interest
	= 1	Covariance of forces to be computed and printed
	= -1	Covariance of forces to be computed but not printed
IFST(3)	= 0	Autocorrelation functions of forces not of interest
	= 1	Autocorrelation functions of forces to be computed and printed
	= -1	Autocorrelation functions of forces to be computed but not printed
IFST(4)	= 0	Apparent frequencies of force not of interest
	= 1	Apparent frequencies of force to be computed and printed
	= -1	Apparent frequencies of force to be computed but not printed

Card 2C (omit if IFORCE≠-1)

Card 2C(i) (I5)

NFN = Number of nodes for which nodal force STATS are required

Card 2C(ii)

(JFN(I), I=1, NFN) Actual node numbers (arranged in ascending order) for which STATS of nodal forces are wanted.

(Note: Error message is issued if IFORCE≠0 but IFST(1)=IFST(2)=IFST(3)=IFST(4)=0)

Card 3 Information for the calculation and printout of the STATS of primary responses

(omit if IPRIMY=0)

Card 3A (4I5)

IPX	= 0	Only AUTOSTATS of primary responses are of interest
	= 1	Both AUTO- and CROSS-STATS of primary responses wanted
IPD	= 0	Displacement STATS not wanted
	= 1	Displacement STATS wanted
IPV	= 0	Velocity STATS not wanted
	= 1	Velocity STATS wanted
IPA	= 0	Acceleration STATS not wanted
	= 1	Acceleration STATS wanted

(Note: Error message is issued if IPRIMY≠0 but IPD=IPV=IPA=0)

Card 3B(i) (4I5) (omit if IPD=0)

IDD(1)	= 0	Power spectral densities of displacements not of interest
	= 1	Power spectral densities of displacements to be computed and printed

	= -1	Power spectral densities of displacements to be computed but not printed
IDD(2)	= 0	Covariance of displacements not of interest
	= 1	Covariance of displacements to be computed and printed
	= -1	Covariance of displacements to be computed but not printed
IDD(3)	= 0	Correlations of displacements not of interest
	= 1	Correlations of displacements to be computed and printed
	= -1	Correlations of displacements to be computed but not printed
IDD(4)	= 0	Apparent frequencies of displacements not of interest
	= 1	Apparent frequencies of displacements to be computed and printed
	= -1	Apparent frequencies of displacements to be computed but not printed

(Note: Error message is issued if IPD=1 but IDD(1)=IDD(2)=IDD(3)=IDD(4)=0)

Card 3B(ii) (4I5) (omit if IPV=0)

IVV(1)	= 0	Power spectral densities of velocities not of interest
	= 1	Power spectral densities of velocities to be computed and printed
	= -1	Power spectral densities of velocities to be computed but not printed
IVV(2)	= 0	Covariance of velocities not of interest
	= 1	Covariance of velocities to be computed and printed
	= -1	Covariance of velocities to be computed but not printed

IVV(3)	= 0	Correlations of velocities not of interest
	= 1	Correlations of velocities to be computed and printed
	= -1	Correlations of velocities to be computed but not printed
IVV(4)	= 0	Apparent frequencies of velocities not of interest
	= 1	Apparent frequencies of velocities to be computed and printed
	= -1	Apparent frequencies of velocities to be computed but not printed
		(Note: Error message is issued if IPV=1 but IVV(1)=IVV(2)=IVV(3)=IVV(4)=0)

Card 3B(iii) (415) (omit if IPA=0)

IAA(1)	= 0	Power spectral densities of accelerations not of interest
	= 1	Power spectral densities of accelerations to be computed and printed
	= -1	Power spectral densities of accelerations to be computed but not printed
IAA(2)	= 0	Covariance of accelerations not of interest
	= 1	Covariance of accelerations to be computed and printed
	= -1	Covariance of accelerations to be computed but not printed
IAA(3)	= 0	Correlations of accelerations not of interest
	= 1	Correlations of accelerations to be computed and printed
	= -1	Correlations of accelerations to be computed but not printed
IAA(4)	= 0	Apparent frequencies of accelerations not of interest
	= 1	Apparent frequencies of accelerations to be computed and printed

= -1 Apparent frequencies of accelerations to be computed but not printed

(Note: Error message is issued if IPA=1 but IAA(1)=IAA(2)=IAA(3)=IAA(4)=0)

Card 3C (omit if IPRIMY≠1)

Card 3C(i) (I5)

NDNP = Number of selected Displacement Nodes for which Primary responses are to be computed

Card 3C(ii) (16I5)

JPN = Actual displacement node numbers (arranged in ascending order) for which primary responses are to be computed

(JPN(I),I=1,NDNP)

Card 4 (omit if (ISECND=0)

Card 4A (2I5)

ISX = 0 Only AUTOSTATS of secondary responses are of interest

= 1 Both AUTO- and CROSS-STATS of secondary responses are of interest

ISC = 1 Stress STATS only are wanted

= 2 Strain STATS only are wanted

= 3 Both stress and strain STATS are wanted

Card 4B(i) (4I5) (omit if ISC=2)

ISS(1) = 0 Power spectral densities of stresses not of interest

= 1 Power spectral densities of stresses to be computed and printed

= -1 Power spectral densities of stresses to be computed but not printed

ISS(2)	= 0	Covariance of stresses not of interest
	= 1	Covariance of stresses to be computed and printed
	= -1	Covariance of stresses to be computed but not printed
ISS(3)	= 0	Correlations of stresses not of interest
	= 1	Correlations of stresses to be computed and printed
	= -1	Correlations of stresses to be computed but not printed
ISS(4)	= 0	Apparent frequencies of stresses not of interest
	= 1	Apparent frequencies of stresses to be computed and printed
	= -1	Apparent frequencies of stresses to be computed but not printed

Card 4B(ii) (4I5) (omit if ISC=1)

ISN(1)	= 0	Power spectral densities of strains not of interest
	= 1	Power spectral densities of strains to be computed and printed
	= -1	Power spectral densities of strains to be computed but not printed
ISN(2)	= 0	Covariance of strains not of interest
	= 1	Covariance of strains to be computed and printed
	= -1	Covariance of strains to be computed but not printed
ISN(3)	= 0	Correlations of strains not of interest
	= 1	Correlations of strains to be computed and printed
	= -1	Correlations of strains to be computed but not printed
ISN(4)	= 0	Apparent frequencies of strains not of interest
	= 1	Apparent frequencies of strains to be computed and printed

= -1 Apparent frequencies of strains to be computed but not printed

Card 4C (omit if ISECND≠-1)

NGNS = Number of selected geometric nodes for which secondary responses are to be computed

JSEN = Actual geometric node numbers (arranged in ascending order) for which secondary responses are to be computed

(JSEN(I),I=1,NGNS)

(Note: The elements corresponding to these nodes must have been communicated to the stress module as described in the VAST manual.)

Card 5 (omit if NTAU=0)

Card 5A (I5)

ICOREL = 1 1st value of τ (non-zero), RTAU1, and constant increment in values of τ, DELTAU, are provided

= 2 Non-zero NTAU values of τ are provided

Card 5B 2E10.3 (omit if ICOREL=2)

RTAU1 = 1st (non-zero) value of time delay for the computation of correlation functions

DELTAU = Constant increment in values of τ to be used for generating other values of time delay

Card 5C 8E10.3 (omit if ICOREL=1)

RTAU = The NTAU values of time delay for which correlation functions are to be computed
(RTAU(I), I=1, NTAU)

APPENDIX B

Input Data for Program PREHPC

Card 1A (A80) Job title for HPCFEM suite of programs (maximum of 80 characters).

Card 1B (A80) Ship name (maximum of 80 characters)

Card 2 (I5) (Defines the type of the ocean wave spectrum, $S_{\eta\eta}$)

ISPEC = 1 : TEN-PARAMETER JUSZKO SPECTRUM
= 2 : SIX-PARAMETER OCHI-HUBBLE SPECTRUM
= 3 : PIERSON-MOSKOWITZ SPECTRUM (W.R.T. WIND SPEED)
= 4 : PIERSON-MOSKOWITZ SPECTRUM (W.R.T. PEAK FREQUENCY)
= 5 : INTER. SHIP STRUCTURES CONGRESS (ISSC) SPECTRUM
= 6 : JONSWAP SPECTRUM (W.R.T. GRAVITATIONAL ACCLN.)
= 7 : JONSWAP SPECTRUM (W.R.T. SIGNIFICANT WAVE HEIGHT)
= 8 : INTER. TOWING TANK CONFERENCE (ITTC) SPECTRUM
= 9 : BRETSCHNEIDER SPECTRUM

Card 2.1A (5F13.6) (Omit if ISPEC ≠ 1)

PARAM(1) = RL(1) = λ_1
PARAM(2) = RL(2) = λ_2
PARAM(3) = WM(1) = ω_{m_1}
PARAM(4) = WM(2) = ω_{m_2}
PARAM(5) = DEL(1) = δ_1
PARAM(6) = DEL(2) = δ_2

Card 2.1B (4F13.6) (Omit if ISPEC ≠ 1)

PARAM(7) = P(1) = p_1
PARAM(8) = P(2) = p_2
PARAM(9) = THM(1) = θ_{m_1}
PARAM(10) = THM(2) = θ_{m_2}

where PARAM(I), I=1, 2, ..., 10, are the ten parameters that describe the Juszko spectrum whose model description is given by equation (3.21), namely:

$$S_{\eta\eta}(\omega,\theta) = \frac{1}{4}\sum_{i=1}^{2} \frac{\left(\frac{4\lambda_i+1}{4}\,\omega_{m_i}{}^4\right)^{\lambda_i}\delta_i{}^2\, e^{-\left[\frac{4\lambda_i+1}{4}\right]\left[\frac{\omega_{m_i}}{\omega}\right]^4} * \cos^{2p_i}\frac{(\theta-\theta_{m_i})}{2}}{\Gamma(\lambda_i)\,\omega^{4\lambda_i+1}} \qquad (B.1)$$

Card 2.2 (6F13.6) (Omit if ISPEC ≠ 2)

This card defines the six parameters that define the Ochi-Hubble spectrum:

$$S_{\eta\eta}(\omega) = \frac{1}{4} \sum_{i=1}^{2} \frac{\left(\frac{4\lambda_i+1}{4}\,\omega_{m_i}^{4}\right)^{\lambda_i}\delta_i^{2}\; e^{-\left[\frac{4\lambda_i+1}{4}\right]\left[\frac{\omega_{m_i}}{\omega}\right]^{4}}}{\Gamma(\lambda_i)\,\omega^{4\lambda_i+1}} \qquad \text{(B.2)}$$

PARAM(1) = RL(1) = λ_1
PARAM(2) = RL(2) = λ_2
PARAM(3) = WM(1) = ω_{m_1}
PARAM(4) = WM(2) = ω_{m_2}
PARAM(5) = DEL(1) = δ_1
PARAM(6) = DEL(2) = δ_2

Card 2.3 (3F13.6) (Omit if ISPEC ≠ 3)

This card defines the three parameters of the Pierson-Moskowitz spectrum described in terms of the wind speed:

$$S_{\eta\eta}(\omega) = \alpha g^2 \omega^{-5} \exp\left[-0.74\left(\frac{wU_\omega}{g}\right)^{-4}\right] \qquad \text{(B.3)}$$

PARAM(1) = ALPHA = α (Fixed at 0.0081)
PARAM(2) = GAC = g = gravitational acceleration
PARAM(3) = VW = U_ω = wind speed

Card 2.4 (3F13.6) (Omit if ISPEC ≠ 4)

This card defines the three parameters of the Pierson-Moskowitz spectrum described in terms of the frequency of spectral peak (ω_o):

$$S_{\eta\eta}(\omega) = \alpha g^2 \omega^{-5} \exp\left[-1.25\left(\frac{\omega}{\omega_o}\right)^{-4}\right] \qquad \text{(B.4)}$$

PARAM(1) = ALPHA = α (Fixed at 0.0081)
PARAM(2) = GAC = g = gravitational acceleration
PARAM(3) = WO = ω_o = frequency of spectral peak

Card 2.5 (2F13.6) (Omit if ISPEC ≠ 5)

This card defines the two parameters of the International Ship Structures Congress (ISSC):

$$S_{\eta\eta}(\omega) = 0.1107\ H_S^2\ \frac{\bar{\omega}^4}{\omega^5}\ \exp[-0.4427(\frac{\bar{\omega}}{\omega})^{-4}]\ , \qquad (B.5)$$

where $\omega = 1.296\ \omega_o$

PARAM(1) = HS = H_S = significant wave height
PARAM(2) = WO = W_o = peak frequency

Card 2.6 (4F13.6) (Omit if ISPEC ≠ 6)

This card defines the four parameters of the JONSWAP spectrum described with respect to gravitational acceleration:

$$S_{\eta\eta}(\omega) = \alpha g^2 \omega^{-5}\ \exp[-1.25\ (\frac{\omega}{\omega_o})^{-4}\ \gamma\ \exp[-\frac{(\omega-\omega_o)^2}{2\tau^2\omega_o^2}] \qquad (B.6)$$

PARAM(1) = ALPHA = α (Usually taken to be 0.0081)
PARAM(2) = GAC = g = gravitational acceleration
PARAM(3) = WO = ω_o = peak frequency
PARAM(4) = GAMA = γ = peakedness parameter

Card 2.7 (3F13.6) (Omit if ISPEC ≠ 7)

This card defines the three parameters fo the JONSWAP spectrum described with respect to significant wave height:

$$S_{\eta\eta}(\omega) = \alpha^* H_S^2\ \frac{\omega^{-5}}{\omega_o^{-4}}\ \exp[-1.25(\frac{\omega}{\omega_o})^{-4}]\ \gamma\ \exp\ [\frac{-(\omega-\omega_o)^2}{2\tau^2\omega_o^2}]\ , \qquad (B.7a)$$

where

$$\alpha^* = \frac{0.0624}{0.230 + 0.0336\gamma - 0.185\ (1.9+\gamma)^{-1}} \qquad (B.7b)$$

PARAM(1) = HS = H_S = significant wave height
PARAM(2) = WO = ω_O = peak frequency
PARAM(3) = GAMA = γ = peakedness parameter

Card 2.8 (3F13.6) (Omit if ISPEC ≠ 8)

This card defines the three parameters of the International Towing Tank Conference (ITTC):

$$S(\omega) = \alpha g^2 \omega^{-5} \exp[-\frac{4\alpha g^2 \omega^{-4}}{H_s^2}] \qquad \text{(B.8a)}$$

where $\alpha = \frac{0.0081}{k^4}$ (B.8b)

and $k = \frac{\sqrt{g/\sigma}}{3.54\omega_z}$ (B.8c)

in which $\sigma = \sqrt{m_o} = \frac{1}{4} H_s$. (B.8d)

In the above, σ is the standard deviation (r.m.s. value) of the water surface elevation, m_n is the nth moment of the spectrum defined as

$$m_n = \int_0^\infty \omega^n S_{\eta\eta}(\omega) d\omega \ , \qquad \text{(B.8e)}$$

and the average zero crossing frequency or apparent frequency (defined in Chapter 2), ω_z is:

$$\omega_z = \{ \frac{m_2}{m_o} \}^{\frac{1}{2}} \qquad \text{(B.8f)}$$

PARAM(1) = ALPHA = α (calculated as given by (B.8b)
PARAM(2) = GAC = g = gravitational acceleration
PARAM(3) = HS = H_S = significant wave height

Card 2.9 (2F13.6) (Omit if ISPEC ≠ 9)

This card defines the two parameters of the Bretscheider spectrum:

$$S_{\eta\eta}(\omega) = 0.1687 H_s^2 \frac{\bar{\omega}^4}{\omega^5} \exp[-0.675(\frac{\bar{\omega}}{\omega})^{-4}] \ , \qquad \text{(B.9a)}$$

where $\omega_s = \frac{2\pi}{T_s}$, $T_s = 0.946 T_o$. (B.9b)

PARAM(1) = HS = H_S = significant wave height
PARAM(2) = TO = T_o = peak period.

Card 3 (2F15.5; 2E10.3)

CDEN = Density of the seawater (eg. 1.025 tonnes/m^3)
CACC = Acceleration due to gravity (eg. 9.81 m/s^2)

(User must ensure that the units of CDEN and CACC are consistent with units used for defining the VAST finite element model.)

Card 4 (5F15.5; 5E10.3)

RLOA = Length overall
RLBP = Length between perpendiculars
BM = Maximum beam
TD = Mean draught
TR = Trim (positive by the stern)

Card 5 (2I5)

ISYM = 0 : ship has no symmetry
= 1 : ship has symmetry about X=0 only
= 2 : ship has symmetry about Y=0 only
= 3 : ship has symmetry about both X=0 and Y=0

ISPED = 1 : ship speed is in m/s
= 2 : ship speed is in knots

Card 6 (2I5)

IMAS = 1 : sectional mass data is provided in this input data file
= 2 : sectional mass data computed from the finite element mesh of the ship is available on file PREFX.LWD (generated by subprogram HGLWD) of module HVAST

NSEC = No. of stations along the global X-axis at which sectional masses are defined

Card 7 (4F15.5; 4E10.3) (To be provided NSEC times)(Omit if IMAS = 2)

SMASS = Sectional mass
XM = X coordinate of the C.O.G. of the sectional mass
YM = Y coordinate of the C.O.G. of the sectional mass
ZM = Z coordinate of the C.O.G. of the sectional mass

(C.O.G. = centre of gravity)

Card 8 (4I5) (Omit if ISYM = 0)

NAFT1 = Number of nodes used to define the aftend of the ship
NAFT2 = Number of facets that make up the aftend of the ship
NFOR1 = Number of nodes used to define the forend of the ship
NFOR2 = Number of facets that make up the forend of the ship

Card 9 (I5, 3E10.3)(Provide NAFTI Cards)(Omit if ISYM = 0)

NODEN = Number of identifier of the aftend node point
XCO = X coordinates of the node point
YCO = Y coordinates of the node point
ZCO = Z coordinates of the node point

Card 10 (5I5)(Provide NAFT2 Cards)(Omit if ISYM = 0)

NF = Facet number for this aft end facet
(NN1, NN2, NN3, NN4) = Connectivities of this facet

Facets Cards (Applicable to both aftend and forend cards)

NF is the facet identifier. 1-36 are the facet identifiers for the facets on the water-line, starting from the stern centre-line and rotating in a clockwise fashion, looking from above. The facets around the girth (starting from the port-side) and directly under the water-line facet with identifier N are numbered N01, N02, N03, .. etc. N1, N2, N3, N4 are the node numbers that make up that facet. The numbering system is in sequential clock-wise order looking from outside the ship and starting from the top right-hand corner of the facet.

Card 11 (I5, 3E10.3) (Omit if ISYM = 0)

NODEN = Number identifier of the forend node point
XCO = X coordinates of the node point
YCO = Y coordinates of the node point
ZCO = Z coordinates of the node point

Card 12 (5I5) (Omit if ISYM = 0)

NF = Facet number for this forend facet (NN1, NN2, NN3, NN4) = connectivities of this facet.

Card 13A (I5) (Omit if ISYM = 0)

NLONG = No. of longitudinal positions at which automatic panels are to be generated by HPCFEM program

Card 13B (3E10.3, I5) (Omit if ISYM = 0)

XX = Longitudinal position (expressed as fraction of the length) (Note: 0.0 corresponds to aft perpendicular and 10.0 corresponds to fore perpendicular)
NP = No. of panels required to model the half girth

Card 14A (2I5)

NSEC2 = No. of two-dimensional sections for which body plan offsets are defined

IDATA = 1 : horizontal and vertical body plan offsets are provided in this input data file
2 : the horizontal and vertical offsets are provided by the output file of the digitizing program DIGHLL

Card 14B (Omit if IDATA = 2) (To be provided NSEC2 times)

RSEC(I) = Station number (Station No. 0.0 corresponds to A.P.; Station No. 10.0 corresponds to F.P.)
Y(I) = Horizontal offset, measured from the centre-line starting at the keel, all values positive
Z(I) = Vertical offset, measured from the base-line starting at the keel, positive upwards

Card 15 (E10.3)(i.e. free format)

DAMP = Damping ratio factor

Card 16 (I5, 4E10.3)

NSPEED = No. of ship speeds (max. of 4)
SPED(I) = Values of the ship speeds
(I=1, NSPEED)

Card 17A (I5)

NHEAD = No. of ship headings (max. of 13)

Card 17B (8E10.3) (Provide 1 or 2 cards as required)

HEAD = Values of ship headings in degrees

Card 18A (I5)

NFREQ = No. of wave frequencies (max. of 15)

Card 18B (8E10.3) (Provide 1 or 2 cards as required)

FREQ(I) = Wave frequencies in rad/s
(I = 1, NFREQ)

Card 19A (I5)

NLPFOM = 0 forces and moments on ship not desired
≠ 0 no of longitudinal positions for which forces and moments on ship are to be calculated and output

Card 19B (8G10.3) (Provide as many cards as required)

(XL(I), I = 1, NLPFOM)
= Longitudinal positions, expressed as a fraction of the length, for calculation of forces and moments
(Note: A.P. = 0.0, F.P. = 1.0)

Card 20 (I5)

INTOPT = Interpolation option parameter
= 1 the closest hydrodynamic pressure point to required point
= 2 weighted average of hydrodynamic pressure points closest to the required point
= 3 linear interpolation between the hydrodynamic pressure points

UNCLASSIFIED
SECURITY CLASSIFICATION OF FORM
(highest classification of Title, Abstract, Keywords)

DOCUMENT CONTROL DATA

(Security classification of title, body of abstract and indexing annotation must be entered when the overall document is classified)

1. ORIGINATOR (the name and address of the organization preparing the document Organizations for whom the document was prepared, e.g. Establishment sponsoring a contractor's report, or tasking agency, are entered in section 8.)

MARTEC LIMITED
Suite 400, 1888 Brunswick Street
Halifax, N.S. B3J 3J8

2. SECURITY CLASSIFICATION (overall security classification of the document including special warning terms if applicable).

Unclassified

3. TITLE (the complete document title as indicated on the title page. Its classification should be indicated by the appropriate abbreviation (S,C,R or U) in parentheses after the title).

Development of Random Response Analysis Capability for the VAST Finite Element Program - Phase 1

4. AUTHORS (Last name, first name, middle initial. If military, show rank, e.g. Doe, Maj. John E.)

Orisamolu, I.R., Norwood, M.E. and Chernuka, M.W.

5. DATE OF PUBLICATION (month and year of publication of document)

March 1991

a. NO OF PAGES (total containing information Include Annexes, Appendices, etc).

6. NO. OF REFS (total cited in document)

6. DESCRIPTIVE NOTES (the category of the document, e.g. technical report, technical note or memorandum. If appropriate, enter the type of report, e.g. interim, progress, summary, annual or final. Give the inclusive dates when a specific reporting period is covered).

DREA Contractor Report

8. SPONSORING ACTIVITY (the name of the department project office or laboratory sponsoring the research and development. Include the address).

Defence Research Establishment Atlantic
PO Box 1012, Dartmouth, N.S.. B2Y 3Z7

9a. PROJECT OR GRANT NO. (If appropriate, the applicable research and development project or grant number under which the document was written. Please specify whether project or grant).

9b. CONTRACT NO. (If appropriate, the applicable number under which the document was written).

Contract No. W7707-0-0956/01-OSC

10a. ORIGINATOR'S DOCUMENT NUMBER (the official document number by which the document is identified by the originating activity. This number must be unique to this document).

MARTEC TR 91-2

10b. OTHER DOCUMENT NOS. (Any other numbers which may be assigned this document either by the originator or by the sponsor).

DREA CR 91/424

11. DOCUMENT AVAILABILITY (any limitations on further dissemination of the document, other than those imposed by security classification)

(X) Unlimited distribution
( ) Distribution limited to defence departments and defence contractors; further distribution only as approved
( ) Distribution limited to defence departments and Canadian defence contractors; further distribution only as approved
( ) Distribution limited to government departments and agencies; further distribution only as approved
( ) Distribution limited to defence departments; further distribution only as approved
( ) Other (please specify):

12. DOCUMENT ANNOUNCEMENT (any limitation to the bibliographic announcement of this document. This will normally correspond to the Document Availability (11). However, where further distribution (beyond the audience specified in 11) is possible, a wider announcement audience may be selected).

UNCLASSIFIED
SECURITY CLASSIFICATION OF FORM

DCD03 2/06/87-M

13. ABSTRACT (a brief and factual summary of the document. It may also appear elsewhere in the body of the document itself. It is highly desirable that the abstract of classified documents be unclassified. Each paragraph of the abstract shall begin with an indication of the security classification of the information in the paragraph (unless the document itself is unclassified) represented as (S), (C), (R), or (U). It is not necessary to include here abstracts in both official languages unless the text is bilingual).

This report contains a description of the work done in the first phase of a contract awarded by the Defence Research Establishment Atlantic (DREA) for the provision of an in-house random response analysis capability. A concise description of the theoretical basis of the finite element random vibration analysis methodology is given. A description of available procedures for computing the assembled cross-spectral density matrix for a finite element model of structures excited by distributed random loads is also presented. Special emphasis is given to marine structures subjected to random pressure loads induced by random ocean waves. Computer programs for performing random vibration analysis developed during the course of this work have been incorporated into the VAST finite element program as a new module called RANVIB. A suite of computer programs for the generation of random loads for ship structures were also developed. Descriptions of all programs together with operational procedures and input data preparation are provided. Example problems illustrating the operation of RANVIB are given. The report also gives some remarks about the capabilities developed and recommendations for future work.

14. KEYWORDS, DESCRIPTORS or IDENTIFIERS (technically meaningful terms or short phrases that characterize a document and could be helpful in cataloguing the document. They should be selected so that no security classification is required. Identifiers, such as equipment model designation, trade name, military project code name, geographic location may also be included. If possible keywords should be selected from a published thesaurus. e.g. Thesaurus of Engineering and Scientific Terms (TEST) and that thesaurus-identified. If it not possible to select indexing terms which are Unclassified, the classification of each should be indicated as with the title).

Random Response
Structural Analysis
Finite Elements
Ship Structures
Marine Structures